Effect of trifluoroacetate, a persistent degradation product of halogenated hydrocarbons, on photosynthesis of C_3 and C_4 crop plants.

Thesis submitted in partial fulfilment of the degree
Masters in Environmental Science (M.Env.Sci)
in the School of Environmental Sciences and Development,
North-West University, Potchefstroom Campus, South Africa.

Martin Francis Smit
(B.Sc)

Supervisor:
Prof GHJ Krüger

Co-supervisor:
Dr PDR van Heerden

2006
Potchefstroom Campus

Acknowledgements

My sincere thanks to the following persons:

- my supervisor Prof. Gert Krüger (NWU) for his input, enthusiasm and for introducing me to the wonderful and exciting world of plant physiology and specifically photosynthesis.
- my co-supervisor Dr. Riekert van Heerden (NWU) for his input and critical evaluation of all aspects of my thesis.
- Prof. Kobus Pienaar (NWU) for additional financial assistance and technical support.
- Prof. Reto Strasser (Bioenergetics Laboratory, University of Geneva) for his valuable assistance regarding calculation and interpretation of the chlorophyll a fluorescence data.
- Dr. Anine Jordaan, for her help on the interpretation of TEM micrographs.
- Miss. Wilna Pretorius, for all her assistance with the preparations for TEM work.
- Dr. Ludwig Weissflog and Dr. Karsten Kotte (Helmholtz Centre for Environmental Research - UFZ, Leipzig) for their valuable input toward the end of my studies.
- Emile and Sherlock for all their assistance with the oxygraph measurements and the bioassay work.
- my parents for their encouragement to pursue my interests and for providing me the opportunities that I know they never had. I will always be grateful for all their sacrifices.
- my sister, Thelma and brother, Stefan, for their support
- my friends and co-students at the School of Environmental Science and Development for their help and encouragement throughout my post-graduate studies. Especially Riaan for his help and friendship.
- Peter Mortimer, for all the conversations and advice when I needed it.

I hereby declare that this thesis presented for the degree *Masters in Environmental Science (M. Env. Sci.)*, at the North-West University (Potchefstroom Campus), is my independent work and has not previously been presented for a degree at any other university or faculty.

Preface

In 1974, Sherwood Rowland and Mario Molina of the University of California proposed the theory that Chlorofluorocarbons (CFCs) may cause stratospheric ozone depletion. This was vigorously contested by the chemical industry but in 1985 scientists reported a loss of stratospheric ozone over Antarctica. These events lead to the 1987 signing of the Montreal Protocol which called for an reduction in non-essential uses of CFCs. Hydrofluorocarbons (HFCs) and Hydrochlorofluorocarbons (HCFCs) was identified as possible safe replacements for CFCs and at a cost of billions CFCs was replaced.

These compounds that served as replacements fulfilled the requirements with regard to their minimal effects on the atmosphere and consequently global change. Soon however the long-lived degradation products of these compounds notably trifluoroacetic acid (TFA), which shared molecular similarities with known toxic substances such as monofluoroacetic acid (MFA), and trichloroacetic acid (TCA) raised concern. TFA levels in nature was however already higher than would be expected and this led to the search for alternative sources which were soon found in the form of thermolysis of fluoropolymers. Basic toxicological studies were funded which showed no effects by TFA on plants and a number of organisms in standard ecotoxicological tests at environmental levels. No in depth studies were however done after this initial work in which the participating scientists identified the need to understand the possible mechanism of TFA phytotoxicity that was observed at different concentrations. In the light the conflicting views of the predicted future levels of TFA, the experiments in this thesis is the first step to understand at least part of the effects of TFA on terrestrial plants (of differing photosynthetic pathways) with regard to the process of photosynthesis.

The concern regarding TFA and other degradation products is best described by a rhetorical question of well know scientist in the field of TFA biomonitoring, Scott Mabury: "Does it matter that we are producing compounds that won't degrade over reasonable timescales?"

Abstract

Effect of trifluoroacetate, a persistent degradation product of halogenated hydrocarbons, on photosynthesis of C_3 and C_4 crop plants

Hydrofluorocarbons (HFCs) and hydrochlorofluorocarbons (HCFCs) have been the main substitutes for CFCs since the signing of the Montreal Protocol in 1987. According to the literature HFCs can degrade in the troposphere by the action of OH, NO and O_2 radicals, amongst others to trifluoroacetic acid (TFA). Studies have also shown that thermolysis of fluoropolymers, such as Teflon, can lead to the formation of HFCs. Water bodies with little or no outflow and high evaporation rate may have the potential to accumulate TFA, and can potentially achieve levels as high as 100 $\mu g.l^{-1}$ in as little as 30 years. The occurrence of TFA has been detected in water and air samples from many geographical areas and studies have confirmed the fact that TFA is a ubiquitous contaminant of the hydrosphere with levels as high as 41 $\mu g.l^{-1}$. Although information is available for the analogous compound trichloroacetic acid (TCA), little is known about the phytotoxic effects of TFA. The prediction of higher estimated future concentrations of TFA, highlights the necessity for research on the phytotoxic relevance of TFA.

Both *P. vulgaris* and *Z. mays*, representative crop plants of the C_3 and C_4 photosynthetic pathways, have been used as test plants in this study. Initial experiments were carried out over a 3 day NaTFA treatment period with plants grown and treated in sand culture. In order to obtain better control over treatment levels, later experiments were carried out over a 14 day treatment period with plants grown and treated in water culture. In both experiments *in vivo* photosynthetic gas exchange and fast phase chlorophyll a fluorescence measurement were routinely measured during the treatment period. In the case of the water culture treatments additional measurements with respect to chlorophyll content and plant development were carried out. At the end of the water culture experiment freeze clamp samples were taken for *in vitro* Rubisco analysis, and dry weight of roots and shoots were measured. In a separate experiment the effect of trifluoroacetate (NaTFA) and trichloroacetate (NaTCA) on photosynthetic electron transport was studied by measuring oxygen evolution of isolated thylakoids. Motivated by observations of NaTFA treatment on plant growth, a further simple experiment was done to determine the effect of NaTFA and NaTCA on cell growth by means of a bioassay.

The results of this study have shown that trifluoroacetate affects not only photosynthesis, but also the utilisation of photosynthates. Photosynthetic gas exchange measurements indicated

that stomatal conductance were initially (day 4 and 8 of treatment) increased by low NaTFA concentrations (0.625 $mg.l^{-1}$) and then subsequently reduced by higher concentrations (40-160 $mg.l^{-1}$) for both *P. vulgaris* and *Z. mays*. Photosynthetic gas exchange data indicated increasing reduction of Rubisco and/or PEP-case activity with increasing NaTFA concentration. The reduction in Rubisco activity was also confirmed by Rubisco activity assays, which displayed decreases with increasing NaTFA treatment levels (0.625-160 $mg.l^{-1}$), for both *P. vulgaris* and *Z. mays*. The photosynthetic gas exchange data also showed a decline in J_{max} which suggested that RuBP regeneration became limiting with increasing NaTFA concentrations, especially in the case of *Z. mays*. This finding was corroborated by the chlorophyll a fluorescence data, indicating that the formation of reducing equivalents (φ_{R0}) was reduced by NaTFA treatment. *In vitro* measurements of oxygen evolution on isolated thylakoid membranes revealed that trifluoroacetate partly inhibited the photosynthetic electron transport between Q_A and Q_B, as well as on the electron acceptor side of PSII (OEC), similarly to inhibition induced by trichloroacetate. These last two mentioned sites of inhibition were however shown not to be the primary point of inhibition of photosynthesis by chlorophyll a fluorescence measurements, and that FNR was also inhibited. Photosynthesis in *Z. mays* was more severely affected, possibly due to the complex nature of the C_4 photosynthetic pathway.

The accumulation of starch in chloroplasts of treated plants (observed by TEM, in *Z. mays*) and the observation that all NaTFA concentrations severely reduced root growth, suggested that the inhibition of root growth (more severe for *Z. mays*) and photosynthate utilisation was an additional cause of the phytotoxic effects of trifluoroacetate. Furthermore the fact that it has been shown that trifluoroacetate affects plant growth and development, in both species, may be due to induced changes in auxin activity.

The combination of subtle effects of root growth inhibition and simultaneous stimulation of stomatal conductance suggest that trifluoroacetate may have marked effects on crops and natural vegetation, even at low environmental relevant concentrations, if an additional stress such as drought is added. The fact that this study has shown some phytotoxic effect of trifluoroacetate at much lower concentration than previously reported (0.625 mg NaTFA.l^{-1}) and the fact that environmental concentrations are predicted to rise by orders of magnitude, point out the relevance of this work in the understanding of this pollutant's phytotoxicity.

Opsomming

Invloed van trifluoroasetaat, 'n blywende afbraakproduk van gehalogeneerde koolwaterstowwe, op fotosintese van C_3 en C_4 oesgewasse

Hidrofluorokoolstowwe (HFCs) en hidrochlorofluorokoolwaterstowwe (HCFCs) is die hoof plaasvervanger vir CFCs sedert die ondertekening van die Montreal protokol in 1987. Volgens die literatuur ontbind HFCs in die troposfeer deur die inwerking van OH, NO en O_2 radikale, onder andere na trifluoroasynsuur (TFA). Navorsing het aangetoon dat termolise van fluoropolimere, soos Teflon, kan lei tot die vorming van HFCs. Watermassas met klein of geen uitvloei en met 'n hoë verdampingstempo besit die potensiaal om TFA te akkumuleer met die potensiële vermoë om konsentrasies so hoog as 100 $\mu g.l^{-1}$ te bereik binne 30 jaar. Die voorkoms van TFA is reeds in water- en lugmonsters van verskeie geografiese gebiede bepaal en ondersoeke het bevestig dat TFA 'n alomteenwoordige kontaminant in die hidrosfeer, met vlakke so hoog as 41 $\mu g.l^{-1}$, is. Ofskoon inligting bestaan aangaande die analoë verbinding, trichloroasynsuur (TCA), is min bekend aangaande die fitotoksiese invloed van TFA. Die voorspelling van toekomstige hoër TFA-besoedelingsvlakke, beklemtoon die noodsaaklikheid vir navorsing t.o.v. die fitotoksiese relevansie van TFA.

P. vulgaris en *Z. mays*, verteenwoordigers van die C_3 en C_4 fotosintetiese reaksieweë, is as proefplante in hierdie ondersoek gebruik. Aanvanklik is die proefplante vir 'n periode van 3 dae blootgestel aan NaTFA in sandkultuureksperimente. Ter wille van beter beheer oor die effektiewe konsentrasie van die behandelings is latere eksperimente oor 'n periode van 14 dae in waterkultuur uitgevoer. In alle eksperimente is fotosintetiese gaswisseling en chlorofil a fluoressensie roetinematig *in vivo* gemeet oor die proeftydperk. In die geval van die waterkuultuureksperimente is addisionele metings t.o.v. van chlorofilinhoud en plantontwikkel uitgevoer. Aan die einde van die waterkultuureksperiment is vriesklamp-blaarmonsters geneem vir die *in vitro* bepaling van Rubisco-aktiwiteit. Die droëmassa van wortels en stingels is bepaal. In 'n afsonderlike eksperiment is die invloed van verskillende konsentrasies trifluoroasetaat (NaTFA) en trichloroasetaat (NaTCA) op fotosintetiese elektrontransport in geïsoleerde tilakoïede met behulp van 'n oksigraafstelsel bepaal. Op grond van waarnemings t.o.v. die invloed van NaTFA op die groei van die proefplante, is 'n verdere eenvoudige bioessaiëring uitgevoer om die invloed van NaTFA en NaTCA op selgroei te bepaal.

Die resultate van die studie het aangetoon dat trifluoroasetaat nie slegs fotosintese beïnvloed nie, maar ook die benutting van fotosinteseprodukte. Fotosintetiese

gaswisselingsanalise het aangetoon dat stomageleiding van die proefplante (beide *P. vulgaris* en *Z. mays*) aanvanklik (dag 4 en 8 van behandeling) by lae NaTFA-konsentrasies (0.625 mg.l^{-1}) gestimuleer is, waarna dit afgeneem het met verhoging in die konsentrasie (40-160 mg.l^{-1}). Die fotosintetiese gaswisselingsdata het verder ook aangetoon dat Rubisco- en/of PEPkase-aktiwiteit toenemend gerem is met toenemende NaTFA-konsentrasie. Die afname in Rubisco-aktiwiteit is ook bevestig deur die *in vitro* metings wat aangetoon het dat die aktiwiteit toenemend afneem met verhoogde NaTFA-konsentrasie by albei spesies. Die gaswisselingsdata het ook aangetoon dat toenemende NaTFA konsentrasies J_{max} toenemend onderdruk het wat dui op 'n toenemende verlaging in RuBP-regenereringskapasiteit, veral in die geval van *Z. mays*. Hierdie bevinding is ondersteun deur die chlorofil a fluoressensiedata wat aangetoon het dat die kwantumdoeltreffendheid vir die vorming van reduksie-ekwivalente (φ_{R0}) afgeneem het met toenemende NaTFA-behandeling. Met die *in vitro* bepaling van suurstofvrystelling deur tilakoïede het dit geblyk dat NaTFA elektrontransport gedeeltelik rem tussen Q_A en Q_B sowel as aan die elektronontvangerkant van PSII (OEC), soortgelyk aan die effek geïnduseer deur trichloroasetaat soos voorheen aangetoon deur ander navorsers. Chlorofilfluoressensiemetings het egter aangetoon dat remming van elektrontransport nie slegs by genoemde posisies plaasvind nie, maar dat FNR ook beïnvloed word. Fotosintese in *Z. mays* was sterker beïnvloed, waarskynlik weens die komplekse aard van die C_4 fotosintetiese meganisme.

Die akkumulering van stysel in die chloroplaste van behandelde plante (waargeneem by *Z. mays* deur TEM) en die waarneming dat NaTFA wortelgroei sterk onderdruk het, het daarop gedui dat wortelgroeiremming (die ergste by *Z. mays*) en onderdrukking van fotosintaatverbruik van die belangrike gevolge was van die fitotoksiese effek van trifluoroasetaat. Daar is ook aangetoon dat die negatiewe invloed van trifluoroasetaat op plantgroei en –ontwikkeling by albei spesies toegeskryf moet word aan steurings in ouksienwerking.

Die kombinasie van subtiele versteurings van wortelgroei en die gelyktydige stimulering van stomageleiding, voorspel dat trifluoroasetaat oesgewasse en natuurlike plantegroei ernstig sal benadeel, self by lae omgewingsrelevante konsentrasies, veral as addisionele stremming soos droogte van toepassing is. Met hierdie ondersoek is aangetoon dat trifluoroasetaat nadelige effekte veroorsaak by baie laer konsentrasies as wat voorheen gerapporteer is (0.625 mg NaTFA.l^{-1}). Die feit dat daar voorspel word dat omgewingskonsentrasies daarvan met ordegroottes kan styg, beklemtoon die relevansie van hierdie gegewens t.o.v. die fitotoksisiteit van trifluoroasetaat.

Table of contents

List of abbreviations

A_{350}	CO_2 assimilation rate at ambient CO_2 concentration (350 µmol mol^{-1})
A_0	CO_2 assimilation rate at an intercellular CO_2 concentration of 350 µmol mol^{-1} or above where no stomatal limitation is present
ABS/CS_M	Phenomenological energy flux (per excited cross section of leaf) for light absorption
ABS/RC	The specific energy flux (per PSII reaction centre) for light absorption
BCF	Bioaccumulation factor
C_a	Atmospheric CO_2 concentration
CE	Carboxylation efficiency
CFCs	Chlorofluorocarbons
C_i	Intercellular CO_2 concentration
CS	Excited cross section of leaf
DCMU	3-(3,4-dichlorophenyl)-1,1-dimethylurea
DF	Driving force for photosynthesis
dw	Dry weight
ET	Electron transport
ET_0/CS_M	Phenomenological energy flux (per excited cross section of leaf) for electron transport
ET_0/RC	Specific energy flux (per PSII reaction centre) for electron transport
FeCy	Potassium hexacyanoferrate
FNR	Ferredoxin $NADP^+$ reductase
F_V/F_M	Quantum yield of primary photochemistry
fw	Fresh weight
g_s	Stomatal conductance
HCFCs	Hydrochlorofluorocarbons
HFCs	Hydrofluorocarbons
J_{max}	Maximum CO_2 assimilation rate at saturating CO_2 concentration

K_{ow}	Octanol-water partition coefficient
I	Relative stomatal limitation of photosynthesis
NADPH	β-Nicotinamide adenine dinucleotide
NaTCA	Sodium trichloroacetate
NaTFA	Sodium trifluoroacetate
OEC	Oxygen Evolving Complex
PEA	Plant Efficiency Analyser
PEP-case	Phosphoenol pyruvate carboxylase
PI_{ABS}	Performance index expressed on absorption basis
PLC	Photosynthetic leaf chamber
PQ	Plastoquinone
PSI	Photosystem I
PSII	Photosystem II
PVPP	Polyvinylpolypyrrollidone
φ_{EO}	Quantum yield of electron transport
φ_{RO}	Quantum efficiency of the formation of reducing equivalents
ψ_0	Efficiency of converting a trapped exciton to electron transport further than Q_A^- into the electron transport chain
Ψ_L	Leaf water potential
Q_A	Primary bound quinone
Q_A^-	Primary bound quinone in reduced state
Q_B	Secondary bound quinone
Q_B^-	Secondary bound quinone in reduced state
RC	Photosystem II reaction centre
RC/ABS	The density of active PSII reaction centres on a chlorophyll basis
RC/CS_M	The density of active PSII reaction centres per excited cross section
Γ	CO_2 compensation concentration
RuBP	Ribulose-1,5-bisphosphate
Rubisco	Ribulose-1,5-bisphosphate carboxylase/oxygenase

SiMo	12-molydosilicic acid hydrate
TCA	Trichloroacetic acid
TECE	Tetrachloroethene
TFA	Trifluoroacetic acid
TFM	Trifluoromethyl
TR	Trapping of excitation energy
TR_0/CS_M	The phenomenological energy flux (per excited cross section of leaf) for trapping
TR_0/RC	The specific energy flux (per PSII reaction centre) for trapping
VOCs	Volatile Organic Compounds
WUE	Water use efficiency
XVOCs	Halogenated Volatile Organic Compounds

List of Figures

List of tables

Chapter 1

Introduction and background

1.1 Air pollution and vegetation

The effect of air pollution can be very subtle. Gradual declines in vegetation or loss in crop production may be difficult to assess since these processes can take years (Treshow & Anderson, 1989). Air pollutants differ in their relative phytotoxicity, but most display clear visible symptoms at high concentrations in susceptible species. Visible symptoms are mostly prominent in leaves and flowers and include the following: rolling of leaves, necrotic or chlorotic lesions and flower or fruit abortion (Jacobson & Hill, 1970). These symptoms are, however, not seen often any more due to strict policies on specific air pollutant emissions, although these symptoms were previously common around large industrial centres.

Over the past few years the focus has shifted away from the identification of visible symptoms and lethal doses to long-term effects of smaller doses and the actual mechanism of pollutant toxicity. Near-background level or chronic low-level pollutant exposures are of interest today (Treshow & Anderson, 1989; Mauzerall & Wang, 2001)

The basis for visible symptoms and other effects are found at the molecular and cellular level, and effects are sometimes present even though no visible injuries are apparent. Air pollution causes negative effects on photosynthesis, respiration, growth and development (Unsworth, 1982).

Air pollution may also influence plant performance at higher levels of organisation, for example at population and ecosystem level. Changes in competitive relationships between species may be caused by air pollution effects on the more sensitive species (Posthumus, 1991). The influence that air pollutants have on plant populations can also be influenced by factors other than the pollutant itself, such as changes in climatological conditions or parasite and plant interactions (Mansfield *et al.*, 1986).

1.2 Halogenated volatile organic compounds and halogenated acetates

In 1974, Sherwood Rowland and Mario Molina of the University of California proposed the theory that chlorofluorocarbons (CFCs) may cause stratospheric ozone depletion. This was vigorously contested by the chemical industry, but in 1985 scientists reported a loss of stratospheric ozone over Antarctica (Farman *et al.*, 1985). These events lead to the 1987 signing of the Montreal Protocol which called for a reduction in non-essential uses of CFCs.

After this initial action, following conferences in Johannesburg and Kyoto lead to the further agreement to control the production and use of semihydrated fluorochlorohydrocarbons and perfluoronatedhydrocarbons. Hydrofluorocarbons (HFCs) and hydrochloro-fluorocarbons (HCFCs) were identified as possible alternatives for CFCs and at a cost of billions, CFCs were replaced by these compounds.

Halogenated volatile organic compounds (XVOCs) do not only play a role in their interactions with ozone and other pollutants. XVOCs also get exposed to oxidative, photolytic and hydrolytic processes, which can alter their original structure and their chemical and physical properties. In this manner these secondary pollutants can alter the potential phytotoxicity of XVOC. For example it is well known for trichlororoacetic acid (TCA) which is formed amongst others by the atmospheric degradation of tetrachloroethene (TECE) (Ahlers *et al.*, 2003, Section 1.2.2). Similarly, HCFCs and HFCs as well as a number of other chemicals can be degraded in the atmosphere to trifluoroacetic acid (TFA) (Figure 1.1, Section 1.2.1).

For many XVOCs natural sources are well documented, and in some cases they can be orders of magnitude higher than anthropogenic sources (Hoekstra & De Leer, 1995). Of these pollutants, TCA is well known for its phytotoxic potential. Since very little work has been done on TFA's environmental impacts, experimental work reported in this thesis was aimed at studying TFA's phytotoxic effects.

1.2.1 Trifluoroacetic acid and trifluoroacetate

Under natural conditions trifluoroacetic acid (TFA) is completely deprotonated due to its strong acidity (pK_a = 0.25), and thus only found as trifluoroacetate in environmental compartments. Although literature sometimes wrongly refers to TFA and its phytotoxic potential, most studies are actually done on sodium trifluoroacetate (NaTFA) (See following sections). In the present thesis only NaTFA was used to test the phytoxic potential of trifluoroacetate.

1.2.1.1 Origin

Hydrofluorocarbons (HFCs), such as HFC-134a, and hydrochlorofluorocarbons (HCFCs) have been the main substitutes for the refrigerants CFC-11 and CFC-12 since the signing of the Montreal Protocol in 1987 (IPCC, 1996). According to literature (Tang *et al.*, 1998) HFC-134a is transformed in the troposphere by the action of OH radicals, NO and O_2, to TFA (Figure 1.1). TFA is also produced during the degradation of other organofluorine compounds (Table 1.1) such as halothane and isoflurane anaesthetics (Tang *et al.*, 1998).

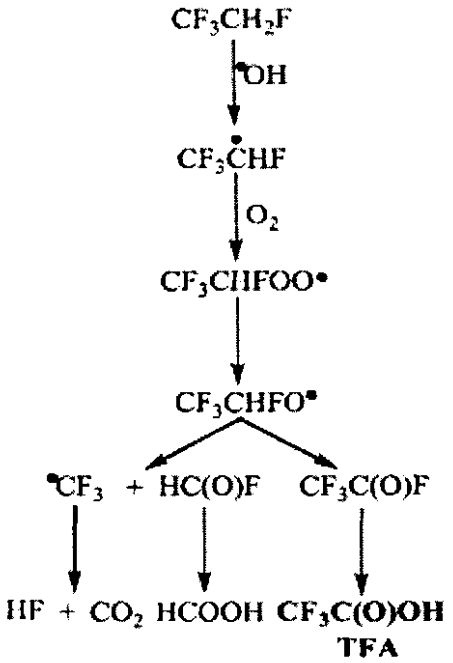

Figure 1.1: Scheme for the atmospheric degradation of a fluorinated organic compound, CF_3CH_2F (HFC-134a) to TFA (Ellis *et al.*, 2002).

Table 1.1: Compounds known to produce TFA in the atmosphere. Molar TFA yield is the fraction of TFA formed per mol of the original compound. Halothane and isoflurane are, however, regarded as negligible sources of TFA (US Global Change Research Information Office, 2006).

Compound	Molecular Weight ($g.mol^{-1}$)	Common name	Molar TFA yield	Atmospheric lifetime (years)
$CF_3CHClBr$	197.5	Halothane	0.6	1.2
$CF_3CHClOCHF_2$	184.5	Isoflurane	0.6	5.0
CF_3CHCl_2	153.0	HCFC-123	0.6	1.5
CF_3CHFCl	136.5	HCFC-124	1.0	6.0
CF_3CH_2F	102.0	HFC-134a	0.13	14.6
CF_3CHFCF_3	170.0	HFC-227ea	1.0	36.5

Another source of TFA according to literature is the breakdown of trifluoromethyl (TFM) and trifluoromethyl-containing agrochemicals such as trifluralin (Ellis *et al.*, 2000). Studies have also showed that fluoropolymers such as Teflon can degrade to form fluorinated carbon molecules (Figure 1.2), including TFA. Longer chain polyfluorocarboxylic acids and

perfluorinated alkenes, which may be as persistent as TFA, also form during fluoropolymer thermolysis, having half-lives of up to 2000 years in the troposphere (Ellis *et al.*, 2001).

TFA derived by fluoropolymer thermolysis can account for up to 25% of the TFA found in rainwater around urban areas, and may also be the source of the high TFA concentrations measured in water around such areas (Jordan *et al.*, 1999; Wujcik *et al.*, 1999; Christoph, 2002). The weathering of fluorites has also been proposed as a source of TFA, although no TFA has been detected originating from these materials (Harnisch *et al.*, 2000). Frank *et al.* (1996) measured TFA concentrations in rainwater and surface waters in Europe and Israel, which were too high to be explained only by the atmospheric degradation of HFC-134a and other chlorofluorocarbon substitutes. This finding was confirmed by Scott *et al.* (2005) who found elevated levels of TFA in ocean waters and suggested that thermal vents may be a source of TFA.

e.g. Teflon

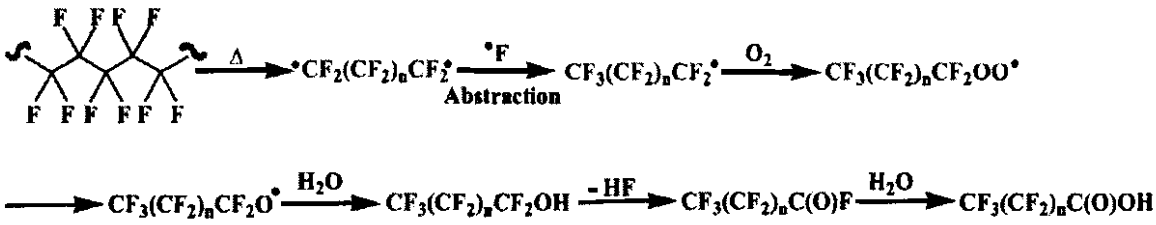

Figure 1.2: Proposed pathways of the thermal decomposition of fluoropolymers such as Teflon to TFA. Longer chain diradicals are formed which can undergo fluorine abstraction or reaction with carbonyl fluoride to form radical fluorinated alkenes or ethers. These radicals then react with oxygen and water to form perfluorinated acids including TFA; Δ = heat (Ellis *et al.*, 2002).

1.2.1.2 Environmental distribution

In the years 1990 to 2003 the production of HFC-134a increased from 0.2 to 166.9 kilotons per year. In the same period the global release of the chemical increased from 0.1 to 114.8 kilotons annually (AFEAS, 2006). Using assumptions for emissions and atmospheric degradation Franklin *et al.* (1993) calculated that the deposition of TFA in rainwater would be 45 kilotons per year in the years 2010 to 2020. Aqueous discharges of HFC-134a are expected to have a half-life of days to a few weeks. HFC-134a's longer atmospheric half-life of 14.6 years is expected to result in a more or less uniform distribution in the atmosphere (Franklin *et al.*, 1993). TFA is inevitably deposited into large water bodies. Such water bodies, with little or no outflow and high evaporation rates, may have the potential to accumulate TFA, and according to a model of Tromp *et al.* (1995) can achieve levels as high as 100 $\mu g.l^{-1}$ in as little as 30 years.

The presence of TFA has been detected in water and air samples from many geographical areas including USA, Canada, Australia, South Africa, Germany, Israel, France, Switzerland, Finland and China. These studies confirmed the fact that TFA is a ubiquitous contaminant of the hydrosphere (Table 1.2) and levels as high as 41 $\mu g.l^{-1}$ have been reported (Zehavi *et al.*, 1996; Christoph, 2002; Zhang *et al.*, 2005). Although the current levels are very low, research has now shown that the increase in chemical activity of the troposphere, due to stratospheric ozone depletion and resulting higher UV-B, might lead to much higher levels of TFA (orders of magnitude), as well as other degradation products of XVOCs, than is currently predicted (Solomon *et al.*, 2003).

TFA has a very high water solubility (Table 1.3) and a low octanol-water partition coefficient (K_{ow} = -2.1) (i.e. very lipophobic/hydrophilic) and is thus not likely to bio-accumulate in the aquatic food chain, although accumulation has been observed in terrestrial plants (Tang *et al.*, 1998; Boutonnet *et al.*, 1999). Most soils do not retain TFA strongly, but soils high in organic matter and some soils rich in iron and aluminium exhibit strong TFA retention. Studies showed the greatest TFA retention to be in organic soils from wetlands, peatlands and boreal forests (Richey *et al.*, 1994). TFA is furthermore a very stable ion in the aqueous phase and no significant loss process such as hydrolysis, photolysis, or formation of insoluble salts has been identified (Tang *et al.*, 1998). In some cases TFA degradation has been reported under certain conditions in the laboratory, but these conditions are difficult to extrapolate to natural conditions (Visscher *et al.*, 1994; Kim *et al.*, 2000; Hori *et al.*, 2003). Although no natural degradation is known for TFA, the possible interactions with organic molecules (Foy, 1969; Chang & Cai, 2005) may act like a natural sink.

Table 1.2: **Tri**fluoroacetate levels in different environmental compartments (Christoph, 2002).

Environmental compartment	High	Low
Air	120 $pg.m^{-3}$	10 $pg.m^{-3}$
Precipitation	1160 $ng.l^{-1}$	2 $ng.l^{-1}$
Fog	3779 $ng.l^{-1}$	237 $ng.l^{-1}$
Rivers	41 000 $ng.l^{-1}$	60 $ng.l^{-1}$
Lakes	41 000 $ng.l^{-1}$	10 $ng.l^{-1}$

1.2.1.3 Effects of trifluoroacetate on plants

Studies funded by AFEAS showed no effect on germination or growth of soybean grown in NaTFA-treated soils at a concentration of 1mg.kg^{-1} soil. However, toxic effects were observed at 10 and 100 mg.kg^{-1} respectively (Thompson & Windeatt, 1994a). Work done at the University of Newcastle showed effects on soybean leaf size after foliar spraying of laboratory-grown plants to simulate 10 mm of rainfall at a concentration of 100 mg TFA.l^{-1} (Davison & Pearson, 1997). In a separate study no effects were observed in a variety of crop plants at concentrations ranging from 1 to 1000 mg.l^{-1} (Tang *et al.*, 1998). The accumulation of NaTFA, applied as a mist (150 and 10000 ng.l^{-1}), has been demonstrated in *Pinus ponderosa,* but no effect on plant morphology, photosynthetic rates or stomatal conductance was observed (Benesch & Gustin, 2002). Sunflower seedlings exposed to a single dose of radio-labelled TFA displayed a bioaccumulation factor (BCF) of 22 in the leaves and an average BCF of 10 for the whole plant, with no degradation of TFA in plants (Thompson *et al.*, 1994b). In a separate study on wheat, the BCF in leaves was found to be 27. The concentrations in the tips of the leaves were approximately four times higher than in the rest of the leaves (AFEAS, 1996). In one study TFA (1 mM) was shown to significantly reduce the growth of the symbiotic nitrogen fixing bacteria *Bradyrhizobium japonicum* on the roots of *Glycine max*. However this effect was attributed to pH effects since trifluoroacetic acid instead of NaTFA was used (Oehrle *et al.*, 2004).

As yet, no in-depth studies on the photosynthetic and biochemical influence of TFA on higher plants have been done.

1.2.2 Trichloroacetic acid

As for TFA, trichloroacetic acid (TCA) is normally found in the deprotonated form in the environment due to its strong acidity (pK_a = 0.77). Although literature sometimes refers to TCA and its phytotoxic potential, most studies are done with sodium trichloroacetate (NaTCA).

Dalapon (2,2-dichloro-propionic acid), a well-known herbicide, and TCA share some similarities in chemical structure, and TCA and Dalapon are known to have similar mechanisms of phytotoxicity (Ashton & Crafts, 1973). Thus information about phytotoxic effects of Dalapon are included along with information on TCA, as this information gives crucial clues on the mechanism of TFA's possible phytotoxicity.

In the UK, TCA was for the first time introduced as a non-selective organic herbicide in 1950 (Hance & Holly, 1963) and was used in the control of monocotyledonous grasses at an application level of 15-30 kg NaTCA.ha^{-1} (Brain, 1976). Thus, TCA is known to be phytotoxic.

TFA has a similar chemical structure to TCA (Figure 1.3) and it is plausible that these two chemicals could have similar phytotoxic effects. Since very little is known about the effects of NaTFA, it was deemed necessary to study the available information on the effects of NaTCA (and Dalapon) on plant growth and metabolism thoroughly. This was done in order to plan the experiments and formulate the hypotheses for this study on trifluoroacetate's effects on plants.

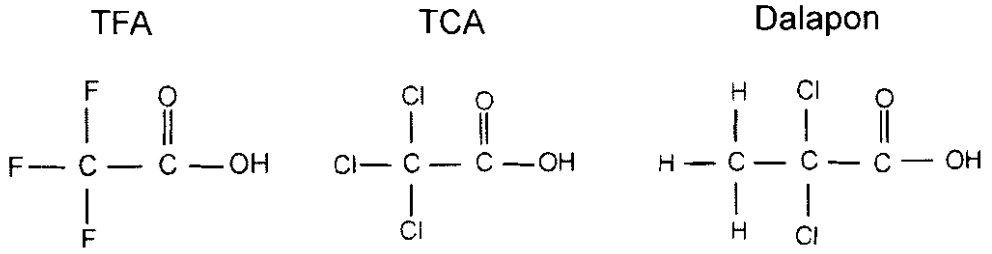

Figure 1.3: Chemical structures of TFA, TCA and Dalapon (2,2-dichloro-propionic acid), an herbicide with an analogous action to TCA.

1.2.2.1 Origin

Highly volatile chemicals such as hydrochlorocarbons, e.g. TECE, can react with radicals (e.g. reactive oxygen species) in the atmosphere to form TCA (Pienaar & Helas, 1996). TECE has a lifetime of 84 days in the atmosphere (Franklin, 1994) and about 95% of all anthropongenicaly produced TECE escapes into the environment (Western European marked = 54 MTons, 2004). Anthropogenic sources of hydrochlorocarbons include: burning of coal in power stations, burning of waste, bleaching of pulp and chlorine treatment of water (Weissflog *et al.*, 2001). Additional amounts of hydrochlorocarbons originating from natural sources include: biomass burning, volcanic activity, salt lakes and iron catalysed reactions of chlorides with humic and fulvic acids (Keppler *et al.*, 2000; Weissflog *et al.*, 2001; Weissflog *et al.*, 2005; Khalil *et al.*, 1999). Elevated TCA levels are often measured around industrialised regions and areas surrounding salt lakes (Weissflog *et al.*, 2001; Weissflog *et al.*, 2006) due to the emissions of the precursors for TCA in these areas. The oxidation of TECE to TCA does not only occur in the atmosphere, but this same process can also take place in plants (Weissflog *et al.*, 2001; Weissflog *et al.*, 2007).

1.2.2.2 Effects of trichloroacetate on plants

1.2.2.2.1 Absorption and translocation

Trichloroacetate is translocated throughout the entire plant, including the leaves, stem and shoot apex. The highest trichloroacetate concentrations are normally located in the oldest leaves (Blanchard, 1954). Trichloroacetate is readily absorbed by the roots and leaves and is

primarily transported via the transpiration stream. Trichloroacetate seems to be largely confined to the apoplast (Hance & Holly, 1963; Ashton & Crafts, 1973) but small amounts are also transported via the symplast system (Blanchard, 1954). In one study with Dalapon (Santelmann & Willard, 1955) it was conclusively shown that Dalapon was translocated with the photosynthate by symplastic movement. This finding was corroborated by Pickering (1965), who showed with the use of historadioautographic techniques, that Dalapon was present in both the xylem and phloem. Trichloroacetate has also been shown to degrade further in plants to form other toxic compounds namely phosgene, which further degrades to chloroform and finally HCl (Weissflog *et al.*, 2007).

1.2.2.2.2 Growth

The mode of the inhibitory action of TCA on plants has been shown to be similar to that of Dalapon (Ashton & Crafts, 1973). The phytotoxic symptoms of TCA include growth inhibition, leaf chlorosis and formative effects especially at the shoot apex. Funderburk and Davis (1960) noted that the reduction in height of maize after Dalapon application was a result of shortening of the internodes. Foliar necrosis may also occur at high NaTCA concentrations (Mayer, 1957; Hance & Holly, 1963; Ashton & Crafts, 1973). Damage to different species of trees has been reported after a single application of 0.1 to 6 g NaTCA.m^{-2} or after long term exposure to TECE (Weissflog *et al.*, 2001; Lange *et al.*, 2004). In the same study, *Pinus sylvestris* (10-year-old) showed accumulation after chronic exposure to TECE (up to 70 µg TCA.kg^{-1} dw). Although low concentrations of NaTCA and TECE increased the performance index (PI_{ABS}) of *Pinus sylvestris* a 58% decrease in performance index relative to controls was observed after drought stress was induced. (Lange *et al.*, 2004). NaTCA causes growth inhibition of both roots and shoots at high concentrations, but stimulation of root growth at low concentrations has been reported by Mayer (1957). This phenomenon contradicted the reports of Ingle and Rogers (1961), which showed that Dalapon inhibits root elongation in maize and cucumber. Prasad and Blackman (1964) reported that the primary effect of Dalapon on the roots of plants was an interference with the meristematic activity of the root tip and that mitotic activity ceased at prophase. Reduced wax excretions by leaves as a result of NaTCA exposure have been attributed to alterations of cell membranes and changes in membrane permeability (Mayer, 1957; Dewey *et al.*, 1962; Hance & Holly, 1963; Franich *et al.*, 1979). NaTCA and Dalapon have been reported to change the character of surface waxes making them more wetable to spraying (Dewey *et al.*, 1962). Reduction in wax excretion has also been reported on pine needles (Franich & Wells, 1980). Mashtakov *et al.* (1967) also found a reduction in cuticle thickness in NaTCA treated *Lupinus lutens*.

1.2.2.2.3 Biochemical responses

TCA has been shown to affect a range of processes including aspects of carbohydrate, lipid and nitrogen metabolism. These effects are, however, thought to be secondary responses brought about by primary effects of TCA on protein conformation, since these changes could affect enzyme activity (Hance & Holly, 1963). Foy (1969) noted that it is theoretically possible for halogenated acetates to alkylate the sulfhydryl or amino groups in proteins causing conformational changes. Dalapon has also been reported to inhibit lipid synthesis (Ashton & Crafts, 1973) and it has also been shown to reduce glucose and increase sucrose in sorghum (McWhorter, 1961). TCA also affects the enzymes involved in the conversion of ammonia to amides causing the accumulation of toxic-free ammonia (Treshow & Anderson, 1989). TCA displays some effects on plant hormone relations, for example TCA increases the amount of bound auxin while decreasing the amount of free auxin possibly due to enzyme inactivation (Parshakova & Mashtakov, 1967), however, it has also been shown to increase auxin content of seed tissue (Mashtakov *et al.*, 1967). Sutinen *et al.* (1997) reported higher potassium and nitrogen concentrations in young pine needles after treatment with low NaTCA concentrations and concluded that the changes where probably due to hormonal changes induced by sub lethal levels of trichloroacetate.

Analysis of Rubisco activity revealed that NaTCA decreased the activation state of the enzyme in both maize and bean plants (Strauss *et al.*, 2004). This same study also showed that NaTCA: (i) affected C_4 plants more adversely than C_3 plants; (ii) at low concentrations (0.05 $g.m^{-2}$) had a stimulatory effect; (iii) inhibited photosynthetic gas exchange due to both mesophyll and stomatal limitation; and (v) had an inhibitory affect on photosynthetic electron transport beyond Q_A. The latter observation corroborated the findings of Govindjee *et al.* (1997), indicating that the inhibition of photosynthetic electron transport by trichloroacetate and other chlorinated acetates occurred mainly between Q_A^- and Q_B, and to a lesser degree at the level of the oxygen evolution complex (OEC). The inhibitory effects on Q_A^- to Q_B were shown to be caused by effects on the two-electron gate in the D1-D2 protein, where a number of other chemicals such as quinones, bicarbonate and some herbicides are known to bind.

1.2.3 Differences in chemical properties of TFA and TCA

Although it is expected that trifluoroacetate and trichloroacetate would have similar phytotoxic effects, their chemical properties suggest that their degree of phytotoxicity may differ (Table 1.3).

Table 1.3: Chemical and physical properties of TFA and TCA.

Properties	Trifluoroacetic acid (TFA)	Trichloroacetic acid (TCA)
Molar Mass	114.03 $g.mol^{-1}$	163.4 $g.mol^{-1}$
Melting point	-15°C	58°C
Boiling point	72.4°C	197.5°C
Acidity (pK_a)	0.25	0.77
Octanol/water partition coefficient (Log K_{ow})	-2.1	1.7
Water solubility	Over 1 000 $g.l^{-1}$	13 $g.l^{-1}$

1.3 Differential photosynthetic pathways in C_3 and C_4 plants

To understand the possible difference in affects between *Z. mays* (maize) and *P. vulgaris* (beans) caused by trifluoroacetate it is necessary to understand the difference in their metabolism and anatomy. *P. vulgaris* is a so-called C_3 plant because of the fact that the first product to incorporate CO_2 is a 3-carbon acid namely 3-phosphoglycerate (PGA) (Figure 1.4a). More than 90% of all plants on earth falls into this category, however, in many families of higher plants an additional system has evolved to accumulate CO_2 before passing it to the photosynthetic carbon reduction or Calvin cycle (PCR cycle). One of these groups is the so-called C_4 plants, which first incorporate CO_2 into a 4-carbon molecule namely oxaloacetate (OAA), by means of the enzyme phosphoenol pyruvate carboxylase (PEP-case), before passing it to the PCR cycle (Figure 1.4b). This pathway was first described by Hatch and Slack (1966) in an effort to describe the initial formation of C_4 acids in sugarcane. *Z. mays* falls into this latter group and more specifically into a group of C_4 plants called NADP-malic enzyme type (Figure 1.5), because OAA is first converted to malate, which is then transferred to the bundle sheath cells where it is enzymatically converted to pyruvate and CO_2. This CO_2 is then reincorporated by the enzyme Rubisco to form PGA in the normal PCR cycle, while the pyruvate is transferred back to the mesophyll cells where it is enzymatically converted back to phosphoenol pyruvate (PEP) (Lawlor, 1993). C_4 plants thus possess a CO_2 concentrating mechanism.

To facilitate this metabolic pathway C_4 plants have, however, developed certain anatomical features. The photosynthetic parenchyma cells in a typical C_3 leaf are organised into two distinct tissues namely an upper region of tightly packed palisade cells and loosely arranged

mesophyll cells bordering large air spaces. A typical C_4 leaf, on the other hand, is much thinner than a C_3 leaf, the vascular bundles are closer together and air spaces are smaller. C_4 plants also differ in the fact that they contain an additional type of mesophyll cell that is found surrounding the vascular bundles, known as bundle sheath cells. These bundle sheath cells contain large amounts of unique bundle sheath chloroplast. The high bundle sheath chloroplast density is necessary to process the high concentration of CO_2 generated by the C_4 system (Laetsch, 1974). The phenomenon of chloroplast dimorphism thus exists in C_4 plants. The above-mentioned typical C_4 anatomy is known as Kranz-anatomy and was first described by Haberland in 1914.

When the energetics of C_4 plants are compared to C_3 plants, they are less efficient, since it requires considerable movement of assimilates across cell membranes at a considerable energy cost. In the case of the NADP malic enzyme type, 2 ATP and 1 NADPH are required in the mesophyll cell to convert pyruvate to PEP. Bundle sheath chloroplasts do not posses granal stacks and thus have little PSII and may synthesise ATP by cyclic photophosphorylation. Oxygen levels are consequently kept very low in the bundle sheath cells. If NADPH supply is insufficient in the bundle sheath for the PCR cycle it is provided by DHAP, from the mesophyll, which is then oxidised to 3PGA giving NADPH and ATP (Lawlor, 1993).

C_4 metabolism, however, offers plants a unique edge in dry, hot and high light conditions. This is possible because of a number of factors. Firstly C_4 photosynthesis allows efficient CO_2 assimilation, even in diluted CO_2 (since PEP-case C_4 plants' primary CO_2 fixing enzyme has a higher affinity for CO_2 than Rubisco and is not affected by O_2), and stomatal conductance is smaller and thus conserving water. Secondly, they have an overall higher CO_2 fixation rate and consequently exhibit faster growth rates. Thirdly, photorespiration does not occur in C_4 plants due to low oxygen levels and relative high CO_2 levels in the bundle sheath cells. Lastly, CO_2 supply limits photosynthesis in C_3 plants causing light saturation to occur at fluence rates lower than full sunlight, while C_4 plants never fully saturate, even at full sunlight (Gifford, 1974).

Possible differences in the effects of trifluoroacetate on *P. vulgaris* and *Z. mays* might be related to these metabolic and anatomical differences. For example, differences in the C_4 pathway sensitivity might be related to:

- higher sensitivity of enzymes associated with C_4 photosynthesis, such as PEP-case.
- effects on membrane permeability could have a negative effect on the transport of malate and pyruvate between mesophyll and bundle sheath chloroplasts/cells.

- higher bundle sheath cells/chloroplasts sensitivity. Even if unaffected mesophyll cells/chloroplasts generate reducing power and ATP they cannot reduce carbon since they do not possess the PCR-cycle and are dependant on the bundle sheath cells.

Not all differences in effects of TFA on *Z. mays* and *P. vulgaris* can, however, be attributed to the differences in carbon assimilation pathways. Differences are also present with regard to growth form and overall anatomy since *Z. mays* is monocotyledonous and *P. vulgaris* is dicotyledonous.

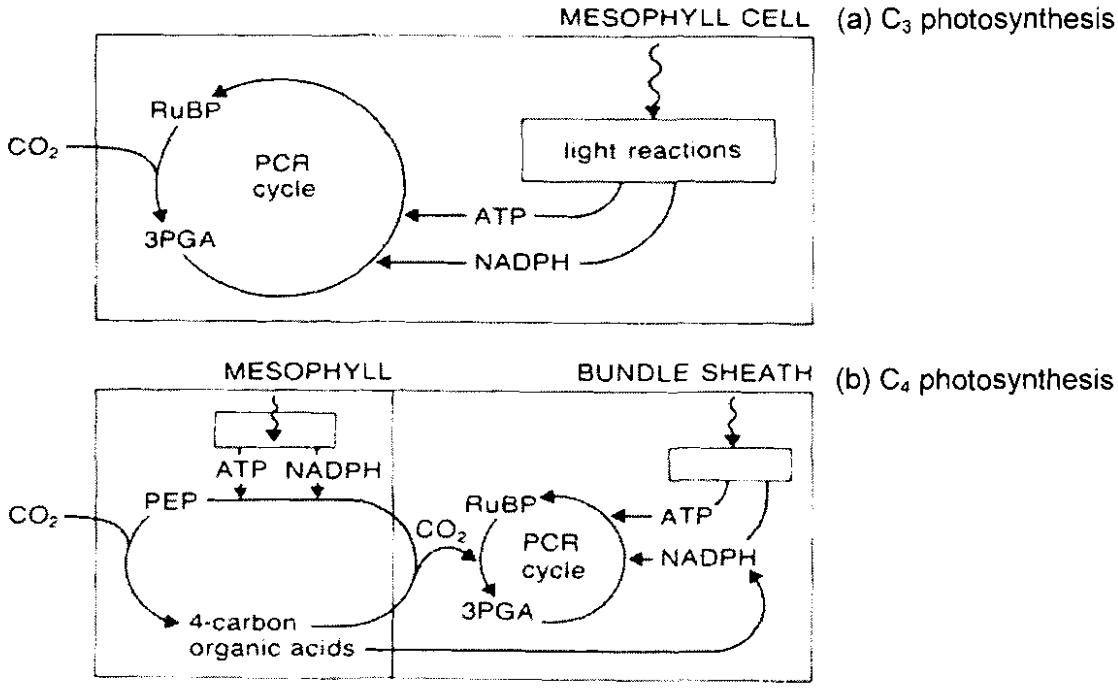

Figure 1.4: Simplified schematic representation of (a) normal C_3 photosynthesis (Note that carbon reduction by the PCR cycle takes place in one cell) and (b) C_4 photosynthesis (Note that light reactions takes place in both mesophyll and bundle sheath cells while the PCR cycle is present in only in the bundle sheath cell and primary carbon reduction takes place only in the mesophyll cell) (Lawlor, 1993).

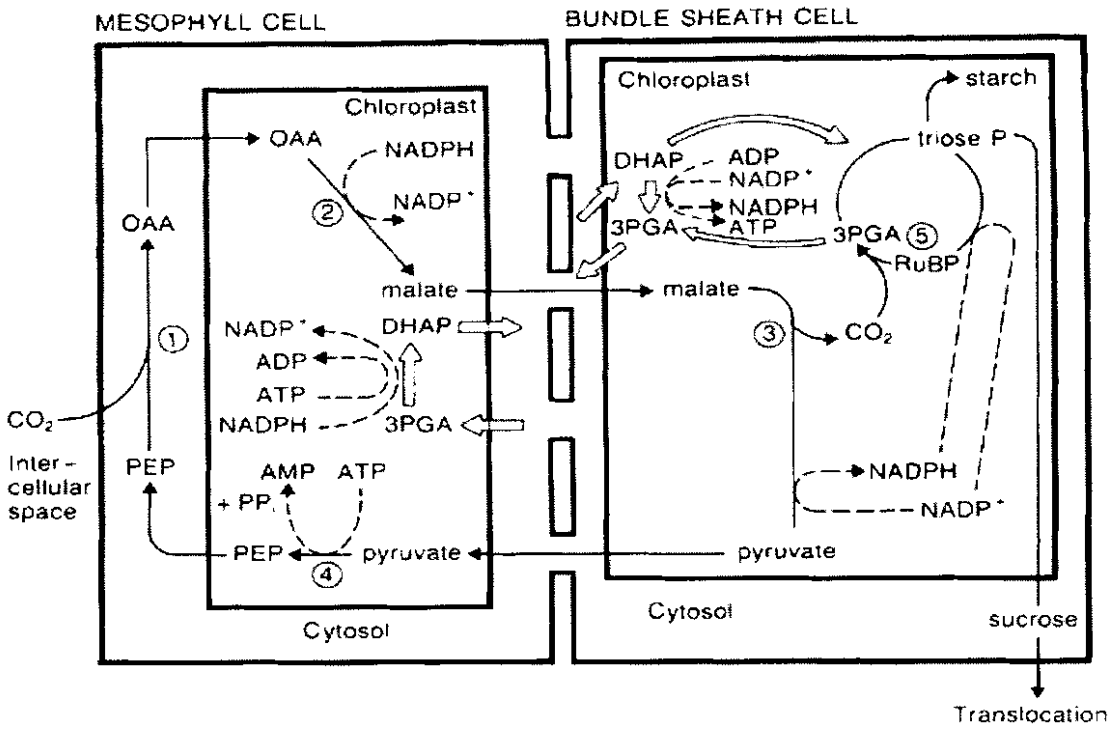

Figure 1.5: Schematic representation of the C_4 pathway (Malic enzyme type found in *Zea mays*). (1) Carboxylation of PEP by PEP-case form OAA in the mesophyll cells without net gain in energy; (2) OAA is converted to malate by NADP malate dehydrogenase which is then transported to the bundlesheath cells; (3) Malate is decarboxylated by NADP malic enzyme to pyruvate; (4) Pyruvate is then transported back to the mesophyll cells to regenerate PEP enzymatically by means of pyruvate phoshate dikinase; (5) CO_2 formed as a result of malate decarboxylation is then assimilated by Ribulose-1,5-carboxylase/oxygenase with a net gain in energy (Lawlor, 1993).

1.4 Quantifying effects of environmental stress on photosynthesis

A stressor, for example an air pollutant, can reduce canopy photosynthesis via a decrease in leaf area, stomatal closure (stomatal limitation) or a decrease in the efficiency of carbon assimilation (mesophyll limitation) of individual leaves (Kramer, 1983; Frederick *et al.*, 1989). Studies have shown that mesophyll factors play an important role in reducing CO_2 assimilation since inhibition of CO_2 assimilation occurred simultaneously with stomatal closure without changes in intercellular CO_2 concentration (Farquhar & Sharkey, 1982; Frederick *et al.*, 1989). These mesophyll factors include photosystem I and II activities (Mayoral *et al.*, 1981), inhibition of reductive carbon metabolism and photophosphorylation activity (Sharkey & Badger, 1982). It is also important to remember that photosynthesis is connected to a whole range of other processes, which can also influence photosynthesis when these processes are affected. It is thus important to distinguish between primary effects and secondary effects on photosynthesis.

While measuring photosynthetic gas exchange is useful in detecting direct physiological effects, using it in parallel with indirect measurements such as chlorophyll a fluorescence, which sheds light on the specific effects including among others photosystem II (PSII) function, promotes interpretation and quantification of plant stress effects (Krüger *et al.*, 1997). Since the shape of fluorescence transients has been found to be very sensitive to stress caused by different stressors, for example chemical influences, cold stress and drought stress (Ouzounidou *et al.*, 1997; Strauss *et al.*, 2006), the quantification of these changes provides a useful tool for the *in vivo* investigation of the behaviour of the photosynthetic apparatus, especially PSII. *In vivo* techniques such as photosynthetic gas exchange measurements and chlorophyll a fluorescence measurements, in conjunction with *in vitro* techniques such as measurement of photosynthetic electron transport and enzyme assays, thus have the potential to elucidate much of the effects of certain environmental stressors on photosynthesis.

Studies done, utilising these techniques, have revealed that TCA, a chemical analogue of TFA, induces both stomatal and mesophyll limitation. This limitation of carbon assimilation was caused by: reduction of ribulose-1,5-bisphosphate regeneration capacity; impairment of PS II function; and reduction of Rubisco activity (Strauss *et al.*, 2004).

The effect of TFA on photosynthesis has received little attention from the scientific community and thus very little information is currently available. The fact that TFA can potentially be derived from the refrigerant HFC-134a, other halogenated hydrocarbons and fluoropolymers that are used in increasing quantities worldwide make an investigation of its physiological/biochemical action on C_3 and C_4 crop plants highly topical.

1.5 Hypotheses

- Due to the structural similarity of TFA to TCA, TFA is believed to be phytotoxic.
- It is expected that C_4 plants would be more sensitive to TFA since a previous study demonstrated maize plants to be more sensitive to TCA than bean plants (Strauss *et al.*, 2004).
- Since TCA and other chlorinated acetates have been shown to directly inhibit photosynthetic electron transport, it is assumed that TFA will have a similar effect (Govindjee *et al.*, 1997).
- Since it has been shown that TCA can increase/decrease auxin levels, it is believed that TFA treatment may also affect auxin levels.

1.5.1 Aim of the study

The aim of the study was to investigate the effect of trifluoroacetate on the photosynthetic metabolism of C_3 and C_4 crop plants under controlled conditions and to shed more light on the mechanism of phytotoxicity.

The investigation was aimed at elucidating the mechanism of TFA phytotoxicity by:

- determining its effect on chlorophyll content, growth and shoot/root biomass;
- determining the possible hormonal effects of TFA and TCA by means of a bioassay;
- quantifying its effects on photosynthetic gas exchange;
- measuring fast phase chlorophyll fluorescence to assess primary processes of photochemistry and to identify the sites of action;
- measuring *in vitro* activity of Rubisco;
- determining the *in vitro* effects of TFA and TCA on photosynthetic electron transport of isolated thylakoids.

Chapter 2

Material and methods

2.1 Experimental plants

Phaseolus vulgaris (cultivar: Jenny) and *Zea mays* (cultivar: Panthera) were used as experimental plants representing C_3 and C_4 crop plants respectively. Seeds of each species were obtained from the Agricultural Research Council, Potchefstroom.

2.2 Growth conditions

Experimental plants were grown under controlled conditions in growth chambers (Conviron PGW 36, Controlled Environment Ltd, Winnipeg, Canada) with sufficient incandescent light bulbs and fluorescent lamps to maintain light intensities as high as 1000 µmol photons.m^{-2}.s^{-1} at plant level. Plants were subjected to a 15-hour light period and 9-hour dark period. A temperature of 26°C was maintained during the light period and 20°C during the dark period. The CO_2 concentration was automatically kept at 350 µmol.mol^{-1}.

2.2.1 NaTFA treatment of plants cultivated in sterilised sand

Plants were germinated in pots containing sterilised sand. After germination the number of plants in each pot was reduced to two. Every third day plants received complete Hoagland's nutrient solution (Table 2.1 & 2.2) (Hoagland & Arnon, 1950). After two weeks TFA was administered as sodium salt solution (Merck, sodium trifluoroacetate, S31820 311) to the growth medium of the experimental plants. The concentrations applied in the present study of plants, cultivated in sterilised sand, was 0.05, 0.2, 0.8, 3.2 and 12.8 g NaTFA.m^{-2} respectively. The control pots received no NaTFA. These concentrations were in the same range as the NaTCA concentrations used in a previous study on the effects of NaTCA on plants (Strauss *et al.*, 2004). The same experimental methodology was used as in this previous study (Strauss *et al.*, 2004) in order to compare data. The study of Strauss *et al.* (2004) included much lower and higher concentrations of NaTCA than those used in field experiments on trees by Weissflog *et al.* (2001). The NaTFA and NaTCA concentration ranges in the study of Strauss *et al.* (2004) and the present study, using sand and water culture, were originally based on the concentration range of NaTCA applied per m^2 used in field studies with trees (Weissflog *et al.*, 2001; Lange *et al.*, 2004). Although the lowest

NaTFA concentration used in the present sand culture study were higher than current environmental levels, however Solomon *et al.* (2003) predicts that environmental levels will rise by orders of magnitude.

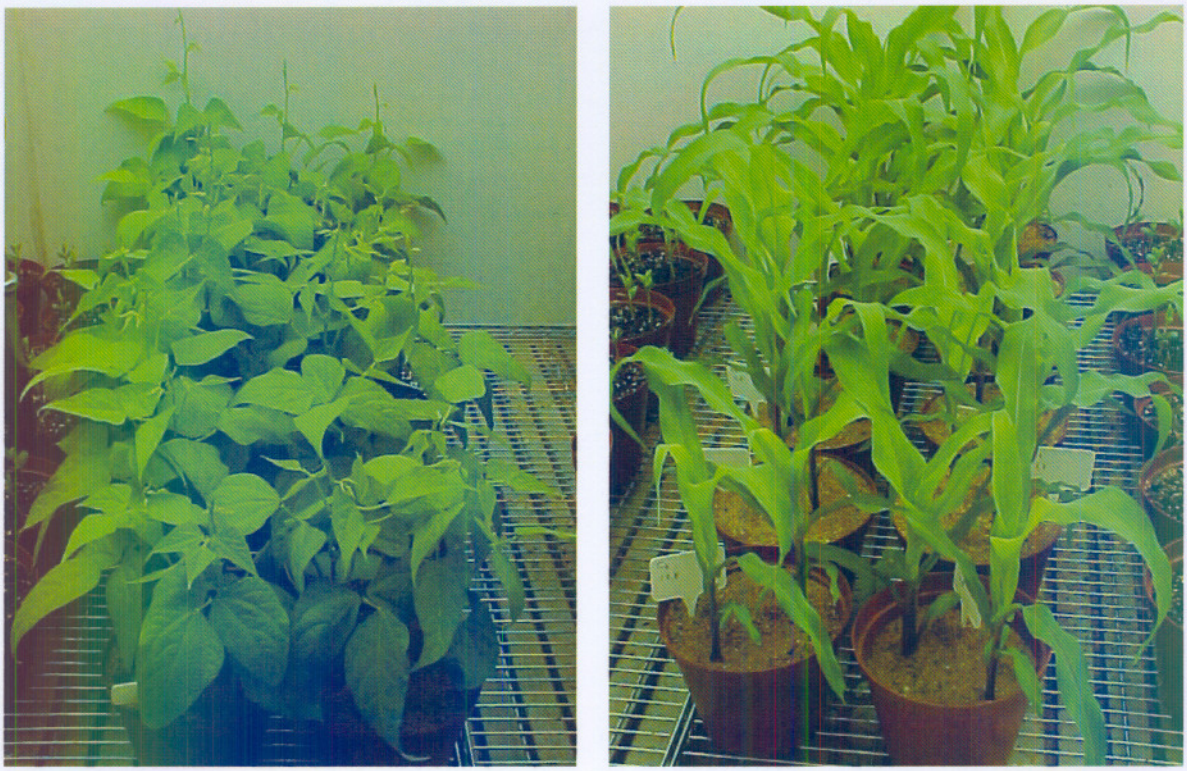

Figure 2.1: *Phaseolus vulgaris* (left) and *Zea mays* (right) cultivated in sterilised sand under controlled conditions.

The surface area of the pots was determined and used to calculate the NaTFA dosage level for each treatment. The NaTFA was dissolved in 100 ml distilled water before it was applied to the soil. Three days after a single application, various measurements were made (see below). Note that only photosynthetic gas exchange and fast phase fluorescence measurements were taken on *P. vulgaris* and *Z. mays* cultivated and treated in sand culture. To compare the results of the treatments per area basis to that of the water culture the volume of the pots were used to calculate the amount of NaTFA per volume sand (Table 2.1). Additionally the amount of trifluoroacetate actually applied was also calculated and is also presented in Table 2.1.

Table 2.1: Conversion from NaTFA per area to NaTFA per volume sand and respectively TFA per volume sand.

NaTFA per m^2 (g)	NaTFA per dm^3 sand (mg)	Trifluoroacetate per dm^3 sand (mg)	Trifluoroacetate per pot (mg)
0.05	2.6	2.2	3.3
0.2	10.4	8.7	13.0
0.8	41.7	35.0	52.5
3.2	166.7	139.7	209.6
12.8	666 .7	558.8	838.2

2.2.2 NaTFA treatment of plants cultivated in water culture

After the initial sterilised sand culture experiments, it was deemed necessary to look at longer-term effects and to identify possible recovery. It was, however, decided to use a water culture system, because: firstly, complicating factors such as NaTFA adsorption could be eliminated; secondly, a better control of actual NaTFA concentration and nutrient availability could be realised; and lastly, the capacity of the sand culture system to supply water to bigger plants would become limiting. Experimental plants were germinated in vermiculite. After germination plants were transferred to the water culture system. This system consisted of glass bottles (1l) filled with modified Hoagland's nutrient solution (Hoagland & Arnon, 1950) through which air was constantly bubbled (Table 2.3 & 2.4). When the third leaves reached maturity chlorophyll a fluorescence, photosynthetic gas exchange, chlorophyll content and plastochronindex (in the case of *P. vulgaris*) measurements were taken and NaTFA was applied to the water culture solution. Measurements were taken at 4, 8 and 12 days after application. Fresh nutrient solutions and NaTFA was applied on day 5 and 9. The NaTFA concentration range was chosen in such a way that the lowest NaTFA applications would present a trifluoroacetate concentration corresponding to concentrations currently found in nature (Zehavi *et al.*, 1996). Higher NaTFA concentrations were also selected that would give a more clear insight to the mechanism of possible trifluoroacetate inhibition and because TFA levels in nature are predicted to rise (Solomon *et al.*, 2003). The different NaTFA concentrations applied were 0.625, 2.5, 10, 40 and 160 mg NaTFA.l^{-1}. Control plants received no NaTFA. The amount of trifluoroacetate actually applied as the sodium salt, NaTFA, was also calculated and is presented in Table 2.2.

Figure 2.2: System used to cultivate *P. vulgaris* in water culture under controlled conditions.

Table 2.2: Conversion from mg NaTFA per volume to mg trifluoroacetate per volume water

NaTFA ($mg.l^{-1}$)	TFA ($mg.l^{-1}$)
0.625	0.524
2.5	2.1
10	8.38
40	33.5
160	134.1

Table 2.3: Composition of the water culture nutrient solution (Modified from Hoagland & Arnon, 1950).

Solution	Stock concentration	Mass used (g) per litre stock solution	Volume (ml) per litre nutrient solution
KNO_3	1M	101.1	6
$Ca(NO_3)_2.4H_2O$	1M	236.1	4
$MgSO_4.7H_2O$	1M	246.5	2
$NH_4H_2PO_4$	1M	115.0	1
$MgCl_2.6H_2O$	1M	203.3	4
Trace elements	(B, Mn, Zn, Cu, Mo)	-	1
NaFe-EDTA	3.86 g in 250ml	-	2

Table 2.4: Trace elements' composition.

Trace element	Quantity (mg) in 250ml H_20
H_3BO_3	715
$MnCl_2.4H_2O$	425
$ZnSO_4.7H_2O$	55
$CuSO_4.7H_2O$	20
$NaMoO_4.2H_2O$	7.25

pH was set to pH 6.8 using 1M NaOH.

2.3 Photosynthetic gas exchange

2.3.1 Overview of photosynthetic gas exchange kinetics

Measurement of CO_2 assimilation is an effective non-destructive method for studying short-term effects on carbon gain of individual organs. This provides additional information to effects on long-term carbon gain, which is analysed as the final biomass.

The approach of measuring photosynthetic gas exchange in plant is in essence based on Fick's first law of diffusion which states that the rate of diffusion is directly proportional to the cross-sectional area of the diffusion path and to the concentration or vapour pressure gradient, and it is inversely proportional to the length of the diffusion path.

To study CO_2 assimilation in plants, a number of measurements, terms and units are employed (Von Caemmerer & Farquhar, 1981): The CO_2 assimilation rate (A) is expressed as the amount of CO_2 assimilated per unit leaf area and time (μmol CO_2 m^{-2} s^{-1}). The stomatal conductance (g_s) represents the flux of CO_2 through the stomata, with the same units as for A.

When a portable open-circuit photosynthesis system is used to measure CO_2 assimilation, air is pumped from the photosynthetic leaf chamber (PLC) or cuvette enclosing a leaf into an infrared gas analyser that continuously measures the CO_2 concentration in the air stream. The CO_2 concentration of the air stream will decrease if the leaf inside the PLC assimilates CO_2. The CO_2 assimilation rate equals the change in the amount of CO_2 in the air stream per unit time. Changes in temperature and pressure are compensated for in the calculation of the CO_2 assimilation rate, but humidity has to be controlled, since a rise in transpiration will cause an increase in the amount of water vapour, resulting in dilution of CO_2 in the air stream (Long & Hällgren, 1993).

CO_2 first has to diffuse through the boundary layer on the leaf surface before it is able to enter the leaf. The boundary layer conductance will be at least in order of a magnitude greater than the highest possible g_s under field conditions (Long, 1985). In the Parkinson-type PLC (used in most portable photosynthesis systems) the boundary layer resistance is minimised and kept constant by the fan of the PLC, which keeps the turbulence high, resulting in the removal of the boundary layer. If only diffusion is taken into consideration, the intercellular CO_2 concentration (C_i) can be determined by:

$$C_i = C_a - A/g_t$$

where g_t represents the total conductance, i.e. boundary layer as well as stomatal conductance, and C_a is the atmospheric CO_2 concentration.

An *in vivo* screening of limitations on the photosynthetic CO_2 assimilation can be achieved by means of the construction of so-called CO_2 ($A:C_i$) response curves. By plotting A against C_i at a range of different C_a values, an $A:C_i$ curve can be plotted (Figure 2.3). Photosynthetic CO_2 assimilation is measured at increasing CO_2 concentrations in order to create an artificial situation where no stomatal limitation exists, i.e. $C_i = C_a$. The photosynthetic CO_2 assimilation rate under this condition is then used as reference point to calculate the percentage stomatal limitation (Farquhar & Sharkey, 1982; Von Caemmerer & Farquhar, 1981).

Such studies allow the quantitative assessment of different gas exchange parameters that can be used to quantify the effect of environmental factors on the different steps of photosynthetic CO_2 assimilation pathways. It is possible to separate limitations in the mesophyll from stomatal limitations by employing simultaneous measurements of CO_2 and water vapour fluxes. Separation of the effects on the CO_2 limiting phases is also possible (Farquhar & Sharkey, 1982; Long & Hällgren, 1993).

The demand function, $A = CE(C_i - \Gamma)$, in an $A:C_i$ response expresses the rate of CO_2 assimilation in terms of the effectiveness [C_i] and the capacity of the system to assimilate CO_2 (Farquhar & Sharkey, 1982). The supply function, $A = g_s(C_a - C_i)$, in an $A:C_i$ response expresses the rate of CO_2 assimilation in terms of the difference in concentration between C_a and C_i (the driving force for the inward movement of CO_2) and the prevailing stomatal conductance (g_s) (Farquhar & Sharkey, 1982). The actual assimilation rate, A_{350}, occurs where we find the simultaneous solution of the demand and the supply function, i.e. the operational point (Lange *et al.*, 1987).

To determine the degree of stomatal limitation of photosynthesis, the following equation is employed:

$$\mathbf{l = (A_0 - A_{350})/A_0}$$

where A_{350} = the CO_2 assimilation rate at ambient CO_2 concentration (C_a = 350 µmol mol^{-1}) and A_0 = the CO_2 assimilation rate where no stomatal limitation is present ($C_i \geq$ 350 µmol mol^{-1}) (Farquhar & Sharkey, 1982). Stomatal limitation (l) represents the proportionate decrease in CO_2 assimilation rate that may be attributed to stomatal restrictions.

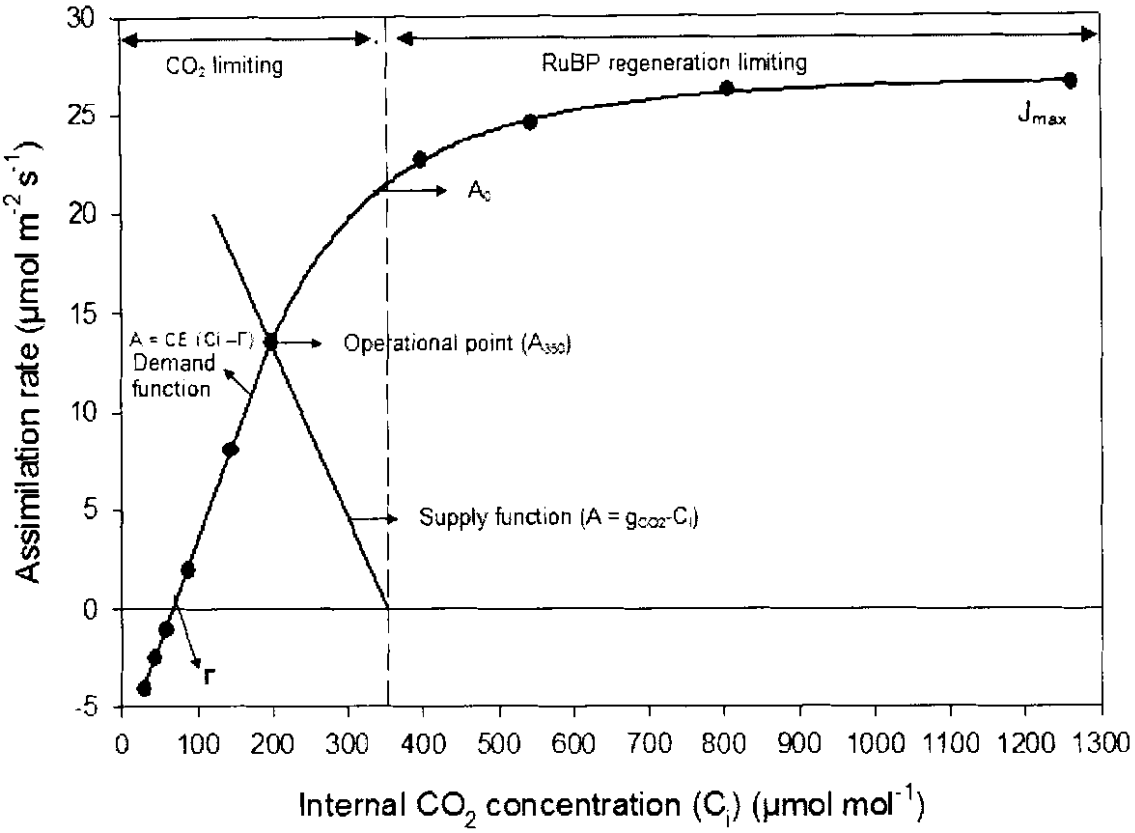

Figure 2.3: Response of CO_2 assimilation rate (A) vs. intercellular CO_2 concentration (C_i). A_{350} is the assimilation rate under atmospheric conditions, i.e. the point of simultaneous solution of the demand and supply functions. Carboxylation efficiency (CE) is represented by the initial slope of the demand function, the CO_2 compensation concentration (Γ) is the intercellular CO_2 level where the net usage of CO_2 equals zero, the maximum rate of assimilation (J_{max}) represents the rate of CO_2 assimilation at saturated levels of CO_2 and A_0 is the rate of assimilation at the point were stomatal limitation is artificially eliminated by raising the internal CO_2 concentration (C_i) to atmospheric CO_2 concentration (interpolation of the value of A from the response curve at C_i = 350 µmol.mol^{-1}) (Lange *et al.*, 1987). The dots are data points generated with an infrared gas analysing system, which is then used to construct an A:C_i response curve.

The apparent carboxylation efficiency of photosynthesis can be deduced from the initial linear response (CE) of the A:C_i response curve which is an *in vivo* estimation of Rubisco activity (Bolhàr-Nordenkampf & Öquist, 1993). The maximal CO_2 assimilation rate at saturating C_i (J_{max}) can be regarded as a reliable indicator of the RuBP regeneration capacity of the leaf.

2.3.2 Measurement of photosynthetic gas exchange on *P. vulgaris* and *Z. mays*

CO_2 gas exchange was measured with an infrared gas analysis system (CIRAS-2, PP-Systems, Hertz, UK). Measurements were taken for each concentration on four different plants. A 2.5 cm^2 section of a leaf was clamed into a standard broad leaf photosynthetic leaf chamber (PLC) with light and temperature control. The light intensity was kept at 1200 µmol photons.m^{-2}.s^{-1} to ensure full activation of Rubisco (Taylor & Terry, 1984) while the leaf temperature was kept at 26°C, during measurements. The ambient CO_2 concentration (C_a) was increased with three-minute increments from 0 to 2000 µmol.mol^{-1}, allowing CO_2 assimilation rate (A) *vs.* intercellular CO_2 concentration (C_i) response curves to be generated.

Figure 2.4: Measurement of photosynthetic gas exchange on a 2.5 cm^2 leaf area of *P. vulgaris* by the automatic PLC of the infrared gas analyser with controlled light intensity, temperature and CO_2 levels.

2.4 Fast phase chlorophyll a fluorescence kinetics

2.4.1 Overview of chlorophyll a fluorescence

Part of the light energy absorbed by the pigments in plants (mostly chlorophyll) is lost by re-emission as fluorescence or as heat from the light harvesting complexes of PSII. Since the decay processes of excited chlorophyll are competitive, changes in photosynthetic rate and/or dissipative heat will lead to complementary changes in emitted fluorescence intensity (Bolhàr-Nordenkampf & Öquist, 1993)

When a dark-adapted leaf is illuminated with a saturated light pulse, characteristic changes in the intensity of chlorophyll *a* fluorescence, known as the Kautsky effect, are observed

(Kautsky & Hirsch, 1931). The Kautsky transient shows a fast rise completed in less than one second, with a subsequent slower decline towards a steady state. It is postulated that the rising phase of the transient reflects the primary reactions of photosynthesis (Krause & Weis, 1991). With the development of fluorimeters with high time resolution and high data acquisition capacity, additional and more accurate information about the kinetics of these transients was obtained (Schreiber & Neubauer, 1987; Strasser & Govindjee, 1992; Strasser *et al.*, 1995). When the OJIP is measured with the Handy Plant Efficiency Analyser (Handy-PEA, Hansatech Instruments Ltd., Kingslynn, UK), direct fluorescence is measured as opposed to modulated fluorescence in the case of many other commercially available instruments. For example, it was demonstrated that the fluorescence rise kinetics of the Kautsky transient is polyphasic when plotted on a logarithmic time scale (Figure 2.5), clearly exhibiting the steps J and I (Strasser & Govindjee, 1992) or I_1 and I_2 (Schreiber & Neubauer, 1987) between the initial O (F_0) and maximum P level ($F_P = F_M$).

Upon excitation with a saturated light pulse, a rapid initial rise occurs in fluorescence intensity from O to the first intermediate step J within ca. 2 ms. This phase is followed by a further rise to the second intermediate step I within ca. 30 ms and to the final peak P in ca. 200 ms. The OJIP fluorescence transient reflects the filling up of the electron acceptor side of PSII (Q_A, Q_B and PQ pool) with electrons from the donor side of PSII (Papageorgiou, 1975; Lavorel & Etienne, 1977; Strasser & Govindjee, 1992). The relationship of these events to the OJIP fluorescence transient was suggested by Strasser *et al.* (1995) to be the following: O, minimal chlorophyll *a* fluorescence yield (highest yield of photochemistry); O to J, reduction of Q_A to Q_A^- (photochemical phase, light intensity dependent); J to I to P, reduction of the PQ pool (non-photochemical phase). Since the OJIP fluorescence transient reflects the kinetics and heterogeneity involved in the filling up of the PQ pool with electrons, it can be used as a sensitive tool to investigate the function and structure of the photosynthetic apparatus *in vivo* (Strasser *et al.*, 1995). The shape of the OJIP fluorescence transient (Figure 2.5) has been found to be very sensitive to various types of stress (Krüger *et al.*, 1997; Lazár & Ilík, 1997; Tsimilli-Michael *et al.*, 1999; Van Heerden *et al.*, 2004; Strauss *et al.*, 2006).

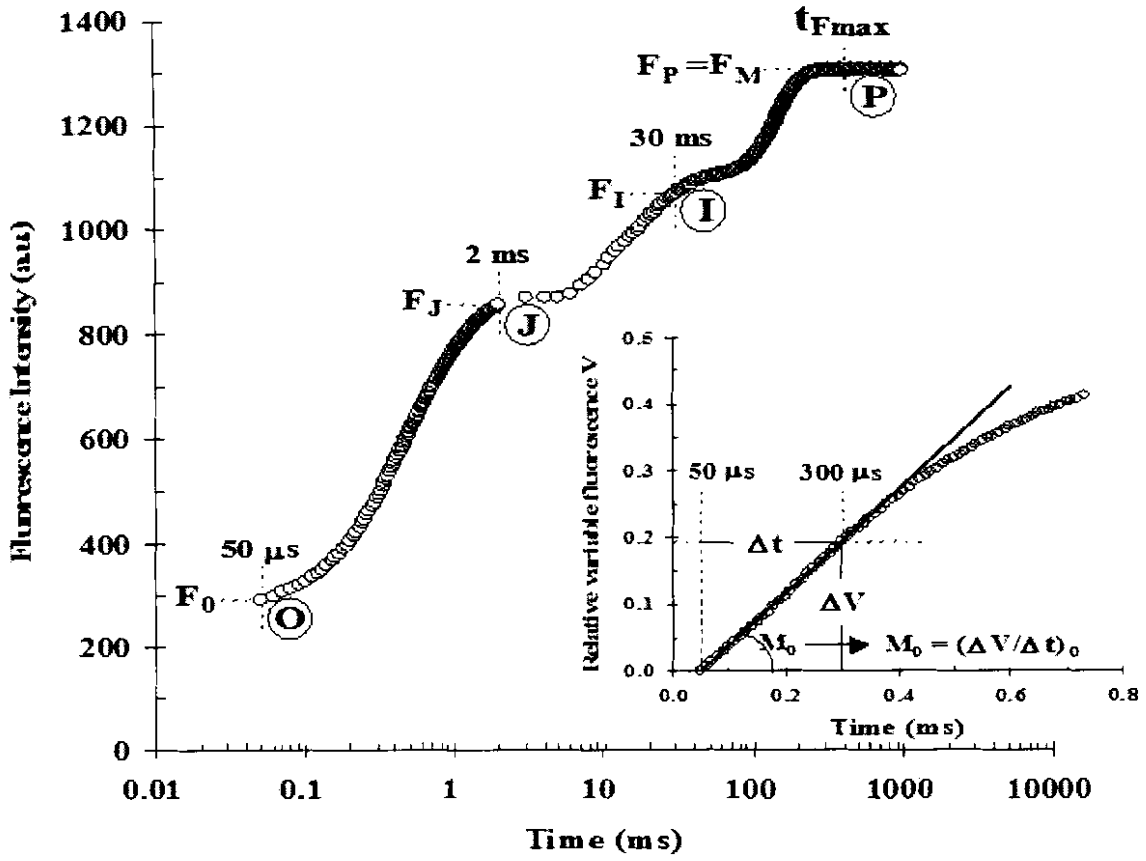

Figure 2.5: An example of a typical polyphasic chlorophyll *a* fluorescence transient OJIP emitted by higher plants representing the accumulation of reduced Q_A. The transient is plotted on a logarithmic time scale from 50 µs to 1 s. The labels refer to the fluorescence data used by the JIP-test for the calculation of various parameters quantifying PSII structure and function with the Biolyser software (Biolyser4HP version 3.06, RM Rodriquez, Bioenergetics Lab, Geneva, Switzerland). The labels are: the fluorescence intensity F_0 (at 50 µs); the fluorescence intensity F_J (at 2 ms); the fluorescence intensity F_I (at 30 ms) and the maximal fluorescence intensity $F_P = F_M$. The inserted figure shows the transient expressed as the relative variable fluorescence, $V = (F - F_0)/(F_M - F_0)$, on a linear time-scale and demonstrates how the initial slope (M_0) is calculated: $M_0 = (D_V/D_t)_0 = (V_{300\mu s})/(0.25\ ms)$. (From Tsimilli-Michael *et al.*, 2000).

2.4.2 Analysis of the chlorophyll a fluorescence transient by the JIP-test

The key expression of the JIP-test is TR_0/RC, in other words the maximal trapping flux at t = 0. This reflects the reduction of Q_A through a single turnover (re-oxidation of Q_A^- blocked by DCMU), in other words only the photochemical reactions. This can be calculated by the initial slope of the fluorescence rise:

$$(dV/dt)_{0,DCMU} = M_{0,\,DCMU}$$

In the absence of DCMU, accumulation of Q_A^- (the netto result of Q_A reduction by PSII and its reoxidation by PSI, in other words multiple turnovers of Q_A to Q_A^-) can be represented by the initial slope:

$$\mathbf{(dV/dt)_0 = M_0}$$

The RC closing rate, i.e. M_0, increases while electron transport beyond Q_A resulting in Q_A^- tends to decrease it. The net rate of closing RCs is represented in the slope:

$$\mathbf{M_0 = TR_0/RC - ET_0/RC}$$

A breakthrough was made by Strasser and Strasser (1995) when it was determined that $M_{0,DCMU}$ can be simulated by multiplying M_0 by $1/V_J$ (V_J is the relative change in fluorescence at F_J, calculated by $(F_J - F_0)/(F_M - F_0)$), thus:

$$\mathbf{M_{0,DCMU} = M_0 / V_J}$$

This implied that the maximal trapping flux could be simulated without the use of DCMU making these measurements non-destructive and creating the opportunity to fully exploit the fluorescence transient.

The following data from the original measurements are used by the JIP-test for calculation of the energy fluxes through PSII and other fluorescence parameters: maximal fluorescence intensity (F_M); fluorescence intensity at 50 µs (considered as F_0); fluorescence intensity at 300 µs ($F_{300\mu s}$) required for calculation of the initial slope (M_0) of the relative variable fluorescence (V) kinetics; and the fluorescence intensity at 2 ms (the J step) denoted as F_J (Figure 2.5).

The JIP-test represents a translation of the original fluorescence data to biophysical parameters that quantify the stepwise flow of energy through PSII at the reaction centre (RC) as well as excited cross-section (CS) level (Strasser & Strasser, 1995; Force *et al.*, 2003; Strasser *et al.*, 2004). The parameters, which all refer to time zero (onset of fluorescence induction), are: (i) the specific energy fluxes (per reaction centre) for absorption (ABS/RC), trapping (TR_o/RC), dissipation at the level of the antenna chlorophylls (DI_o/RC) and electron transport (ET_o/RC); (ii) the flux ratios or yields, i.e. the maximum quantum yield of primary photochemistry ($\varphi_{Po} = TR_o/ABS = F_V/F_M$), the efficiency ($\psi_o = ET_o/TR_o$) with which a trapped exciton can move an electron into the electron transport chain further than Q_A^-, the quantum yield of electron transport ($\varphi_{Eo} = ET_o/ABS = \varphi_{Po} \cdot \psi_o$); the quantum yield of the formation of

reduction equivalents ($\varphi_{R0} = \varphi_{E0} \bullet \delta$) (Personal communication to Krüger GHJ by Strasser RJ, 2006); (iii) the phenomenological energy fluxes (per excited cross section, CS) for absorption (ABS/CS), trapping (TR_o/CS), dissipation (DI_o/CS) and electron transport (ET_o/CS). The fraction of active PSII reaction centres per excited cross section (RC/CS) is also calculated. The formulae in Table 2.5 illustrate how each of the above-mentioned biophysical parameters can be calculated from the original fluorescence measurements.

The initial stage of photosynthetic activity of a RC complex is regulated by three functional steps namely absorption of light energy (ABS), trapping of excitation energy (TR) and conversion of excitation energy to electron transport (ET). Strasser *et al.* (2000) introduced a multi-parametric expression of these three independent steps contributing to photosynthesis, the so-called performance index (PI_{ABS}):

$$\mathbf{PI_{ABS} = RC/ABS \bullet \varphi_{P0}/(1-\varphi_{P0}) \bullet \psi_0/(1-\psi_0)}$$

This expression can be de-convoluted into three JIP-test parameters and estimated from the original fluorescence measurements as $RC/ABS = RC/TR_o \bullet TR_o/ABS = [(F_{2ms} - F_{50\mu s})/4(F_{300\mu s} - F_{50\mu s})] \bullet F_V/F_M$. The factor 4 is used to express the initial fluorescence rise per 1 ms. The expression RC/ABS shows the contribution to the PI_{ABS} due to the RC density on a chlorophyll basis. The contributions of the light reactions for primary photochemistry are estimated according to the JIP-test as $[\varphi_{P0}/(1-\varphi_{P0})] = TR_o/DI_o = k_P/k_N = F_V/F_o$. The contribution of the dark reactions are derived as $[\psi_o/(1-\psi_o)] = ET_o/(TR_o - ET_o) = (F_M - F_{2ms})/(F_{2ms} - F_{50\mu s})$. The JIP-test reveals changes in the behaviour of PSII that cannot be detected by the commonly used parameter $\varphi_{P0} = F_V/F_M$, (quantum efficiency of primary photochemistry) which is the least sensitive of all parameters (Strasser *et al.*, 2004). An additional parameter has been recently developed that gives an indication of the efficiency of the reduction of $NADP^+$ to NADPH, namely φ_{R0}, which is derived as follows $\varphi_{R0} = \varphi_{P0} \bullet \delta = \varphi_{P0} \bullet (1-F_{30ms})/(1-F_{2ms})$ (Personal communication to Krüger GHJ by Strasser RJ, 2006).

Table 2.5: Summary of the JIP-test formulae using data extracted from the chlorophyll a fluorescence transient OJIP (Modified from Strasser & Tsimilli-Michael, 2001).

Extracted and Technical Fluorescence Parameters		
F_0	=	$F_{50\mu s}$, fluorescence intensity at 50μs
$F_{100\mu s}$	=	fluorescence intensity at 100μs
$F_{300\mu s}$	=	fluorescence intensity at 300μs
F_J	=	fluorescence intensity at the J-step (at 2ms)
F_I	=	fluorescence intensity at the I-step (at 30ms)
F_M	=	maximal fluorescence intensity
t_{F_M}	=	time to reach F_M , in ms
V_J	=	relative variable fluorescence at the J-step = $(F_{2ms} - F_0) / (F_M - F_0)$
$(dV / dt)_0 = M_0$	=	fractional rate of PS II reaction centre closure = $4 . (F_{300} - F_0)/(F_M - F_0)$
Quantum Efficiencies or Flux Ratios or yields		
$\varphi_{Po} = TR_0 / ABS$	=	$[1 - (F_0 / F_M)] = F_V / F_M$
$\varphi_{Eo} = ET_0 / ABS$	=	$[1 - (F_0 / F_M)] . \Psi_0$
$\varphi_{Ro} = RE/ABS$	=	$(1-V_I)/(1-V_J) . \varphi_{Eo}$
$\Psi_0 = ET_0 / TR_0$	=	$(1 - V_J)$
Specific Fluxes or Specific Activities		
ABS / RC	=	$M_0 . (1 / V_J) . (1 / \varphi_{Po})$
TR_0 / RC	=	$M_0 . (1 / V_J)$
ET_0 / RC	=	$M_0 . (1 / V_J) . \Psi_0$
DI_0 / RC	=	$(ABS / RC) - (TR_0 / RC)$
Phenomenological Fluxes or Phenomenological Activities		
ABS / CS	=	$ABS / CS_{Chl} = Chl / CS$ or $ABS / CS_0 = F_0$ or $ABS / CS_M = F_M$
TR_0 / CS	=	$\varphi_{Po} . (ABS / CS)$
ET_0 / CS	=	$\varphi_{Po} . \Psi_0 . (ABS / CS)$
DI_0 / CS	=	$(ABS / CS) - (TR_0 / CS)$

Density of Reaction Centres		
RC / CS	=	$\varphi_{Po} . (V_J / M_0) . ABS / CS$
Performance Indexes		
PI_{ABS}	=	$(RC / ABS) . [\varphi_{Po} / (1 - \varphi_{Po})] . [\Psi_0 / (1 - \Psi_0)]$
Driving force		
DF_{ABS}	=	$\log [PI_{ABS}]$

ABS = absorption energy flux; CS = excited cross section of leaf sample; DI= dissipation energy flux at the level of the antenna chlorophylls; ET = flux of electrons from Q_A^- into the electron transport chain; φ_{Do} = quantum yield of dissipation; φ_{Eo} = probability that an absorbed photon will move an electron into electron transport further than Q_A^-; φ_{Po} = maximum quantum yield of primary photochemistry; φ_{R0} = quantum efficiency of the formation of reduction equivalents; PI_{ABS} = performance index; ψ_o = efficiency by which a trapped exciton, having triggered the reduction of Q_A to Q_A^-, can move an electron further than Q_A^- into the electron transport chain; RE = reduction equivalent ;RC = reaction centre of PSII; RC/CS = fraction of active reaction centres per excited cross section of leaf; TR = excitation energy flux trapped by a RC and utilized for the reduction of Q_A to Q_A.

2.4.3 Measurement of chlorophyll a fluorescence induction curves

Chlorophyll a fluorescence induction curves were recorded one hour before the light period in the controlled growth chamber started, i.e. on dark-adapted plants. Measurements were recorded with a Handy Plant Efficiency Analyser (Handy-PEA, Hansatech Instruments Ltd., Kingslynn, UK). Each fluorescence induction curve was induced by a homogenous red light (peak 650nm) of 2000 µmol photons.m^{-2}.s^{-1} and recorded for 1 second on a 4mm diameter area of leaf sample.

2.5 Chlorophyll Content Index (CCI) measurements

The chlorophyll content index (CCI) of leaves was measured before treatment started and then after four, eight and twelve days of treatment. This was measured with a hand-held chlorophyll content meter (CCM-200, Opti-Sciences, Inc., USA), which recorded the chlorophyll content index (CCI) for each leaf. Although only an index value is measured, studies in our lab have verified that a direct correlation exists between the chlorophyll content index values and the actual chlorophyll concentration in leaves (r^2 = 0.9684), with a CCI of 5 to 35 corresponding to a chlorophyll content of 2 to 14.5 µg.ml^{-1} (Strauss *et al.*, 2007).

2.6 Measurement of plant development

The vegetative development of *Phaseolus vulgaris* plants prior to NaTFA treatment was quantified by daily measurements of the plastochronindex (Erickson & Michelini, 1957). All trifoliate leaves with central leaflets exceeding a reference length of 25 mm (L_{ref}) were counted. The length of the youngest central leaflet longer than or equal to 25 mm, as well as the length of the central leaflet (shorter than 25 mm) on the next trifoliate leaf was measured. The plastochronindex of each plant was calculated using the following formula:

$$\textbf{Plastochronindex} = n + (\log L_n - \log L_{ref})/(\log L_n - \log L_{n+1})$$

where n = number of trifoliate leaves with central leaflets longer than the reference length of 25 mm (L_{ref}), L_n = length of the central leaflet on trifoliate leaf L_n (which by definition is longer than or equal to L_{ref}) and L_{n+1} = length of the central leaflet on trifoliate leaf L_{n+1} (which by definition is shorter than L_{ref}).

Similar measurements on *Zea mays* were not possible since its growth form (monocotyledonous) does not lend itself to this technique.

Figure 2.6: Measurement of plant growth by means of the plastochronindex on *P. vulgaris* plants.

2.7 Biomass determination

Thirteen days after treatments started plants were harvested. The shoots and roots were separated and dried at 60°C for 48h. The dried shoots and roots were then weighed and the root to shoot ratios calculated. These measurements were only done on the plants cultivated and exposed to NaTFA in the water culture system.

2.8 Determination of Rubisco activity

Leaf discs (3.14 cm^2) were sampled with a freeze clamp at the temperature of liquid nitrogen, at the end of the NaTFA treatment period. Sampling occurred 4 hours after the light period started. Special care was taken not to shade the portion of the leaf from which the sample was taken, since it would have caused deactivation of Rubisco. The collected leaf discs were stored at – 84°C.

The method of Keys and Parry (1990) was used to assay Rubisco activity. Each leaf disc was ground in liquid nitrogen, insoluble polyvinylpolypyrrollidone (PVPP) and proteinase inhibition cocktail (Sigma proteinase inhibition cocktail for plant extractions; containing 4-(2-aminoethyl) benzenesulfonyl fluoride, bestatin, pepstatinA, E-64, leupeptin and 1,10-phenanthroline), and then rapidly extracted with extraction buffer (pH 8.0) containing 100mM Bicine-NaOH, 20 mM $MgCl_2$ and 50 mM β-mercaptoethanol to form a crude extract. The crude extract was transferred to a pre-cooled micro centrifuge tube and centrifuged at 10000 x g and 4°C for 1min. Of the clarified supernatant 25 µl was then added to a glass scintillation vial containing assay buffer (pH 8.2 and the same composition as the abovementioned buffer but without β-mercaptoethanol), and substrate (RuBP and $NaH^{14}CO_2$). The enzyme reaction was stopped after 1 min with 200 µl formic acid (10 mM). This was done to determine initial activity (enzyme activity at the time of sampling). For total activity (activity after incubation in bicarbonate) the same clarified supernatant was used but substrate (RuBP) was added after a 3 min incubation period. All the acidified samples were dried in an oven. Water (4 ml) and 3.5 ml scintillation cocktail (Packard Ultima Gold) were then added. The incorporation of ^{14}C into 3-phosphoglycerate was determined by liquid scintillation spectrometry using a liquid scintillation analyser (Beckman, LS 6000TA). The soluble protein content of the original supernatants was determined according to the method of Bradford (1976).

2.9 *In vitro* photosynthetic electron transport

Thylakoid membranes were isolated according to the method of Mills and Joy (1980) from *Phaseolus vulgaris* plants, grown under controlled conditions. The chlorophyll a and b

concentrations of the membrane suspension was measured according to the method of Arnon *et al.* (1958) and were used as an approximation of thylakoid membrane concentration. Before measurements took place the light intensity and temperature in the oxygen electrode cuvette were measured by a combined light meter and thermometer (Quantitherm, Hansatech Instruments Ltd., Kingslynn, UK) and adjusted to a light intensity of 3000 µmol photons.$m^{-2}.s^{-1}$ and a temperature of 20°C respectively. Buffer solution (pH 7.6, 200 mM Tricine, 3 mM $MgCl_2$, 20 mM NaCl), artificial electron acceptor and thylakoid membranes were added to the cuvette to give a final chlorophyll concentration of 0.1 $mg.l^{-1}$ and a final volume of 1,5 ml. In this experiment potassium hexacyanoferrate (FeCy) was used as an electron acceptor and electron transport was measured in the system: $H_2O \rightarrow PSII \rightarrow PQ \rightarrow FeCy$ (further electron transport blocked by DBMIB) (Figure 2.7). The oxygen evolution rate was measured, using an oxygen electrode system (Oxygraph, Hansatech, Kingslynn, UK), after an incubation period of 1 min. The light source was then switched on and oxygen evolution measured for 1min after which NaTFA or NaTCA was added. The oxygen evolution rate was then measured for 1 min after this addition. As a control, only buffer solution was added instead of NaTFA or NaTCA. The site of inhibition was also determined using a range of artificial electron acceptors and donors. Since the literature suggested that one of the likely sites of photosynthetic electron transport inhibition by halogenated acetates may well be located between Q_A and Q_B (Govindjee *et al.*, 1997), 12-molybdosilicic acid hydrate (SiMo) was used to test this hypothesis. SiMo changes the polarity of the thylakoid membrane and consequently opens up the stacked regions of the thylakoid where PSII is located, thus making it possible for FeCy to receive an electron directly from Q_A (Trebst, 1999). If trifluoroacetate or trichloroacetate did inhibit photosynthetic electron transport between Q_A and Q_B the addition of SiMo would thus alleviate it.

2.10 Transmission Electron Microscope preparation (TEM)

To study the effect of NaTFA on cellular structures of *Z. mays*, small (2 mm^2) samples of leaf and root material were harvested at the end of the water culture experiment (after 13 days). These samples was then fixated in Todd's fixation solution for 8 hours and then washed in cacolidate buffer and post-fixated by osmiumtetraoxide. After pre-casting with 2% uranyl acetate for 30 min and dehydration in a series of acetone solutions, the material was infiltrated with resin (Spurr, 1969). Ultra thin sections were prepared with a Reichert Ultracut E microtome and contrasted with uranyl acetate and lead citrate (Reynolds, 1963) and then investigated with a Philips CM 10 transmission electron microscope.

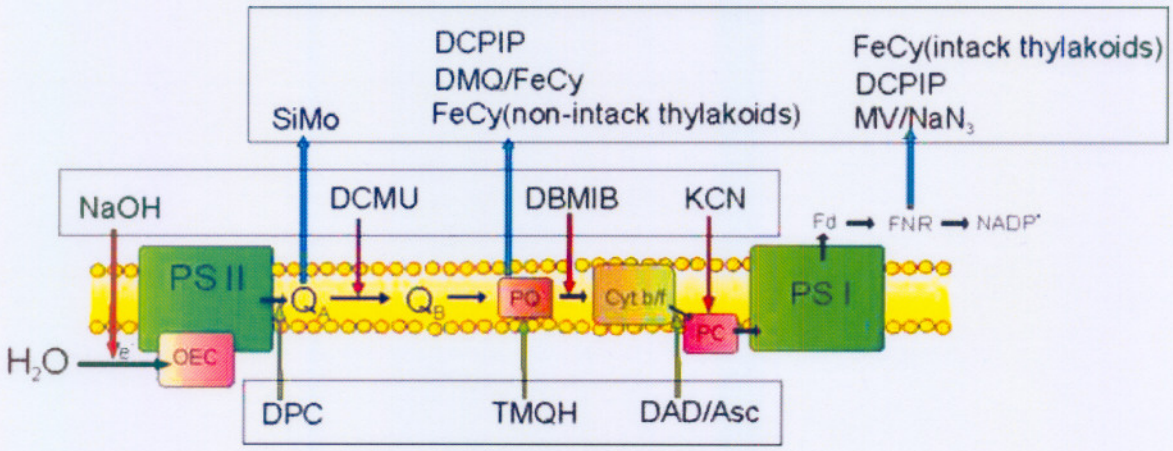

Figure 2.7: Schematic representation of the photosynthetic electron transport chain showing artificial electron acceptors (blue arrows), inhibitors (red arrows) and artificial electron donors (green arrows). Protein complexes are also shown namely: photosystem II (PS II), oxygen-evolving complex (OEC), photosystem I (PS I), cytochrome b/f complex (Cyt b/f), plastocyanin (PC), plastoquinone (PQ). Q_A refers a bound quinone located on the D2 protein of PS II and Q_B refers to a bound quinone on the D1 protein of PS II were plastoquinone (PQ) binds. Synthetic electron acceptors shown are 12-molybdosilicic acid hydrate (SiMo), potassium hexacyanoferrate (FeCy), 2,6-dichlorophenol indophenol (DCPIP), 2,5-dimethylbenzoquinone and potassium hexacyanoferrate (DMQ/FeCy), methylviologen and sodiumazide (MV/NaN_3). Inhibitors shown are sodium hydroxide (NaOH), 3-(3,4-dichlorophenyl)-1,1-dimethylurea (DCMU), 2,5-dibromo-6-isopropyl-3-methyl-1,4-benzoquinone (DBMIB), potassiumcyanide (KCN). Synthetic electron donors shown are Diphenylcarbazide (DPC), trimethyl-p-benzoquinone (TMQH), 2,3,5,6-tetramethyl-p-phenylenediamine and ascorbate (DAD/Asc).

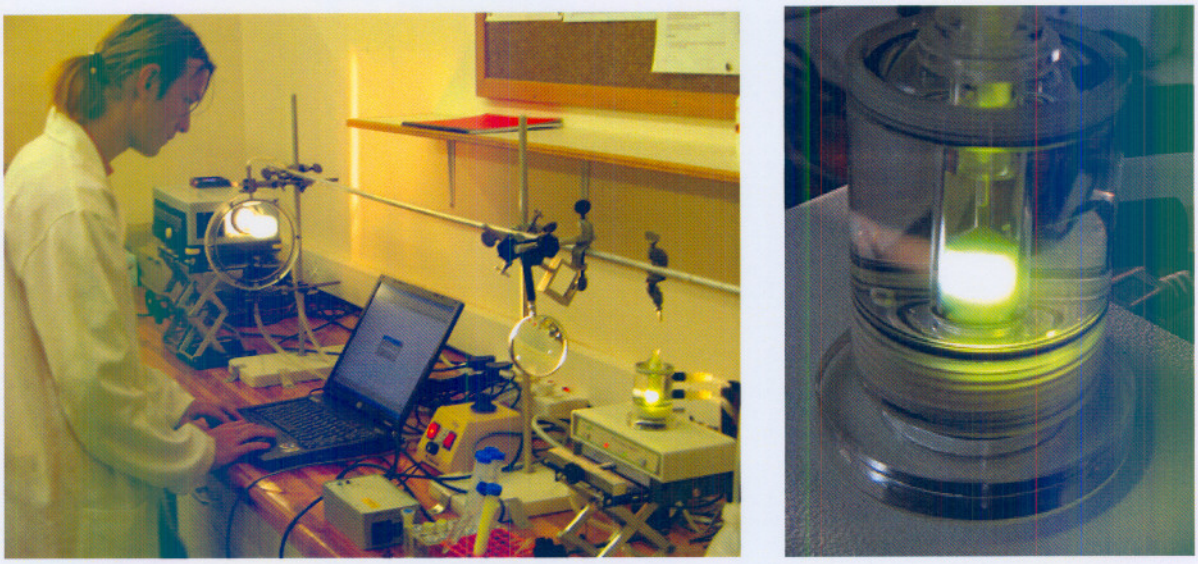

Figure 2.8: Measuring the oxygen evolving rate of isolated thylakoid membranes by means of an oxygraph system (left). The cuvette containing the isolated thylakoid membranes (right) was kept at 20°C and was illuminated by a focussed external light source illuminating the thylakoid suspension in the cuvette at a photon flux density of 3000 µmol photons.m^{-2}.s^{-1}.

2.11 Investigation of short-term hormonal effects and symptoms of NaTFA and NaTCA on excised radish cotyledons

The observed growth responses of the experimental plants upon trifluoroacetate treatment motivated a general investigation of the possible auxin effect of TFA, or possible effects it may have on auxin levels or even cell division rate. These effects were investigated using a simple bioassay system (Letham, 1971). Radish cotyledons were used for this bioassay just as in the original experiment by Letham (1971) since it lends itself to this technique. Since cytokinin levels were saturated by kinetin, any increase in auxin levels would cause an increase in cotyledon expansion and subsequent weight. Radish seedlings were grown in darkness for 3 days, where after their lower cotyledons were excised. Petri dishes were prepared containing a disc of filter paper wetted with 0.5 ml of a 5 µg.ml^{-1} kinetin solution and 0.5 ml of a given NaTFA or NaTCA concentration. The NaTFA and NaTCA concentrations used were 0.1563, 0.625, 2.5, 10, 40, 160 mg.l^{-1}. The Control petri dishes received 0.5 ml distilled water. Ten cotyledons were first weighed and then placed on the filter paper in each prepared petri dishes with their adaxial sides down. The petri dishes were then sealed in transparent containers and incubated for four days in a growth chamber (Conviron PGW 36, Controlled Environment Ltd, Winnipeg, Canada) at a light intensity of 500 µmol photons.m^{-2}.s^{-1}. Cotyledons were subjected to a 15-hour light period and 9-hour dark period. A temperature of 26°C was maintained during the light period and 20°C during the dark period.

After the incubation period the cotyledons were reweighed and the percentage mass increase calculated.

2.12 Statistical analysis

Statistical analysis was conducted with the software package Statistica for Windows version 6 (StatSoft, Inc, USA). In data sets with parametric distribution, significant differences between treatment means were determined using Student's t-test.

Chapter 3

Results and discussion

3.1 Growth

3.1.1 Visual appearance of NaTFA treated plants

Both *P. vulgaris* and *Z. mays* displayed visual symptoms after trifluoroacetate treatment, in particular at higher concentrations (40-160 mg NaTFA.l^{-1}). The severity of the symptoms with regard to plants treated in the sterilised sand compared plants treated in the water culture system however differed. These differences may be attributed to the fact that the sterilised sand experimental plants were only exposed to trifluoroacetate for 3 days compared to 13 days of exposure in the water culture experiment. The expression of symptoms also differed between *P. vulgaris* and *Z. mays*.

3.1.1.1 Sand culture

For *P. vulgaris* treated in sterilised sand, the two lowest NaTFA concentrations, namely 0.05 and 0.2 g.m^{-2}, appeared conspicuously taller and more robust compared to the control plants and higher treatments. Plants treated with the highest NaTFA concentration, namely 12.8 g.m^{-2} were visibly smaller and also displayed signs of epinasty (curling of leaves to the abaxial side) on the young leaves (Figure 3.1). Due to this curling or epinasty the younger leaves also appeared smaller compared to the control plants's leaves. The latter observation corresponded to the reduction in soybean leaf size upon spraying plants with 10 ml of a 100 mg TFA.l^{-1} (Davison & Pearson, 1997). For NaTFA treated *Z. mays* plants no apparent symptoms were visible for any of the treatments after the 3 day treatment period in sterilised sand.

3.1.1.2 Water culture

Both *P. vulgaris* and *Z. mays* plants treated with NaTFA in the water culture system displayed marked visible symptoms. *P. vulgaris* plants cultivated at a low NaTFA concentration of 0.625 mg.l^{-1} were taller and seemed more vigorous (Figure 3.2). This increase in plant height seemed to have been caused by longer internodes which may be attributed to increased auxin levels, since similar increases in auxin levels have been shown to be caused by trichloroacetate (Mashtakov *et al.*, 1967). All higher NaTFA treated plants, from 2.5 to 160 mg NaTFA.l^{-1}, were visibly smaller and adopted a more stocky growth (Figure

3.4). The stocky growth seemed to be caused by a stimulation of axillary bud development, possibly due to reduction of free auxin levels as was reported in studies done on trichloroacetate (Parshakova & Mashtakov, 1967). These above mentioned observations of reduction in plant growth also correlated with the biomass data (Section 3.1.2).

After 3 days of treatment with 40 and 160 mg NaTFA.l^{-1}, epinasty of young leaves of *P. vulgaris* appeared. Thompson *et al.* (1994) reported higher trifluoroacetate levels in the tips of the leaves of plants treated with trifluoroacetate and Davison and Pearson (1997) suggested that the curving of the leaves may be due to a higher inhibition of growth at the edges of the leaves. *P. vulgaris* plants treated with the two highest NaTFA concentrations of 40 and 160 mg NaTFA.l^{-1} also displayed necrotic lesions on the young leaves (Figure 3.3) after 8 days of treatment. This phenomenon once again corroborated the similarity of toxicity symptoms to trichloroacetate (Mayer, 1957; Hance & Holly, 1963; Ashton & Crafts, 1973). These appeared as necrotic spots on the young leaves and appeared first after 8 and 10 days for the 160 and the 40 mg NaTFA.l^{-1} treatments respectively. At the end of the experiment after 13 days these leaves were completely misformed and new leaves also displayed severe inhibition in leaf expansion (Figure 3.3) (Davison & Pearson, 1997). Young leaves of *P. vulgaris* plants treated with the two higher concentrations appeared to be thicker and shinier possibly due to differences of the wax excretions of the cuticle and the leaves seemed to be more susceptible to breakage (Dewey *et al.*, 1956). Older leaves on which measurements were taken displayed no visible symptoms (Figure 3.4).

All NaTFA treated *Z. mays* plants cultivated in water culture displayed signs of increasing chlorosis and reduction in plant height with increasing NaTFA concentration (Figure 3.5). The apparent reduction in chlorophyll content was also confirmed by actual chlorophyll content index measurements (Section 3.1.4). The reduction in plant height due to shorter internodes correlated with similar symptoms caused by Dalapon, as reported by Funderburk and Davis (1960). Similar to *P. vulgaris*, *Z. mays* also displayed visual injury symptoms. After 5 days necrotic spots and apparent thickening of the younger leaves appeared only on the 40 and 160 mg NaTFA.l^{-1} treated plants (Figure 3.6). The leaves of the 160 mg NaTFA.l^{-1} treatment as well as new leaves of these plants started displaying severe curling and wrinkling after 7 days of treatment, suggesting a developmental effect at the shoot apex (Ashton & Crafts, 1973). At the 40 mg NaTFA.l^{-1} and lower treatments these symptoms did not appear, suggesting that the appearance of necrotic spots and wrinkling is not directly connected.

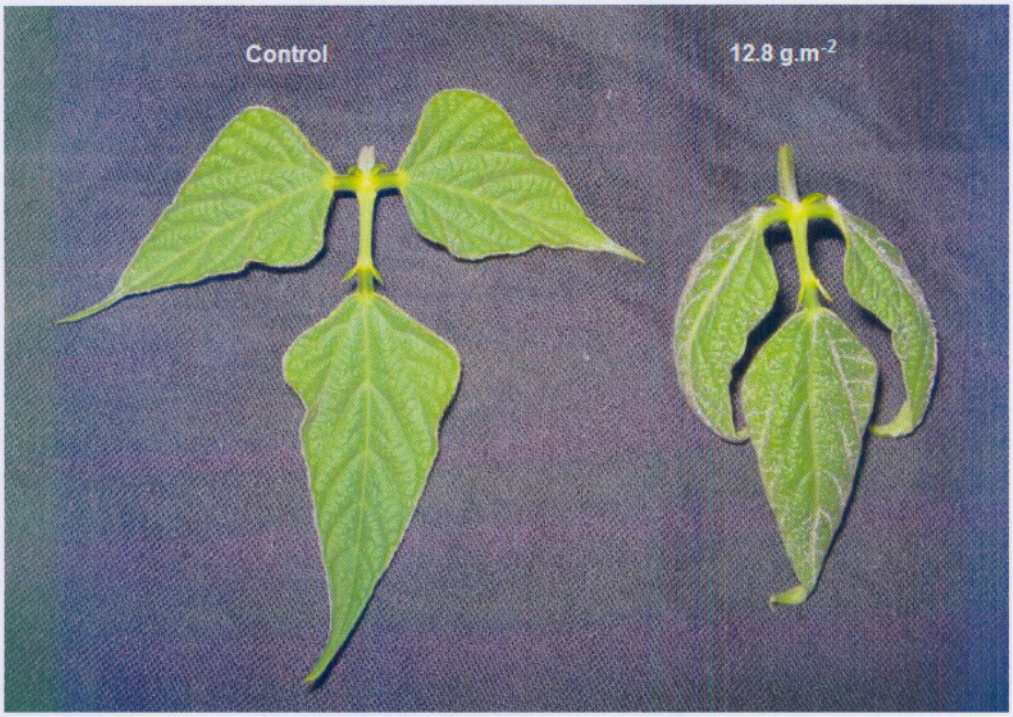

Figure 3.1: Young leaves of *P. vulgaris* plants, grown in sterilised sand, 3 days after treatment with NaTFA. A leaf of a 12.8 g NaTFA.m^{-2} treated plant (right) displaying signs of epinasty compared to the leaf of a control plant (left).

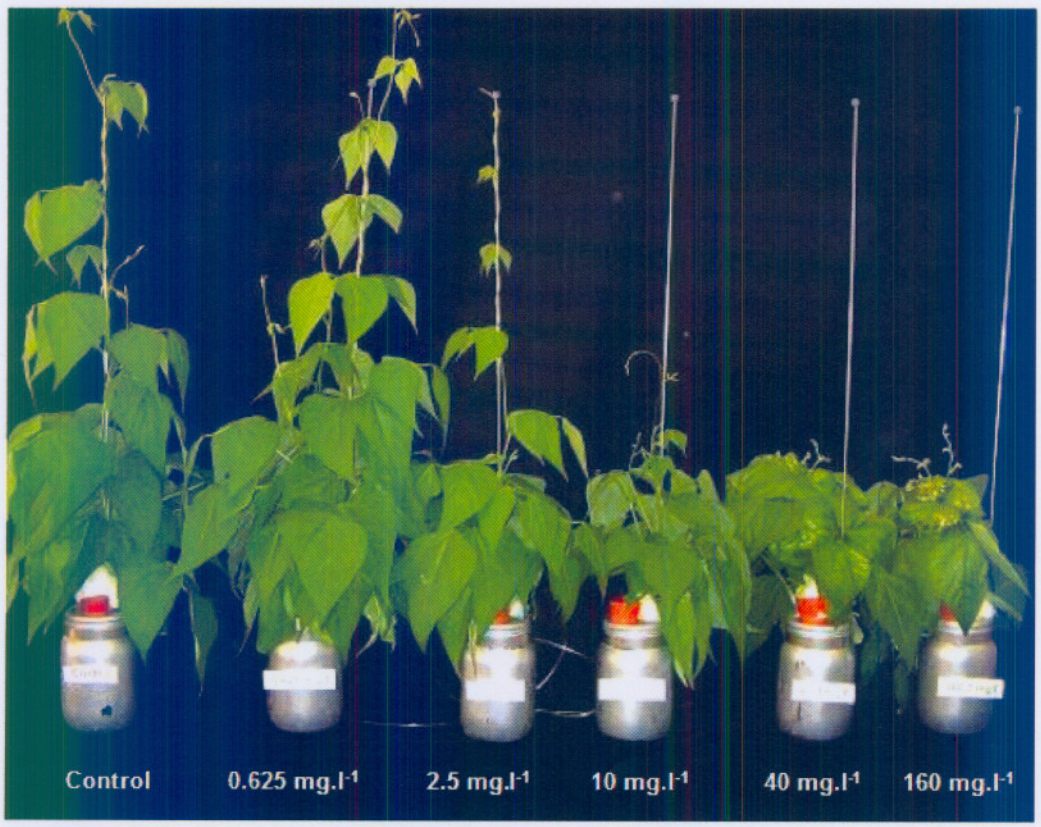

Figure 3.2: *P. vulgaris* cultivated in water culture after treatment with different NaTFA concentrations for a 13 day period.

Figure 3.3: Necrotic spots appearing on leaves of *P. vulgaris* treated with 160 mg NaTFA.l^{-1} after 8 days (left). The same leaves 13 days after treatment started (center). New leaf displaying inhibition (160 mg NaTFA.l^{-1}) of leaf expansion after 13 days of treatment (right).

Figure 3.4: *P. vulgaris* plants treated with 160 mg NaTFA.l^{-1} after 13 days of treatment. Axillary shoot development seemed to be stimulated by NaTFA (left). Only younger leaves displayed signs of epinasty, necrosis and apparent leaf thickening (right).

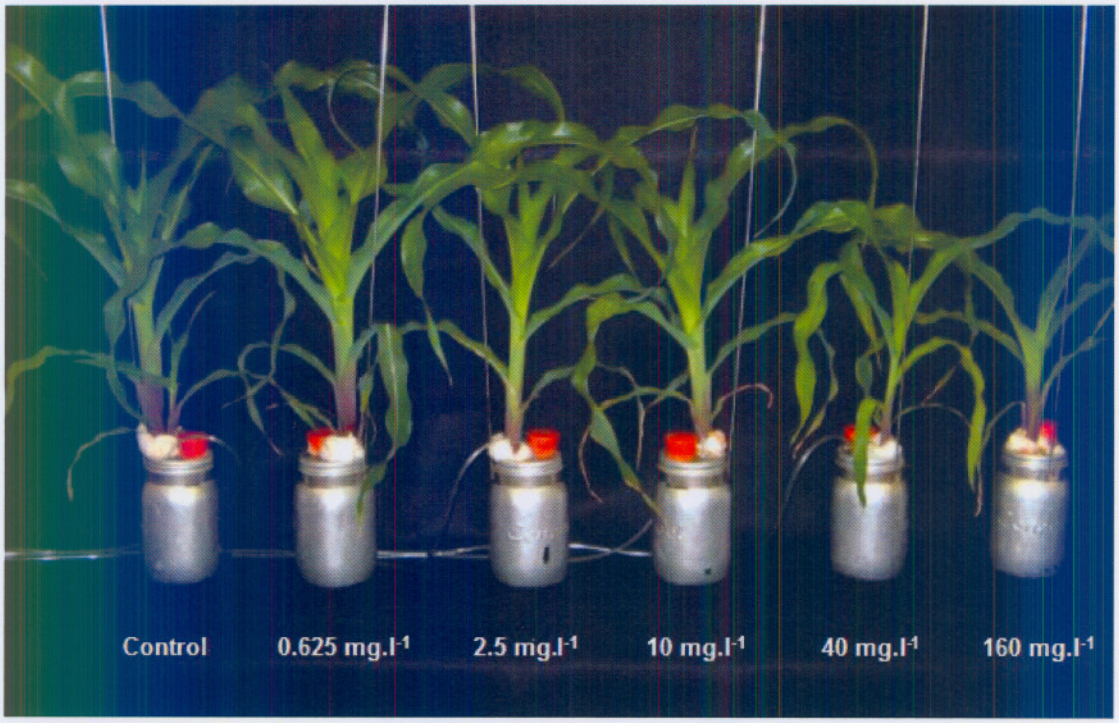

Figure 3.5: *Z. mays* cultivated in water culture after treatment with different concentrations of NaTFA for a 13 day period.

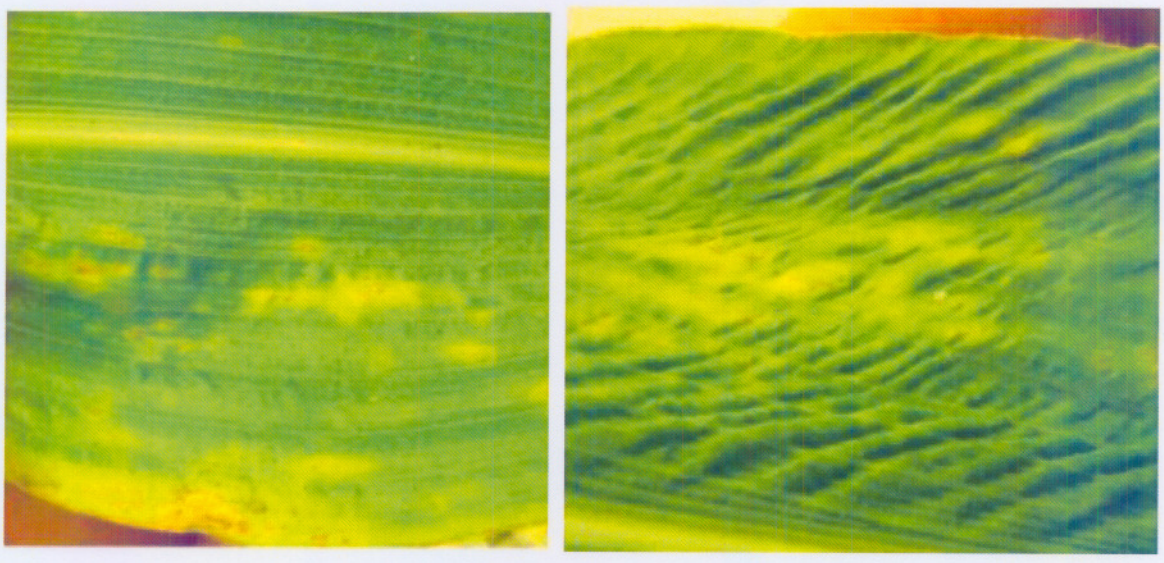

Figure 3.6: Necrotic spots appearing on leaves of *Z. mays* treated with 160 mg NaTFA.l^{-1} after 5 days (left). The same leaf closer to the leaf base started displaying severe wrinkling of leaves 13 days after treatment (right).

3.1.2 Effect of trifluoroacetate on biomass production

The biomass production of both *P. vulgaris* and *Z. mays* was markedly affected by trifluoroacetate, although no statistically significant changes where observed for *P.vulgaris*. NaTFA treated *P. vulgaris* plants displayed a statistically nonsignificant gain of 13% and 5% in shoot biomass for the lowest concentrations of 0.625 and 2.5 $mg.l^{-1}$ (Figure 3.7). The higher NaTFA treatment displayed a decreasing trend of 26%, 23% and 35% at the 10, 40 and 160 $mg.l^{-1}$ treatments. The root mass of *P. vulgaris* displayed a statistically nonsignificant decrease of 26%, 30%, 14% and 28% for the 2.5 to the 160 mg $NaTFA.l^{-1}$ treatments respectively. These effects on the root and shoot masses led to a 36% stimulation in the shoot to root ratio at 2.5 $mg.l^{-1}$, although once again this was not statistically significant (Figure 3.8). It thus seems as though root inhibition appears before shoot inhibition in *P. vulgaris*.

For *Z. mays* the trend with respect to losses in shoot and root biomass was similar to that of *P. vulgaris*. At the low NaTFA concentrations of 0.625 and 2.5 $mg.l^{-1}$ the shoot mass was unaffected. Statistically significant reductions in shoot mass of 39% ($p<0.05$), 65% ($p<0.05$) and 76% ($p<0.01$) occurred at 10, 40 and 160 mg $NaTFA.l^{-1}$ respectively (Figure 3.7). Root mass decreased severely with increasing NaTFA concentrations with reductions of 30% and 38% (stastically nonsignificant) at concentrations of 0.625 and 2.5 $mg.l^{-1}$. Significant reductions in root mass of 70% ($p<0.05$), 66% ($p<0.05$) and 80% ($p<0.01$) were observed at the 10, 40 and 160 mg $NaTFA.l^{-1}$ treatments. These changes in the root and shoot mass of *Z. mays* resulted in increased shoot to root ratios of 50%, 61% ($p<0.05$) and 94% ($p<0.05$) at NaTFA concentrations of 0.625, 2.5 and 10 $mg.l^{-1}$ (Figure 3.8). As in the case of *P. vulgaris*, a loss in root mass occurred before the reduction of shoot mass. Trifluoroacetate thus induces severe root inhibition especially in the case of *Z. mays*. This phenomenon also corresponds with data showing that inhibition of root elongation by Dalapon occurred due to interference with the meristematic activity at the root tip (Prasad & Blackman, 1964). The reduction in root mass also induced a severe strain on nutrient uptake in the case of *Z. mays* (See section 3.1.4 and 3.1.6).

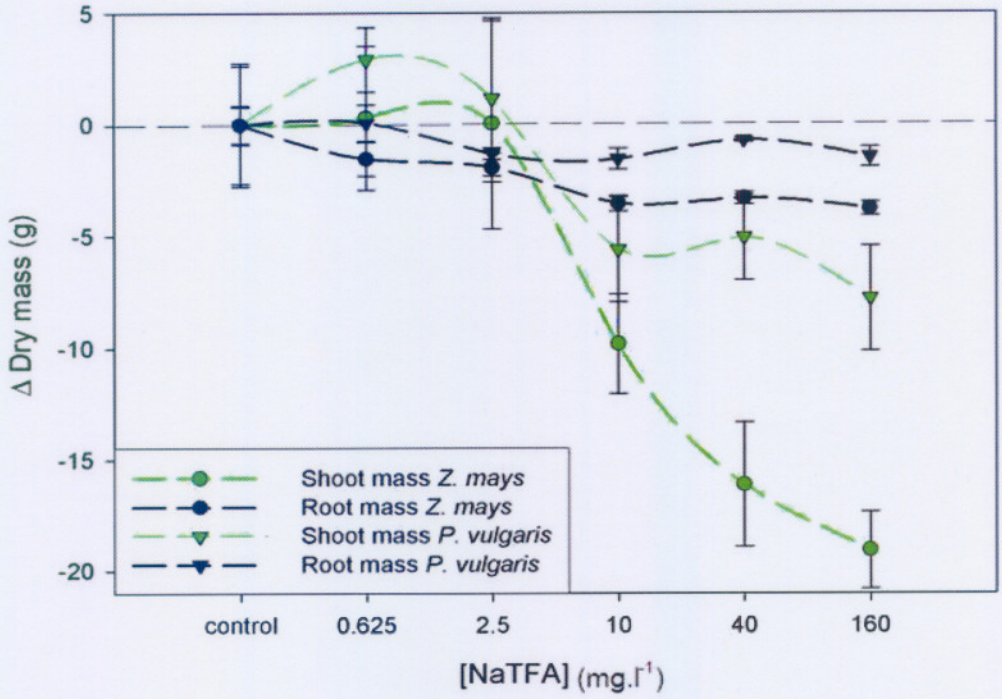

Figure 3.7: The effect of NaTFA on root and shoot mass of both *P. vulgaris* and *Z. mays* plants relative to the control plants after 13 days of exposure to range of increasing NaTFA concentrations in water culture. Each point represents the average of four replicates.

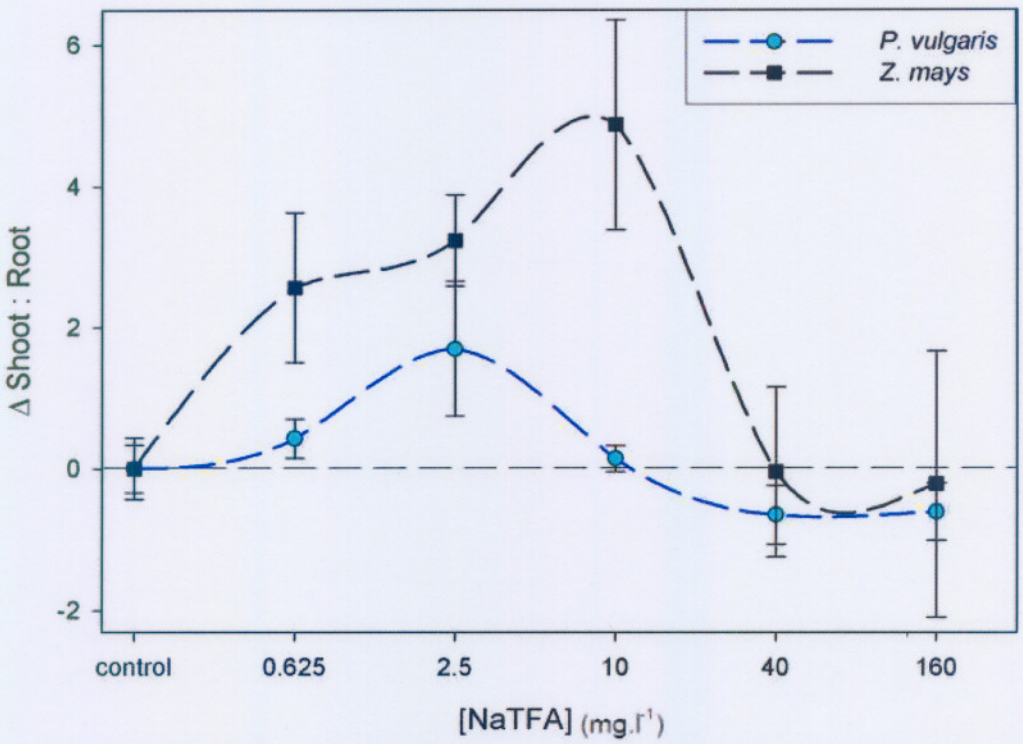

Figure 3.8: The effect of NaTFA on shoot to root ratios of *P. vulgaris* and *Z. mays* plants relative to the control plants after 13 days of exposure to range of increasing NaTFA concentrations in water culture. Each point represents the average of four replicates.

3.1.3 Effect of trifluoroacetate on growth rate of *P. vulgaris*

Over the 13 day experiment, trifluoroacetate applied with increasing concentration, had a marked effect on plant growth as measured by the change in plastochronindex of *P. vulgaris* cultivated in water culture. For the 2 days before and during the first 6 days after treatment no statistically significant differences were observed in growth rate at all concentrations used, although a slight stimulation was observed at 0.625 mg NaTFA.l^{-1} (12%) and decreases in growth at the 2.5 (8%), 10 (13%), 40 (4%) and 160 mg NaTFA.l^{-1} (13%) treatments (Table 3.1). From day 7 to 14 all treatments displayed reduced growth rates for the treatments ranging from 0.625 to the 160 mg NaTFA.l^{-1}. The growth rate reductions were 13%, 12%, 48% ($p<0.01$), 48% ($p<0.01$) and 76% ($p<0.01$), although the reductions at the 0.625 and the 2.5 mg NaTFA.l^{-1} treatments were not statistically significant. At the end of the treatment period there were significant differences in the final plastochronindex values with decreases of 11% ($p<0.05$), 30% ($p<0.01$), 27% ($p<0.01$) and 38% ($p<0.01$) for the NaTFA concentration of 2.5, 10, 40 and 160 mg.l^{-1} respectively (Figure 3.9).

Although the maize plants also displayed an apparent reduction in plant high and growth rate during the treatment it was not possible to measure plastochronindex on these plants due to their monocotyledonous growth form.

Table 3.1: Growth rates (change in Plastochronindex per day) of *P. vulgaris* cultivated in water culture during the test period, with * and ** indicating significant differences ($p<0.05$ and $p<0.01$ respectively) compared to untreated plants. Each value represents the average of four replicates.

	Control	0.625 mg NaTFA.l^{-1}	2.5 mg NaTFA.l^{-1}	10 mg NaTFA.l^{-1}	40 mg NaTFA.l^{-1}	160 mg NaTFA.l^{-1}
(ΔPI per day) Day -1 to 6	0.427±0.032	0.481±0.036	0.394±0.047	0.371±0.025	0.411±0.035	0.371±0.059
(ΔPI per day) Day 7 to 14	0.845±0.078	0.732±0.011	0.744±0.062	0.439±0.027**	0.437±0.049**	0.205±0.011**

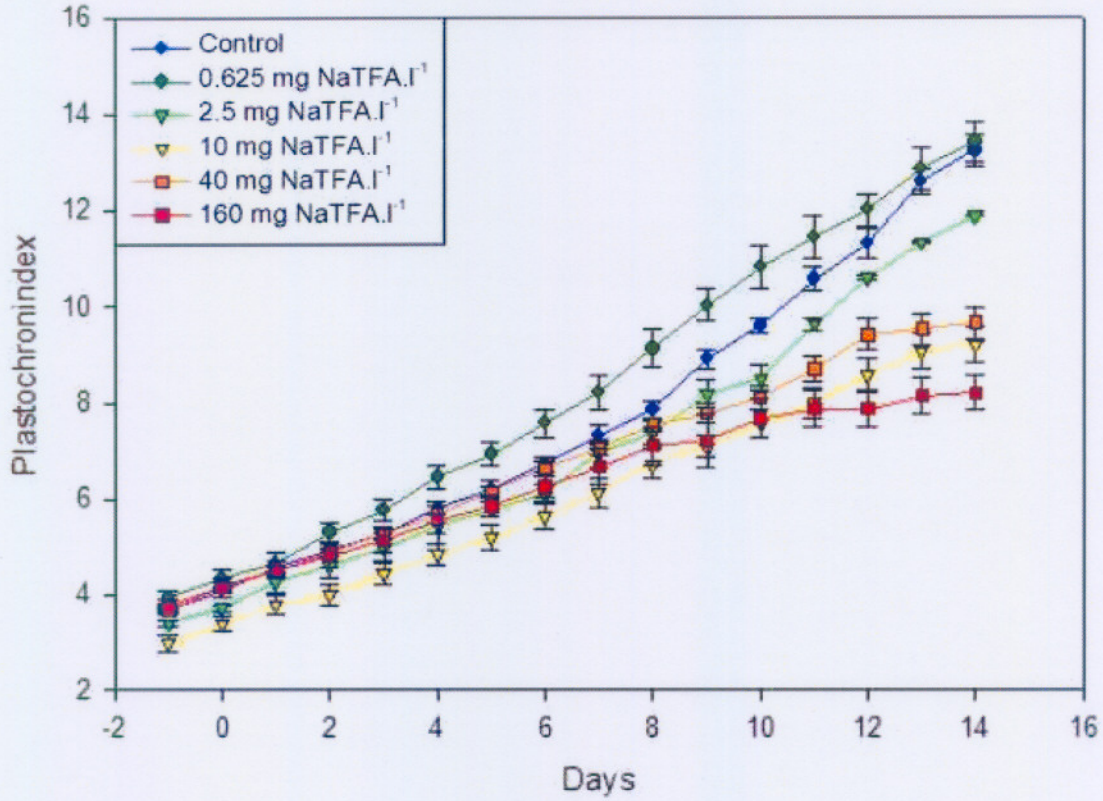

Figure 3.9: Change in Plastochronindex for *P. vulgaris*, treated with different NaTFA concentrations, before and during the test period in water culture. Each point represents the average of four replicates.

3.1.4 Effect of trifluoroacetate on chlorophyll content

For *P. vulgaris*, cultivated in water culture, trifluoroacetate had little effect on the chlorophyll content index (CCI), except for a slight increase occurring on day 4 at the 2.5, 10 and 40 mg.l^{-1} treatments namely 12% ($p<0.05$), 10% ($p<0.05$) and 14% ($p<0.01$) respectively. On day 8 the 2.5 mg.l^{-1} also displayed an increase of 10% ($p<0.05$) (Figure 3.10). All plants displayed reductions in chlorophyll content index on day 12 when compared to their relative values on day 8. These reductions may be attributed to leaf ageing.

For *Z. mays*, cultivated in water culture, the effect of trifluoroacetate on chlorophyll content was severe (Figure 3.11). On day 4 of treatment the 10, 40 and 160 mg NaTFA.l^{-1} treatments already displayed a marked reduction of 33% ($p<0.05$), 37% ($p<0.01$) and 30% ($p<0.05$) respectively in the chlorophyll content index value. After 8 days the 0.625 to the 160 mg NaTFA.l^{-1} treatments displayed respective reductions in the chlorophyll content index of 29% ($p<0.01$), 32% ($p<0.05$), 72% ($p<0.01$), 74% ($p<0.01$) and 69% ($p<0.01$) respectively. After 12 days of treatment severe reductions were still apparent in all treatments: 17% ($p<0.05$), 34% ($p<0.01$), 62% ($p<0.01$), 68% ($p<0.01$), 70% ($p<0.01$) for the respective treatments from 0.625 to 160 mg NaTFA.l^{-1}.

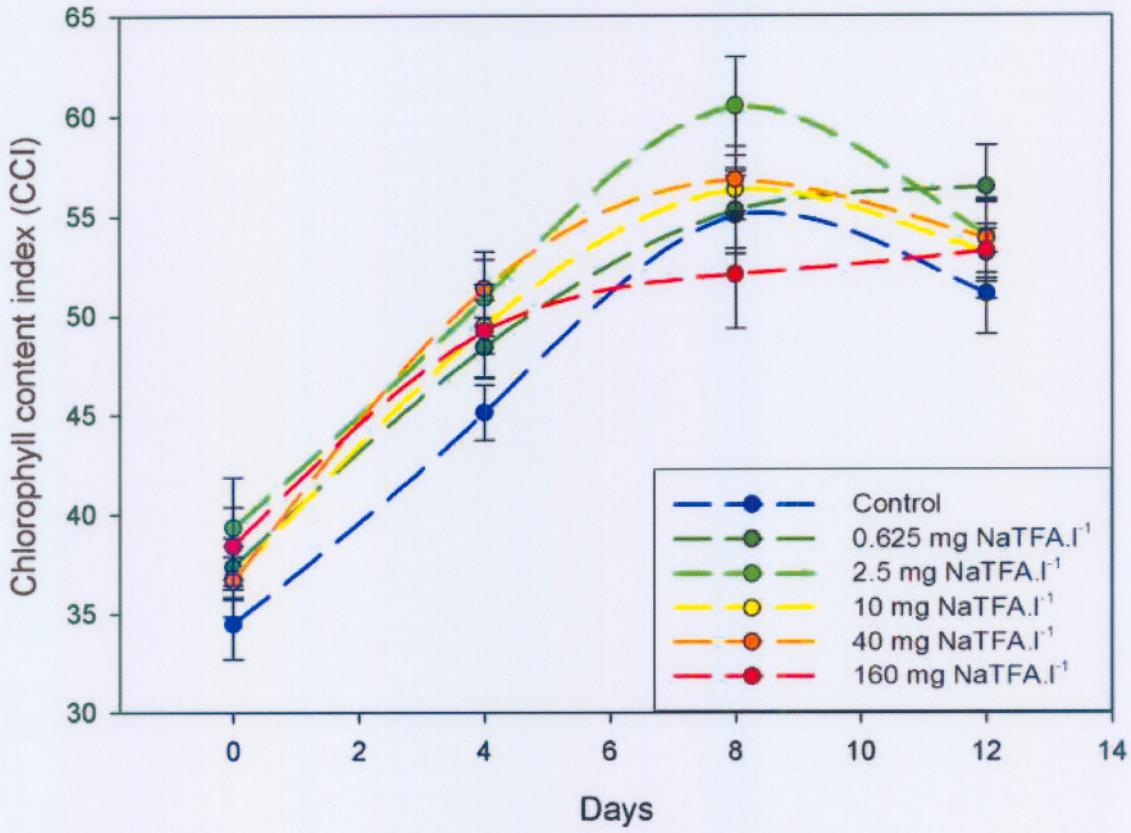

Figure 3.10: Chlorophyll content index (CCI) for *P. vulgaris* treated with a range NaTFA concentrations over 12 days in water culture. Each point represents the average of four replicates. CCI of 5 to 35 corresponds to a chlorophyll content of 2 to 14.5 $\mu g.ml^{-1}$.

These severe reductions in the chlorophyll content index, in the case of *Z. mays*, were probably caused by severe nutrient deficiencies resulting from inhibition of root growth by trifluoroacetate (Section 3.1.2), severely straining nutrient uptake. This observation (of chlorosis) also corresponded to reports by numerous authors in various studies on the phytotoxic effects of TCA and Dalapon (Mayer, 1957; Hance & Holly, 1963; Ashton & Crafts, 1973; Weissflog *et al.*, 2001)

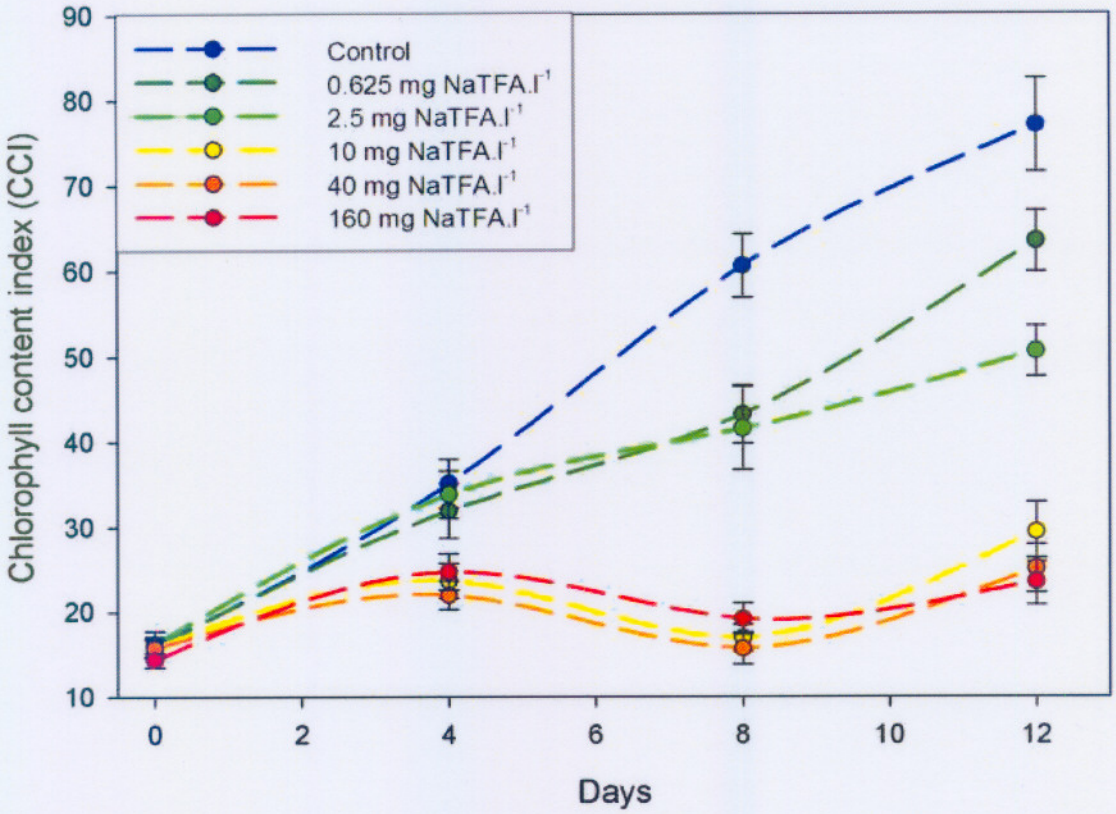

Figure 3.11: Chlorophyll content index (CCI) for *Z. mays* treated with a range NaTFA concentrations over 12 days in water culture. Each point represents the average of four replicates. CCI of 5 to 35 corresponds to a chlorophyll content of 2 to 14.5 $\mu g.ml^{-1}$.

3.1.5 Short term hormonal effects of NaTFA and NaTCA on excised radish cotyledons

Although both NaTFA and NaTCA treated cotyledons displayed symptoms of chlorosis at high concentrations (40 and 160 $mg.l^{-1}$) the NaTCA treatments displayed more severe chlorosis, indicating the greater phytotoxicity of NaTCA (Figure 3.12). These observations however still need to be confirmed by chlorophyll content analysis.

Although there were changes in mass of the cotyledons these were mostly statistically nonsignificant. Both NaTFA and NaTCA had a effect on the % mass increase. At the low NaTCA concentrations of 0.156 and 0.625 $mg.l^{-1}$ the mass increase of the cotyledons were 44% and 156% ($p<0.05$). At the 2.5 to the 160 mg $NaTCA.l^{-1}$ treatments a mass decrease occurred, showing a reduction of 55% (not significant) at the 160 $mg.l^{-1}$ treatment (Figure 3.13). For all NaTFA treatments used, an increase in mass occurred reaching a maximum at the 10 $mg.l^{-1}$ treatment of 98% (not significant). The initial increase in % mass increase may be attributed to an increase in the auxin levels and the decrease in the case of the 160 mg $NaTCA.l^{-1}$ treatment, to a subsequent reduction in auxin levels, since cytokinin levels were

saturated. This view corresponds to work done by Mashtakov *et al.* (1967), which showed an increase in auxin levels in seed tissue treated by trichloroacetate. Once again the initial stimulation and subsequent decrease in % mass increase for NaTCA and stimulation by NaTFA suggest greater sensitivity to NaTCA. The apparent NaTFA-induced auxin increase in the experiment strengthens the hypothesis that the increase in plant height of *P. vulgaris* at low NaTFA concentrations may also be caused by initial increased auxin levels (Section 3.11).

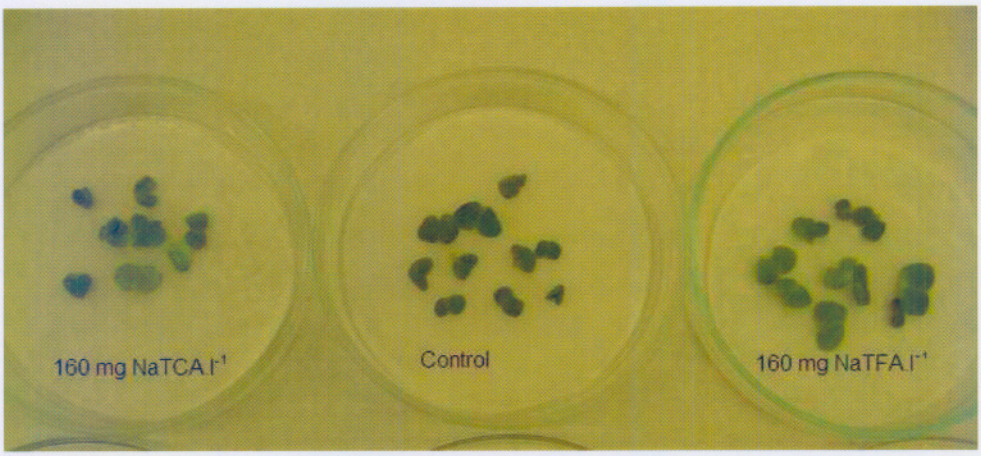

Figure 3.12: Radish cotyledons treated with NaTCA (left) and NaTFA (right) exhibiting marked chlorosis compared to control (center).

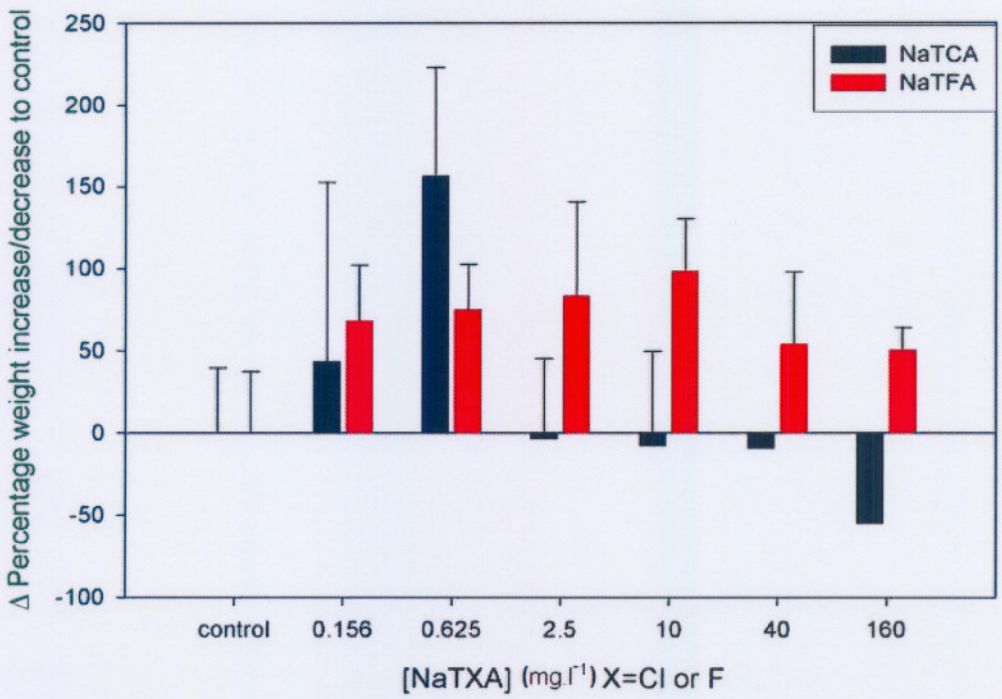

Figure 3.13: The short-term (4 days) effect of NaTFA and NaTCA on the % mass increase of excised radish cotyledons. Each point represents the average of five replicates.

3.1.6 Effect of trifluoroacetate on cell structures of *Z. mays*

To determine the effect of trifluoroacetate on the ultrastructural changes of chloroplasts leaf samples of *Z. mays* cultivated and treated in water culture were taken at the end of the treatment period. Root samples were also taken. These samples were prepared accordingly and used for transmission electron microscopy as well as light microscopy (Section 2.10). Root samples exhibited no apparent change in structure (Figures not shown).

The TEM micrograph shown in Figure 3.14 illustrates that control plants exhibited typical C_4 anatomy with bundle sheath chloroplasts having no granal stacks (1), whereas mesophyll chloroplasts exhibited clear granal stacks. The bundle sheath chloroplasts were typically tightly packed on the mesophyll bordering side of the bundle sheath cells (2). Starch grains were visible only in the bundle sheath chloroplasts whereas electron dense osmiophilic globules were present in both mesophyl and bundle sheath chloroplasts.

The chloroplast structure were affected by the 10 mg NaTFA.l^{-1} treatment as the bundle sheath chloroplasts seemed to be less densely packed around the mesophyll bordering side of the bundle sheath cells (4, Figure 3.15). The thylakoid membranes of the bundle sheath chloroplasts were not well defined and seemed to be disintegrating (3). The number and size of starch grains increased in the 10 mg NaTFA.l^{-1} treatment (6). Although the most conspicuous effects occurred in the bundle sheath chloroplasts, the mesophyll chloroplasts were also affected with less defined thylakoid membranes. Apparent leakage of lipidic globules was evident, indicating damage to the chloroplast envelope (5).

The chloroplast arrangement was markedly affected in the 160 mg NaTFA.l^{-1} treatment (Figure 3.16). Bundle sheath chloroplasts were arranged further away from the mesophyll cell bordering side of the chloroplast (7). Thylakoid membranes of the bundle sheath cell seemed to be markedly affected as the membranes were not well defined. Osmiophilic globules were also apparent in the cytoplasm indicating damage to the chloroplast envelope (11). Increase in the size of lipidic globules was apparent, especially for the 160 mg NaTFA.l^{-1} treatment (8). The remnants of a large amount of starch grains were clearly visible as electron lucent areas (9) and apparently caused deformations in the form of these chloroplast. At the 160mg NaTFA.l^{-1} treatment, irregularities in the mesophyll chloroplast thylakoid membranes were apparent as large electron-lucent areas (10).

Trifluoroacetate clearly affected membrane structures in chloroplast and correlate to the decreases in photosynthesis measured in *Z. mays*. These negative effects on membrane structure may have been caused by trifluoroacetate itself (Hance & Holly, 1963; Foy 1969) or by the formation of reactive singlet oxygen as a result of the inhibition of the photosynthetic electron transport chain by trifluoroacetate (McKersie & Leshem, 1994). Trifluoroacetate also

seemed to affect the carbohydrate partitioning since there was an apparent build up of starch. This change in carbohydrate partitioning may have been caused by trifluoroacetate itself (McWhorter, 1961) or as a result of trifluoroacetate induced nutrient shortages (Ingle & Rogers, 1961) (Section 3.1.2).

Figure 3.14: Transmission electron micrograph of untreated *Z. mays* cultivated in water culture, showing part of the bundle sheath cells and mesophyll cells. bs = bundle sheath cell, bc = bundle sheath chloroplast, g = lipidic globule, m = mesophyll cell, mc = mesophyll chloroplast, s = starch grain. See text for explanation.

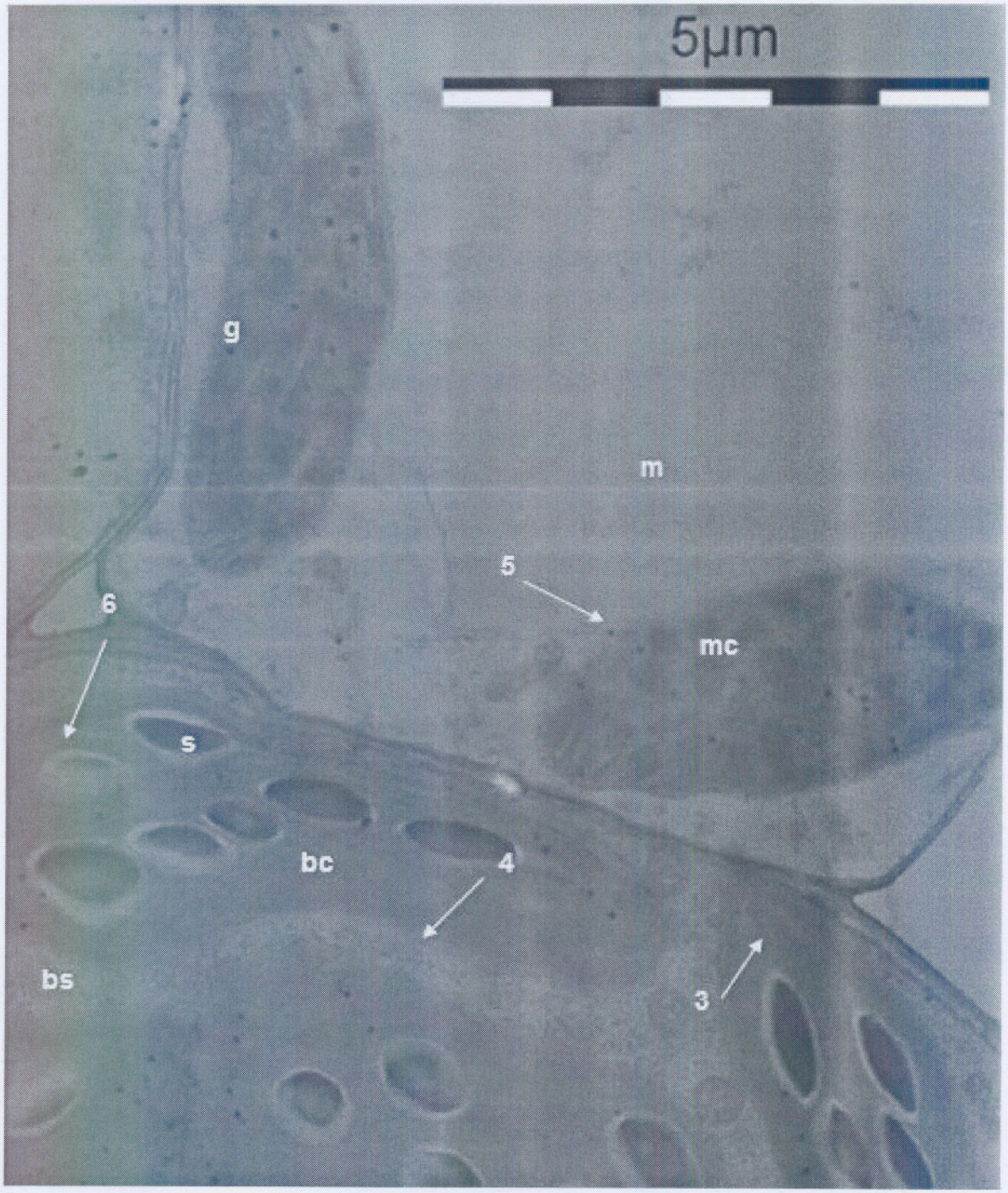

Figure 3.15: Transmission electron micrograph of 10 mg NaTFA.l^{-1} treatment of *Z. mays* cultivated in water culture showing part of the bundle sheath cells and mesophyll cells. bs = bundle sheath cell, bc = bundle sheath chloroplast, g = lipidic globule, m = mesophyll cell, mc = mesophyll chloroplast, s = starch grain. See text for explanation.

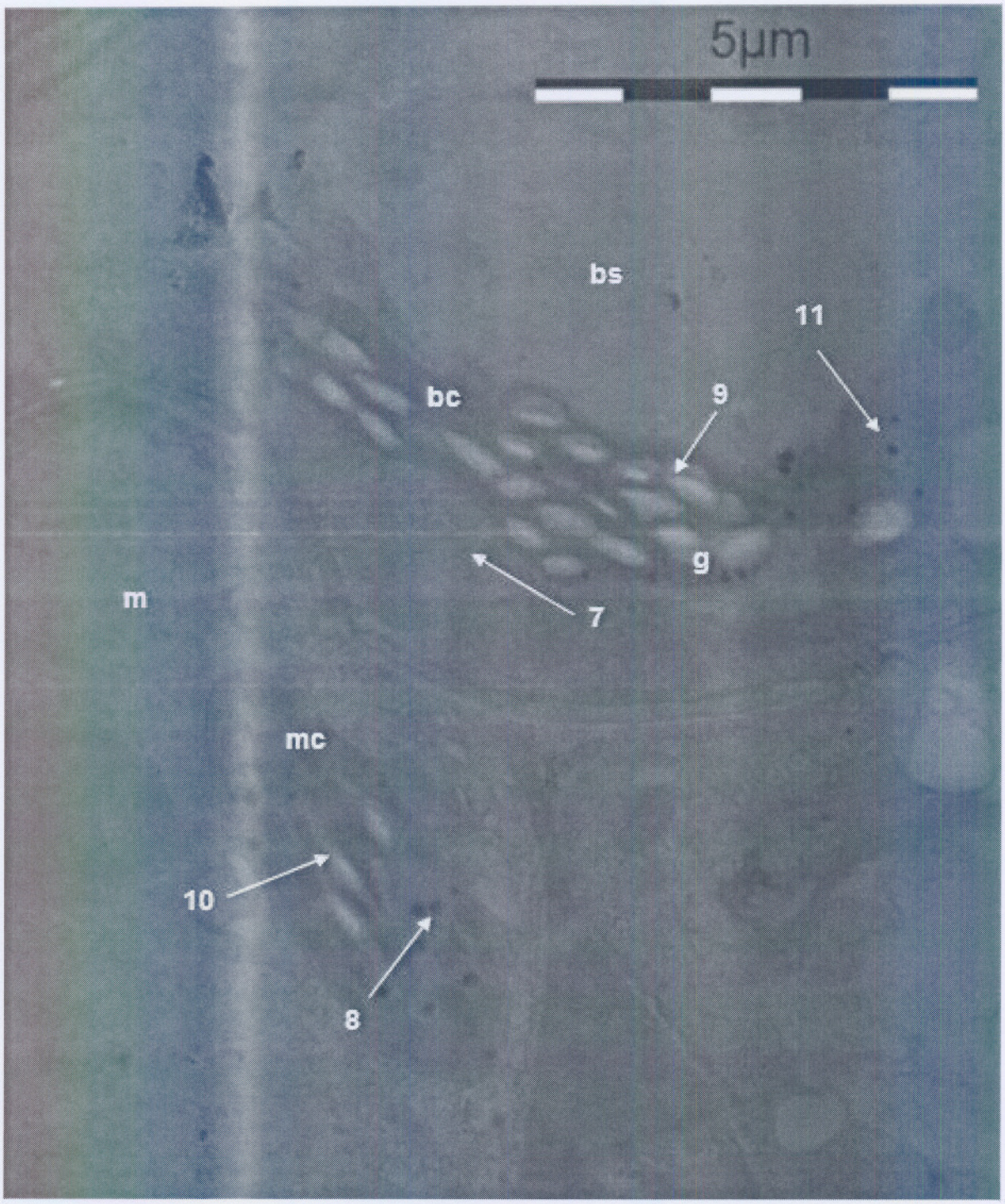

Figure 3.16: Transmission electron micrograph of 160 mg $NaTFA.l^{-1}$ treatment of *Z. mays* cultivated in water culture showing part of the bundle sheath cells and mesophyll cells. bs = bundle sheath cell, bc = bundle sheath chloroplast, g = lipidic globule, m = mesophyll cell, mc = mesophyll chloroplast. See text for explanation.

3.2 Photosynthesis

3.2.1 Photosynthetic gas exchange

3.2.1.1 Sand culture

The A:Ci response curves of *P. vulgaris* plants, treated with different concentrations of NaTFA are depicted in Figure 3.17. It is evident that the A:Ci response of the test plants was markedly affected at all concentration levels used. The photosynthetic gas exchange parameters of all treatments were calculated and are presented in Table 3.2.

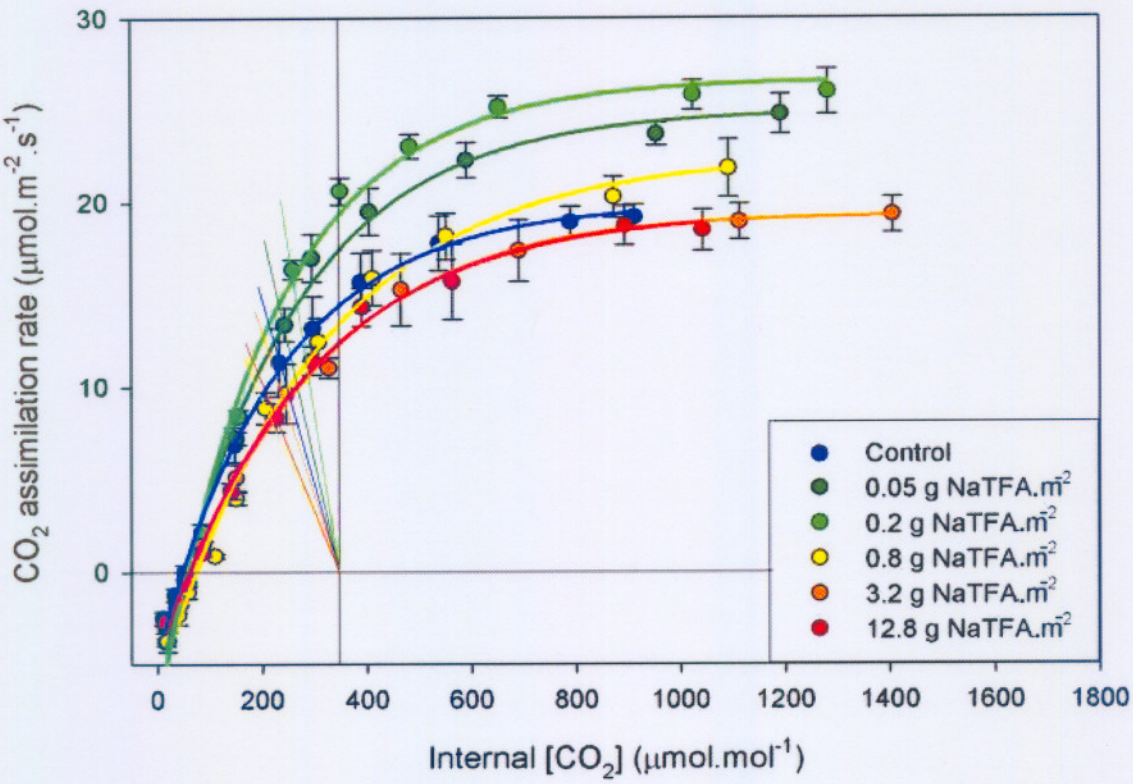

Figure 3.17: CO_2 assimilation rate vs intercellular CO_2 concentration (Ci) response curves for *P. vulgaris* cultivated in sand exposed to NaTFA concentration of 0.05, 0.2, 0.8, 3.2 and 12.8 g.m^{-2} respectively. The plotted values represent the average of four to five replicates.

From the A:Ci response curves of *P. vulgaris* plants (Figure 3.17), treated with a range of increasing NaTFA concentrations, it is evident that the compensation concentration (Γ) increased with increasing treatment levels, from 24% ($p<0.05$) at the 0.05 g NaTFA.m^{-2} treatment to 39% ($p<0.01$) at the 12.8 g NaTFA.m^{-2} treatment. This point at increasing mesophyll limitation with increasing NaTFA concentration (Table 3.2). The carboxylation

efficiency (CE) (i.e. the initial slope of the A:Ci curve) displayed an initial, although statistically nonsignificant, increase of 12% and 24% at the 0.05 and 0.2 g NaTFA.m^{-2} treatments followed by a decrease of 24% ($p<0.05$), 24% and 26 % ($p<0.05$) at the 0.8, 3.2 and 12.8 g.m^{-2} treatments respectively. This decrease in carboxylation efficiency (CE) may be attributed to a decrease in Rubisco activity and this decrease also corroborated the increase in compensation concentration (Γ). The rate of CO_2 assimilation at C_a = 350 µmol.mol^{-1} (A_{350}), increased by 31% ($p<0.05$) at a NaTFA concentration of 0.2 g.m^{-2}, followed by a 33 % in A_{350} ($p<0.05$) at a NaTFA concentration of 12.8 g.m^{-2}. The same trend was also observed in the CO_2 assimilation rate at a C_i = 350 µmol.mol^{-1} (A_0), showing a 36% increase ($p<0.01$) at a NaTFA concentration 0.2 g.m^{-2} and a statistically nonsignificant 14% decrease at a NaTFA concentration of 12.8 g.m^{-2}. Although not statistically significant, a decrease in (C_i) at C_a = 350 µmol.mol^{-1} occurred with increasing NaTFA concentration indicating increased stomatal limitation. This decrease in C_i occurred in spite of a decreased A_{350} and A_0 at higher NaTFA treatments, corroborating an increased stomatal limitation (Figure 3.19). The stomatal conductance (Gs) at ambient CO_2 concentration C_a increased with 49% ($p<0.05$) at 0.2 g NaTFA.m^{-2} and decreased with 43% ($p<0.05$), 46% ($p<0.05$) and 56% ($p<0.05$) at the 0.8, 3.2 and 12.8 g NaTFA.m^{-2} treatments respectively (Table 3.2). The % stomatal limitation of photosynthesis (l) increased statistically significantly at higher NaTFA levels with l increasing 39% ($p<0.05$) at 12.8 g NaTFA.m^{-2}. The decrease in stomatal conductance (Gs) at higher NaTFA concentration corresponds to the concomitant increase in stomatal limitation (l) (Table 3.2). The maximum rate of CO_2 assimilation (J_{max}) increased at all NaTFA treatments, reaching a maximum of a 31% increase ($p<0.05$) at the 0.2 g NaTFA.m^{-2} treatment. As J_{max} is an indication of the capacity for the regeneration of RuBP (Farquhar & Sharkey, 1982) this phenomenon corroborates the fact that the CE (Rubisco activity) was inhibited in the first place rather than the RuBP regeneration capacity. The fact that % stomatal limitation (l) increased; the carboxylation efficiency (CE) displayed a relatively small decrease and the maximal assimilation rate (J_{max}) increased drastically suggests that, both stomatal limitation and to a lesser degree mesophyll limitation played a role in the inhibition of photosynthetic gas exchange in *P. vulgaris*. Changes in the A:Ci response curves (Figure 3.17) as well as the values of the carboxylation efficiency (CE, initial slope), assimilation rate at C_i = 350 µmol.mol^{-1} (A_{350}) and maximal assimilation rate (J_{max}) also show that stimulation of photosynthesis occurred at the two lowest NaTFA concentrations used (Figure 3.19).

Table 3.2: Effect of different NaTFA concentrations on the different parameters of photosynthetic gas exchange parameters of *P. vulgaris* after 3 days of treatment in sand. Rate of CO_2 assimilation (A_{350}) ($\mu mol.m^{-2}.s^{-1}$) at C_a = 350 $\mu mol.mol^{-1}$; Intercellular CO_2 concentration (Ci) ($\mu mol.mol^{-1}$) at C_a = 350 $\mu mol.mol^{-1}$; Rate of CO_2 assimilation (A_0) ($\mu mol.m^{-2}.s^{-1}$) at Ci = 350 $\mu mol.mol^{-1}$; Stomatal conductance (Gs) at C_a = 350 $\mu mol.mol^{-1}$; Carboxylation efficiency (CE) at Γ; Maximum rate of CO_2 assimilation (J_{max}); CO_2 compensation point (Γ) ($\mu mol.mol^{-1}$); % Stomatal limitation of photosynthesis (l) (%) with * and ** indicating significant differences ($p<0.05$ and $p<0.01$ respectively) compared to control plants.

	Control	0.05 g NaTFA.m^{-2}	0.2 g NaTFA.m^{-2}	0.8 g NaTFA.m^{-2}	3.2 g NaTFA.m^{-2}	12.8 g NaTFA.m^{-2}
A_{350}	12.5±1.4	13.4 ±0.7	16.4±0.5*	8.9±0.9*	8.9±0.9*	8.4±0.8*
Ci	243.0±8.8	243.4±7.0	259.8±6.1	206.3±27.5	245.5±9.2	226.0±5.3
A_0	14.6±1.2	17.6±0.8	19.8±0.7**	13.5±1.1	12.7±1.4	12.5±0.7
Gs	311.3±52.7	284.8±34.0	462.5±31.6*	175.5±38.4*	168.0±22.0*	137.8±22.6*
CE	0.092±0.009	0.103±0.007	0.114±0.008	0.070±0.005*	0.070±0.009	0.068±0.006*
J_{max}	19.2±1.5	24.7±0.5*	25.1±1.4*	22.8±1.9	19.8±0.9	19.5±1.5
Γ	43.5±3.4	53.8±2.3*	56.6±1.7*	71.5±4.3**	61.4±2.5**	60.4±2.0**
l	14.8±4.0	23.6±3.2	17.0±0.8	33.7±5.0*	29.5±2.0*	33.4±3.6*

In the case of *Z. mays*, cultivated and treated in sand culture, the A:Ci response was even more severely affected by NaTFA treatment (Figure 3.18). Unlike in the case of *P. vulgaris*, only a nonsignificant initial stimulation in the responses was apparent for *Z. mays*. The small changes with respect to the supply function, indicate that stomatal conductance was not much affected. The effect of NaTFA treatment on the different photosynthetic gas exchange parameters of *Z. mays*, with their statistical significance indicated, are presented in Table 3.3.

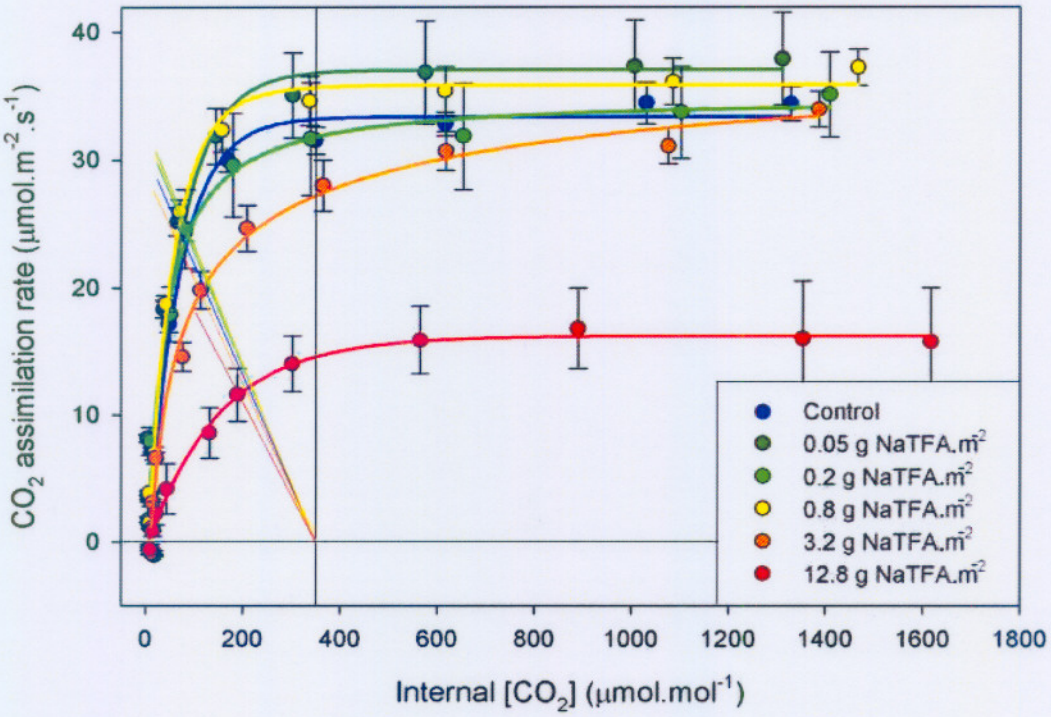

Figure 3.18: CO_2 assimilation rate vs intercellular CO_2 concentration (Ci) response curves for *Z. mays* cultivated in sand and exposed to NaTFA concentration of 0.05, 0.2, 0.8, 3.2 and 12.8 g.m^{-2}. The plotted values represent the average of four to five replicates.

From the A:Ci response curves of *Z. mays* plants (Figure 3.18) treated with a range of increasing NaTFA concentrations it is evident that the compensation concentration (Γ) decrease by 38% at the 0.05 g NaTFA.m^{-2} treatment and increased with 75% (not significant) at 12.8 g NaTFA.m^{-2} treatment, pointing at increased mesophyll limitation from the 0.2 g.m^{-2} NaTFA treatments (Table 3.3). The carboxylation efficiency (CE) increased by 14% and 22% ($p<0.05$) at the 0.2 and the 0.8 g NaTFA.m^{-2} treatments; this was followed by a respective decrease of 38% ($p<0.05$) and 63% ($p<0.05$) at the 3.2 and the 12.8 g NaTFA.m^{-2} treatments. The decrease in CE at higher NaTFA concentrations may be attributed to possible decrease in Rubisco and/or PEP-case activity. The rate of CO_2 assimilation at C_a = 350 µmol.mol^{-1} (A_{350}) increased, however not statistically significantly, at the 0.05, 0.2 and 0.8 g NaTFA.m^{-2} treatments, followed by a significant decrease of 20% ($p<0.01$) and 48% ($p<0.01$) at the 3.2 and 12.8 g NaTFA.m^{-2} treatments (Table 3.3). The same trend was also observed in the CO_2 assimilation rate at C_i = 350 µmol.mol^{-1} (A_0) with A_0 decreasing by 19% ($p<0.05$) and 53% ($p<0.01$) at the 3.2 and 12.8 g NaTFA.m^{-2} treatments. Although the intercellular CO_2 concentration (C_i) at C_a = 350 µmol.mol^{-1} was stable in the plants treated with lower NaTFA treatments, it increased by 52% ($p<0.01$) and 123% ($p<0.01$) at the 3.2 and 12.8 g NaTFA.m^{-2} treatments (Table 3.3). The increase in C_i at higher NaTFA treatments and moderately affected Gs (See small decrease in slope of the supply function, Figure

3.18), indicates strong mesophyll limitation and corroborates the abovementioned possible decrease in Rubisco activity. The stomatal conductance (Gs) at ambient CO_2 concentration (C_a = 350 µmol.mol^{-1}) decreased by 6% ($p<0.05$) at the 0.8 g NaTFA.m^{-2} treatment and decreased by 18% ($p<0.01$) at the 12.8 g NaTFA.m^{-2} treatment. The % stomatal limitation of photosynthesis (l) decreased only significantly at the highest NaTFA levels with l decreasing by 34% ($p<0.05$) at the 12.8 g NaTFA.m^{-2} treatment. No statistically significant increases in the maximum rate of CO_2 assimilation (J_{max}) occurred at low NaTFA levels. J_{max} increased by 11% at the 0.2 g NaTFA.m^{-2} treatment (not significant), but however decreased significantly by 40% ($p<0.01$) at the 12.8 g NaTFA.m^{-2} treatment. The fact that changes in stomatal conductance (Gs) and % stomatal limitation (l) were relatively small, and the fact that CE and J_{max} decreased and C_i and Γ increased suggests that NaTFA inhibits photosynthetic gas exchange in *Z. mays* as a result of strong mesophyll limitation (Figure 3.19).

3.2.1.2 Water culture

P. vulgaris (C_3 crop) cultivated in water culture was markedly affected after 12 days of NaTFA treatments (Figure 3.20) and displayed greater effects than the corresponding 3 day treatments in sand culture. Photosynthetic gas exchange measurements taken on the second and fifth mature leaves showed that the inhibitory effect increased with time. No difference was apparent in the effect of NaTFA treatment on the two leaf sets (Data not shown). These findings also corresponds to the data of the chlorophyll fluorescence measurements carried out on the younger leaf sets which also displayed no difference in the extend of the effect between older and younger leaves (Section 3.2.2). This suggests that the increase in developmental abnormalities in younger leaves and effects on photosynthesis were not connected. For this reason only the photosynthetic gas exchange data measured on the second mature leaves on day 12 will be discussed, even though assimilation rates and chlorophyll content (Figure 3.10) indicated that leaf ageing had commenced.

From the A:C_i response curves of *P. vulgaris* treated with different NaTFA concentrations (Figure 3.20), it is evident that the initial slope (CE), the maximal assimilation rate (J_{max}) and assimilation rate at C_a = 350 µmol.mol^{-1} (A_{350}) were not affected after twelve days of various NaTFA treatments (Figure 3.20). The stomatal conductance (Gs) decreased with increasing concentration (after 12 days of treatment), corresponding to the decrease of the NaTFA treated plants cultivated and treated in sand. The effect of NaTFA treatment on the different photosynthetic gas exchange parameters, of *P. vulgaris*, indicating their statistical significant changes, are presented in Table 3.4.

Table 3.3: Effect of different NaTFA concentrations on the different parameters of photosynthetic gas exchange parameters of *Z. mays* after 3 days of treatment in sand. Rate of CO_2 assimilation (A_{350}) ($\mu mol.m^{-2}.s^{-1}$) at C_a = 350 $\mu mol.mol^{-1}$; Intercellular CO_2 concentration (Ci) ($\mu mol.mol^{-1}$) at C_a = 350 $\mu mol.mol^{-1}$; Rate of CO_2 assimilation (A_0) ($\mu mol.m^{-2}.s^{-1}$) at Ci = 350 $\mu mol.mol^{-1}$; Stomatal conductance (Gs) at C_a = 350 $\mu mol.mol^{-1}$; Carboxylation efficiency (CE) at Γ; Maximum rate of CO_2 assimilation (J_{max}); CO_2 compensation point (Γ) ($\mu mol.mol^{-1}$); % Stomatal limitation of photosynthesis (l) (%) with * and ** indicating significant differences ($p<0.05$ and $p<0.01$ respectively) compared to control plants.

	Control	0.05 g NaTFA.m^{-2}	0.2 g NaTFA.m^{-2}	0.8 g NaTFA.m^{-2}	3.2 g NaTFA.m^{-2}	12.8 g NaTFA.m^{-2}
A_{350}	24.4±0.6	25.5±1.1	25.6±3.1	26.3±0.9	19.5±1.5**	12.7±1.7**
Ci	79.8±4.6	70.8±15.0	78.5±15.4	72.5±8.5	121.3±10.7**	178.0±16.6**
A_0	33.0±1.1	36.8±3.8	33.1±4.5	35.5±1.8	26.7±2.0*	15.6±2.3**
Gs	171.0±1.5	175.3±9.0	180.3±15.7	181.8±5.3*	162±8.2	141±5.5**
CE	0.631±0.042	0.600±0.054	0.717±0.085	0.768±0.062*	0.392±0.023**	0.233±0.109**
J_{max}	33.5±1.2	37.2±3.8	34.7±3.2	36.2±1.7	33.2±2.0	20.1±3.9**
Γ	5.2±1.5	3.2±1.6	5.5±2.3	6.1±1.2	9.0±2.4	9.1±2.5
l	26.2±0.8	29.0±6.1	21.9±2.9	25.9±1.9	27.3±2.1	17.4±3.1*

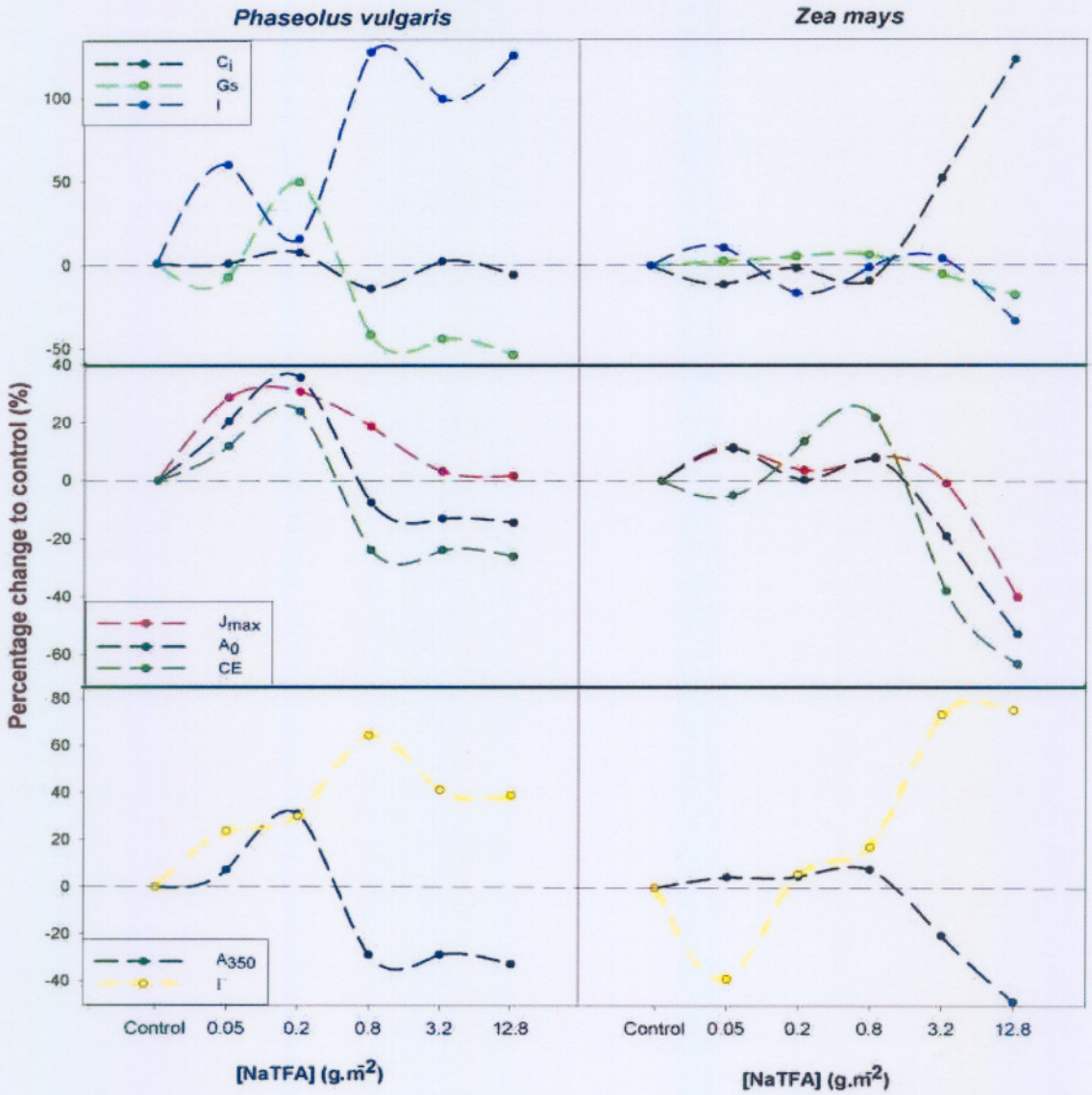

Figure 3.19: Summary of the effect of different NaTFA concentrations on different photosynthetic gas exchange parameters of *P. vulgaris* and *Z. mays* cultivated in sand: Intercellular CO_2 concentration (C_i) at ambient CO_2 concentration; Stomatal conductance (Gs) at ambient CO_2 concentration; Stomatal limitation (l) at ambient CO_2 concentration; Maximum CO_2 assimilation (J_{max}); CO_2 assimilation rate at C_i of 350 µmol.mol^{-1} (A_0); Carboxylation efficiency (CE); Assimilation rate at ambient CO_2 concentration (A_{350}); CO_2 compensation concentration (Γ). The fact that % stomatal limitation (l) was unchanged and assimilation rate (A_{350}), carboxylation efficiency (CE) and maximal assimilation rate (J_{max}) were decreased by the trifluoroacetate treatments, suggest a greater contribution of mesophyll limitation to the inhibition of photosynthesis for *Z. mays* than for *P. vulgaris*. The increases in % stomatal limitation suggest a greater stomatal limitation for *P. vulgaris* compared to *Z. mays*.

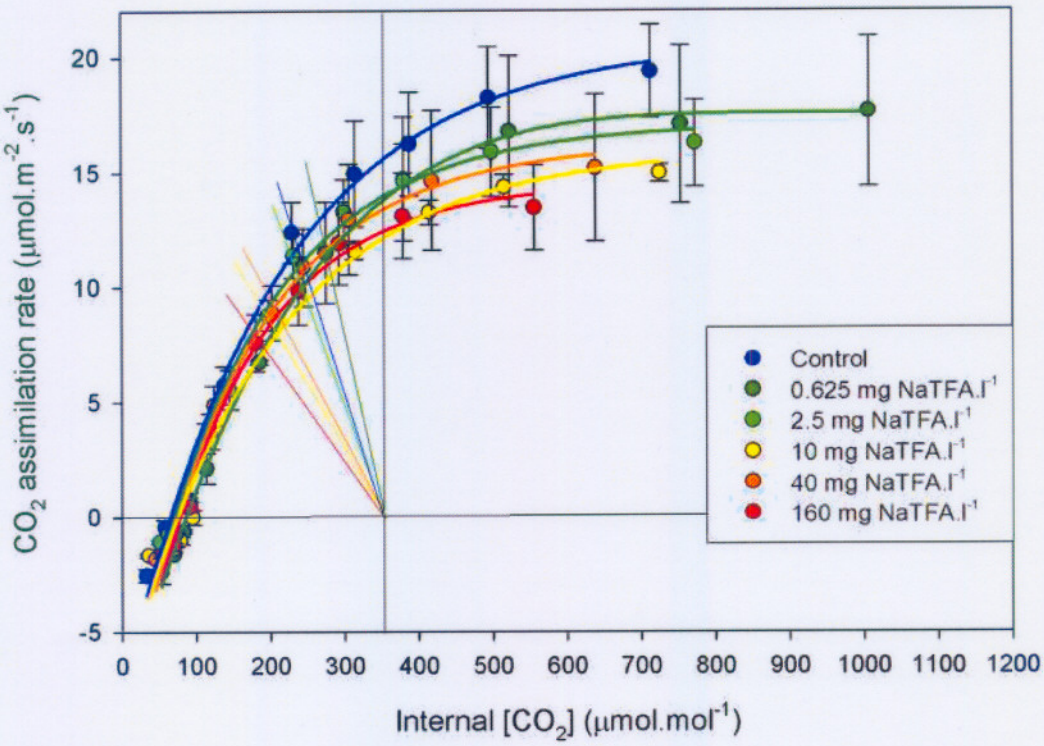

Figure 3.20: CO_2 assimilation rate (A) vs intercellular CO_2 concentration (Ci) response curves for *P. vulgaris* cultivated in water culture after 12 days of treatment with a range of NaTFA concentrations. The values represent the mean of four replicates.

After 12 days of treatment of *P. vulgaris* with a range of increasing NaTFA concentrations, the following changes occurred in the photosynthetic gas exchange parameters on paramenters calculated from the A:Ci response curves. The compensation concentration (Γ) increased slightly (statistically nonsignificantly) with increasing NaTFA concentration, suggesting increased mesophyll limitation (Table 3.4). The carboxylation efficiency (CE) was not statistically significantly affected. The rate of CO_2 assimilation at C_a = 350 µmol.mol^{-1} (A_{350}) decreased with 7%, 8%, 24%, 28% ($p<0.05$) and 39% ($p<0.05$) at the 0.625 to the 160 mg NaTFA.l^{-1} treatments (Table 3.4). The same trend was also observed in the CO_2 assimilation rate at C_i = 350 µmol.mol^{-1} (A_0), with A_0 decreasing by 12%, 12%, 30%, 16% and 20% at the 0.625 to the 160 mg NaTFA.l^{-1} treatments. An initial significant increase of 20% ($p<0.05$) was observed in the intercellular CO_2 concentration (C_i) at C_a = 350 µmol.mol^{-1} at the 0.625 mg NaTFA.l^{-1} treatment, followed by significant decreases of 12 % ($p<0.05$) and 22% ($p<0.05$) at the 40 and the 160 mg NaTFA.l^{-1} treatments respectively. The stomatal conductance (Gs) at ambient CO_2 concentration (C_a = 350 µmol.mol^{-1}) decreased by 11%, 22%, 36% ($p<0.05$), 49% ($p<0.01$), and 58% ($p<0.01$) at the 0.625, 2.5, 10, 40 and the 160 mg NaTFA.l^{-1} treatments respectively. However after 4 days of treatment an increase of 55% was apparent in stomatal conductance (Gs) for the 0.625 mg NaTFA.l^{-1} treatment (See

Appendix CD). The initial increase in C_i at the 0.625 mg NaTFA.l^{-1} treatment may be attributed to mesophyll limitation since the stomatal conductance (Gs) decreased slightly for this treatment while the decreases at higher treatment levels may also be attributed to stomatal limitation (Table 3.4). The % stomatal limitation of photosynthesis displayed an initial decrease of 12% (not significant) followed by an increase up to 78% ($p<0.05$) at the 160 mg NaTFA.l^{-1} treatment. This initial decrease in % stomatal limitation further strengthens the occurrence of initial mesophyll limitation at the 0.625 mg NaTFA.l^{-1} concentration. The maximum rate of CO_2 assimilation (J_{max}) decreased by 13%, 17%, 21%, 20% and 32% ($p<0.05$) from the 0.625 to the 160 mg NaTFA.l^{-1} treatments respectively. The fact that the % stomatal limitation (l) increased with an concomitant decrease in stomatal conductance at higher NaTFA concentrations, suggests relatively large stomatal limitation, while the decrease in assimilation rate at a higher C_i suggests some mesophyll limitation for trifluoroacetate treated *P. vulgaris* plants (Figure 3.22).

Table 3.4: Effect of different NaTFA concentrations on the different parameters of photosynthetic gas exchange parameters of *P. vulgaris* after 12 days of treatment in water culture. Rate of CO_2 assimilation (A_{350}) (µmol.m^{-2}.s^{-1}) at C_a = 350 µmol.mol^{-1}; Intercellular CO_2 concentration (Ci) (µmol.mol^{-1}) at C_a = 350 µmol.mol^{-1}; Rate of CO_2 assimilation (A_0) (µmol.m^{-2}.s^{-1}) at Ci = 350 µmol.mol^{-1}; Stomatal conductance (Gs) at C_a = 350 µmol.mol^{-1}; Carboxylation efficiency (CE) at Γ; Maximum rate of CO_2 assimilation (J_{max}); CO_2 compensation point (Γ) (µmol.mol^{-1}); % Stomatal limitation of photosynthesis (l) (%) with * and ** indicating significant differences ($p<0.05$ and $p<0.01$ respectively) compared to control plants.

	Control	0.625 mg NaTFA.l^{-1}	2.5 mg NaTFA.l^{-1}	10 mg NaTFA.l^{-1}	40 mg NaTFA.l^{-1}	160 mg NaTFA.l^{-1}
A_{350}	12.4±1.3	11.5±2.2	11.4±1.0	9.5±0.7	8.9±1.2*	7.6±1.2*
Ci_{350}	229.5±6.9	275.0±16.3*	231.3±10.3	210.0±20.8	202.3±12.7*	180.3±18.7*
A_0	15.8±1.9	13.9±3.0	13.9±1.4	11.1±2.1	13.3±2.2	12.5±1.6
Gs	225.0±26.0	201.5±110.0	176.7±15.4	143.3±27.9*	115.5±22.5**	95.3±28.6**
CE	0.101±0.015	0.101±0.016	0.096±0.002	0.095±0.013	0.105±0.002	0.102±0.003
J_{max}	20.6±2.1	17.8±3.5	17.0±1.9	16.3±0.9	16.6±3.8	14.1±2.2*
Γ	65.5±3.1	84.5±13.3	69.1±7.2	70.9±2.7	74.5±7.1	79.5±8.1
l	21.3±2.5	16.6±2.1	17.7±3.4	24.8±8.0	29.1±9.4	38.0±7.3*
WUE	3.4±0.2	5.6±1.9	3.8±0.3	4.0±0.4	4.5±0.5*	4.8±0.6*

Similar to the sand culture experiments, NaTFA treatment had marked effects on the A:Ci response curves of *Z. mays* (C_4 crop) cultivated and treated in water culture (Figure 3.21). As in the case of *P. vulgaris*, the effects for treated *Z. mays* increased during the treatment period and no recovery was observed at any of the treatment levels. This corresponded with the chlorophyll a fluorescence measurements (Section 3.2.2), which also displayed no significant recovery during the treatment period. Day 12 of treatment thus displayed the greatest effects and for this reason only photosynthetic gas exchange data of day 12 will be discussed for *Z. mays*. The effect of NaTFA treatment on the different photosynthetic gas exchange parameters, of *Z. mays*, with their statistical significance are presented in Table 3.5.

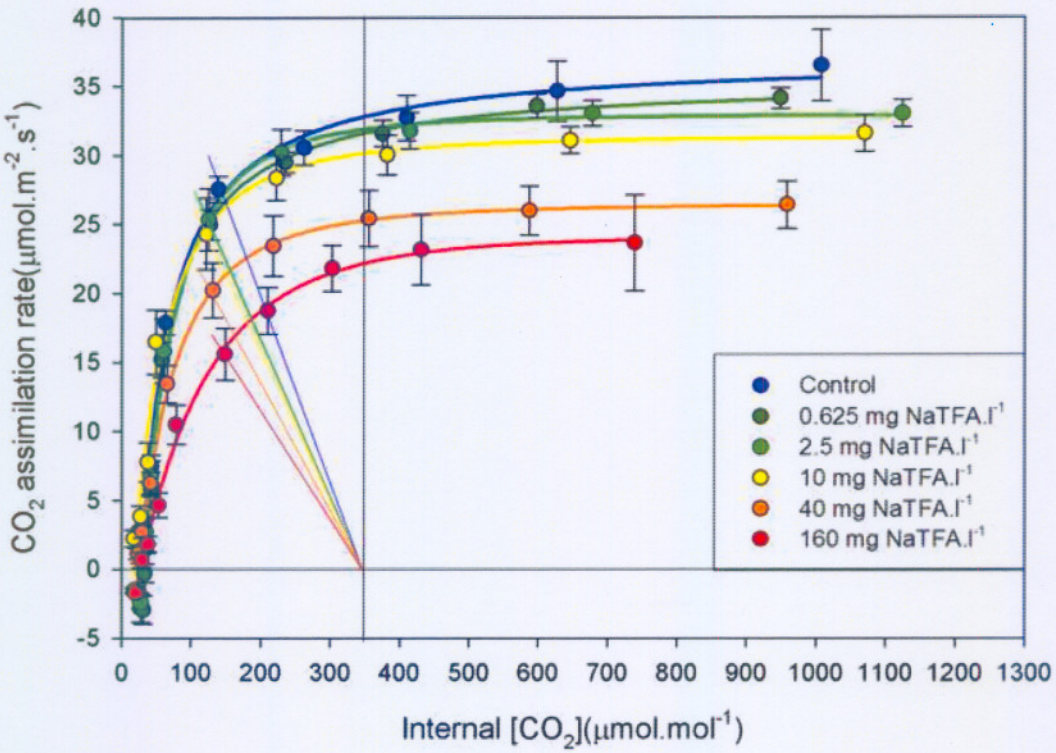

Figure 3.21: CO_2 assimilation rate (A) vs intercellular CO_2 concentration (Ci) response curves for *Zea mays* cultivated in water culture, 12 days after treatment started with a range of NaTFA concentrations. The values represent the mean of four replicates.

From the A:C_i response curves of *Z. mays* after the treatment with a range of increasing NaTFA concentrations (Figure 3.21) it is evident that the compensation concentration (Γ) displayed no statically significant effect at any NaTFA concentration (Table 3.5). The carboxylation efficiency (CE) displayed a respective decrease of 20%, 39% ($p<0.05$), 44% ($p<0.05$), 52% ($p<0.01$) and 70% ($p<0.01$) from the 0.625 to the 160 mg NaTFA.l^{-1} treatment

(Table 3.5). This decrease in CE at all NaTFA concentrations may be attributed to a decrease in Rubisco and/or PEP-case activity. The rate of CO_2 assimilation at C_a = 350 $\mu mol.mol^{-1}$ (A_{350}) decreased by 6%, 8%, 13%, 27% ($p<0.01$) and 44% ($p<0.01$) from the 0.625 to the 160 mg NaTFA.l^{-1} treatments. The same trend was also observed in the CO_2 assimilation rate at a C_i = 350 $\mu mol.mol^{-1}$ (A_0) with a decrease of 24% ($p<0.05$) and 33% ($p<0.05$) at the 40 and 160 mg NaTFA.l^{-1} treatments. The intercellular CO_2 concentration (C_i) at C_a = 350 $\mu mol.mol^{-1}$ displayed no statistically significant changes (Table 3.5). This stability in C_i at all treatments suggests a strong mesophyll limitation since assimilation rate (A_{350}) actually decreased with increasing NaTFA concentration. The stomatal conductance (Gs) at ambient CO_2 concentration (C_a) decreased by 11%, 15%, 20%, 33% ($p<0.01$) and 43% ($p<0.01$) from the 0.625 to the 160 mg NaTFA.l^{-1} treatment. However after 8 days of treatment an 51% increase ($p<0.05$) in stomatal conductance (Gs) was apparent for the 0.625 mg NaTFA.l^{-1} treatment (See Appendix CD). The % stomatal limitation of photosynthesis (l) displayed a statistically nonsignificant tendency to increase with increasing NaTFA concentration and increased up to 70% at the 160 mg NaTFA.l^{-1} treatment. The maximum rate of CO_2 assimilation (J_{max}) displayed a decreasing tendency with increasing NaTFA concentration although only a statistically significant decrease of 33% ($p<0.05$) was recorded at the 160 mg NaTFA.l^{-1} treatment (Table 3.5). The fact that an increases in % stomatal limitation (l) was observed, as well as a marked decrease in carboxylation efficiency (CE), overwhelmingly suggests that trifluoroacetate inhibits photosynthetic gas exchange in Z. *mays* as a result of both stomatal and mesophyll limitation (Figure 3.22).

Table 3.5: Effect of different NaTFA concentrations on the different parameters of photosynthetic gas exchange parameters of *Z. mays* after 12 days of treatment in water culture. Rate of CO_2 assimilation (A_{350}) ($\mu mol.m^{-2}.s^{-1}$) at C_a = 350 $\mu mol.mol^{-1}$; intercellular CO_2 concentration (Ci_{350}) ($\mu mol.mol^{-1}$) at C_a = 350 $\mu mol.mol^{-1}$; Rate of CO_2 assimilation (A_0) ($\mu mol.m^{-2}.s^{-1}$) at Ci = 350 $\mu mol.mol^{-1}$; stomatal conductance (Gs) at C_a = 350 $\mu mol.mol^{-1}$; Carboxylation efficiency (CE) at Γ; maximum rate of CO_2 assimilation (J_{max}); CO_2 compensation point (Γ) ($\mu mol.mol^{-1}$); % stomatal limitation of photosynthesis (l) (%); Water use efficiency (WUE), with * and ** indicating significant differences ($p<0.05$ and $p<0.01$ respectively) compared to control plants.

	Control	0.625 mg NaTFA.l^{-1}	2.5 mg NaTFA.l^{-1}	10 mg NaTFA.l^{-1}	40 mg NaTFA.l^{-1}	160 mg NaTFA.l^{-1}
A_{350}	27.6±1.0	25.9±2.0	25.4±2.2	24.3±2.6	20.2±2.0**	15.6±1.9**
Ci_{350}	138.8±14.5	159.0±52.1	125.0±8.9	121.5±10.5	131.3±17.5	148.5±29.1
A_0	33.2±1.9	31.9±0.5	32.2±0.9	30.1±1.2	25.4±1.9*	22.3±2.8**
Gs	278.3±13.0	247.5±53.5	236.3±33.4	223.5±39.7	188.0±24.0**	159.5±33.9**
CE	1.084±0.153	0.863±0.071	0.665±0.103*	0.613±0.052*	0.516±0.088**	0.326±0.092**
J_{max}	35.6±2.4	34.4±0.7	33.0±1.1	31.2±1.0	27.1±1.3	24.1±3.1*
Γ	26.9±5.0	33.1±4.5	28.4±6.7	17.7±3.8	24.5±3.0	27.2±4.0
l	16.5±2.7	18.9±5.2	21.6±5.1	19.9±5.8	20.4±3.9	28.1±9.2
WUE	5.2±0.3	5.5±0.3	5.6±0.3	5.6±0.3	5.1±0.3	4.8±0.7

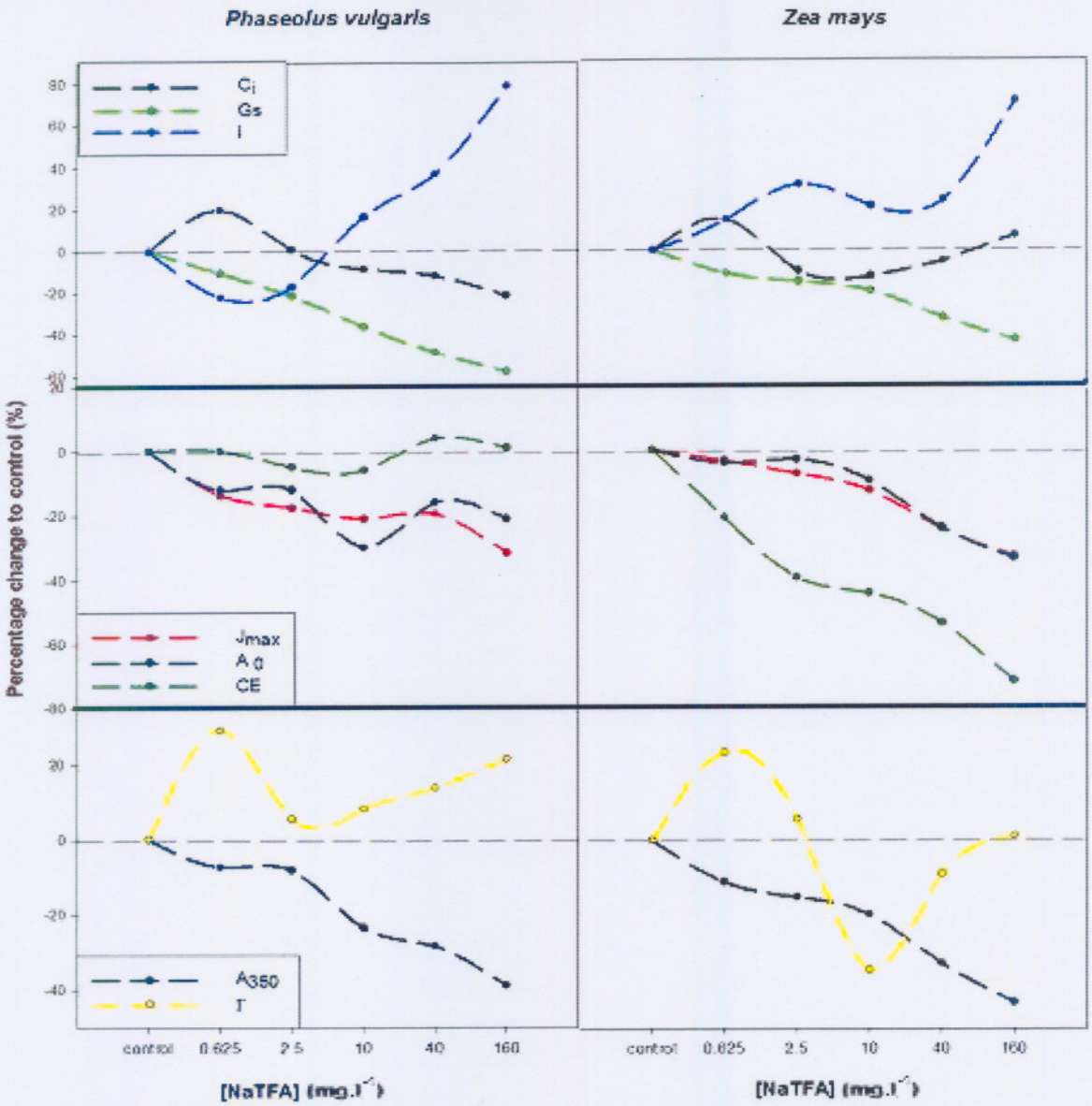

Figure 3.22: Summary of the effect of different NaTFA concentrations on different photosynthetic gas exchange parameters of *P. vulgaris* and *Z. mays*: Intercellular CO_2 concentration (C_i) at ambient CO_2 concentration; Stomatal conductance (Gs) at ambient CO_2 concentration; % Stomatal limitation (I) at ambient CO_2 concentration; Maximum CO_2 assimilation (J_{max}); CO_2 assimilation rate at C_i of 350 µmol.mol^{-1} (A_0); Carboxylation efficiency (CE); Assimilation rate at ambient CO_2 concentration (A_{350}); CO_2 compensation concentration (Γ). The relatively large decrease in carboxylation efficiency (CE) and maximal assimilation rate (J_{max}) by trifluoroacetate treatments for *Z. mays*, suggest a relatively greater contribution of mesophyll limitation to inhibition of photosynthesis than for *P. vulgaris*.

3.2.2 Photosystem II structure and function: chlorophyll a fluorescence kinetics

3.2.2.1 Water culture

Trifluoroacetate treatment clearly displayed concentration dependant effects on the fast phase chlorophyll a fluorescence transients of both *P. vulgaris* and *Z. mays* after 12 days of treatment in water culture (Figure 3.23 and 3.24). The chlorophyll a fluorescence transients of *P. vulgaris* displayed no difference at F_0 but displayed a clear reduction in F_m. In the case of *Z. mays* the chlorophyll a fluorescence transient displayed an apparent decrease in F_m with increasing NATFA concentrations (10 - 40 mg NaTFA.l^{-1}) while no change in F_0 was apparent. This stability of F_0 clearly indicates that the plants were homogenous and that all plants were completely dark adapted, i.e. all RCs were fully open.

When the fluorescence transients were normalised between F_0 and 2 ms, clear differences were visible between NaTFA treatments with regards to the fluorescence rise after 2 ms for both *P. vulgaris* and *Z. mays* (Figure 3.25 and 26). *P. vulgaris* displayed a NaTFA concentration dependant decrease with regard to the fluorescence rise while *Z. mays* displayed an initial stimulation at 10 mg NaTFA.l^{-1} followed by decreases in fluorescence rise with increasing NaTFA concentrations. These normalisations between F_0 and 2 ms clearly point to the fact that the effect is mainly located in the dark reactions of photosynthesis i.e. in the multiple turn-over phase of the fluorescence transient (Tsimilli-Michael *et al.*, 1999).

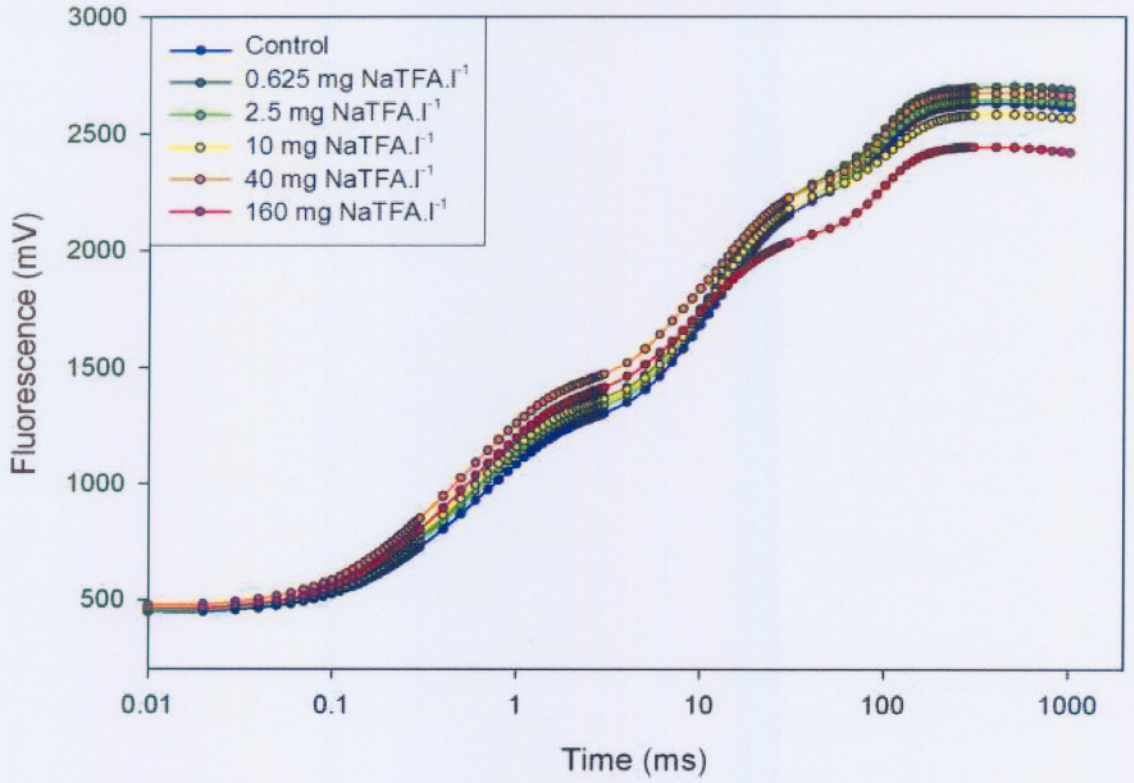

Figure 3.23: Raw chlorophyll a fluorescence transients of *P. vulgaris* plants treated with different NaTFA concentrations in water culture.

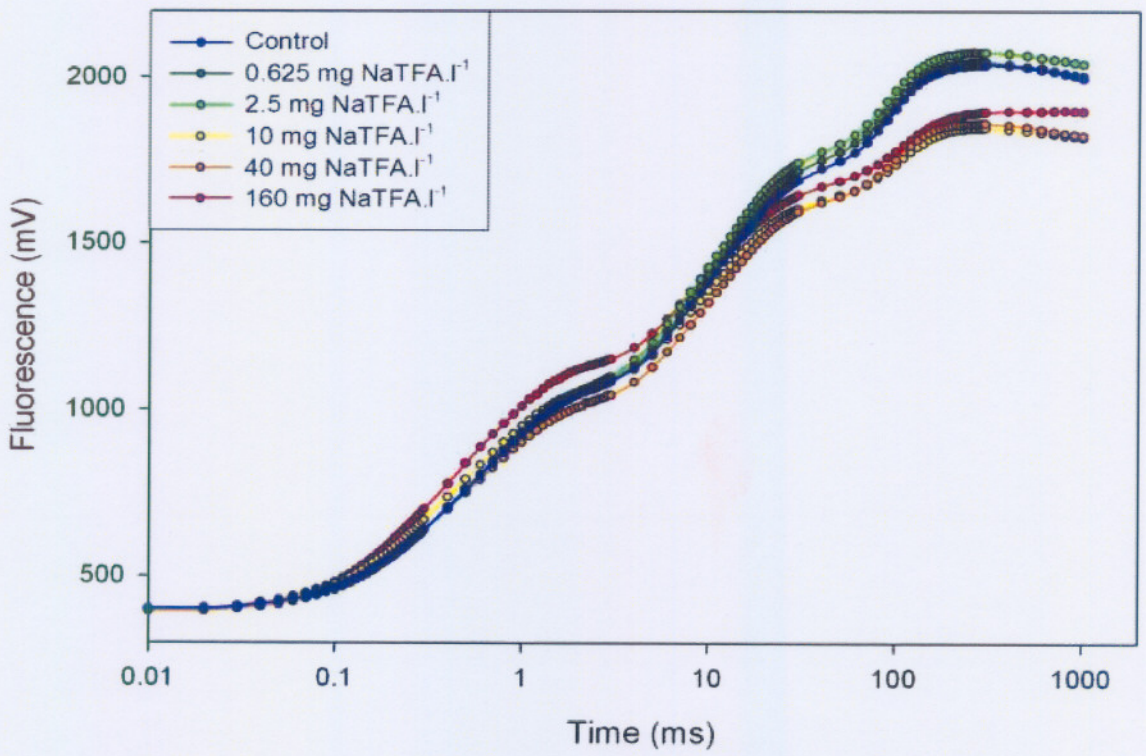

Figure 3.24: Raw chlorophyll a fluorescence transients of *Z. mays* plants treated with different NaTFA concentrations in water culture.

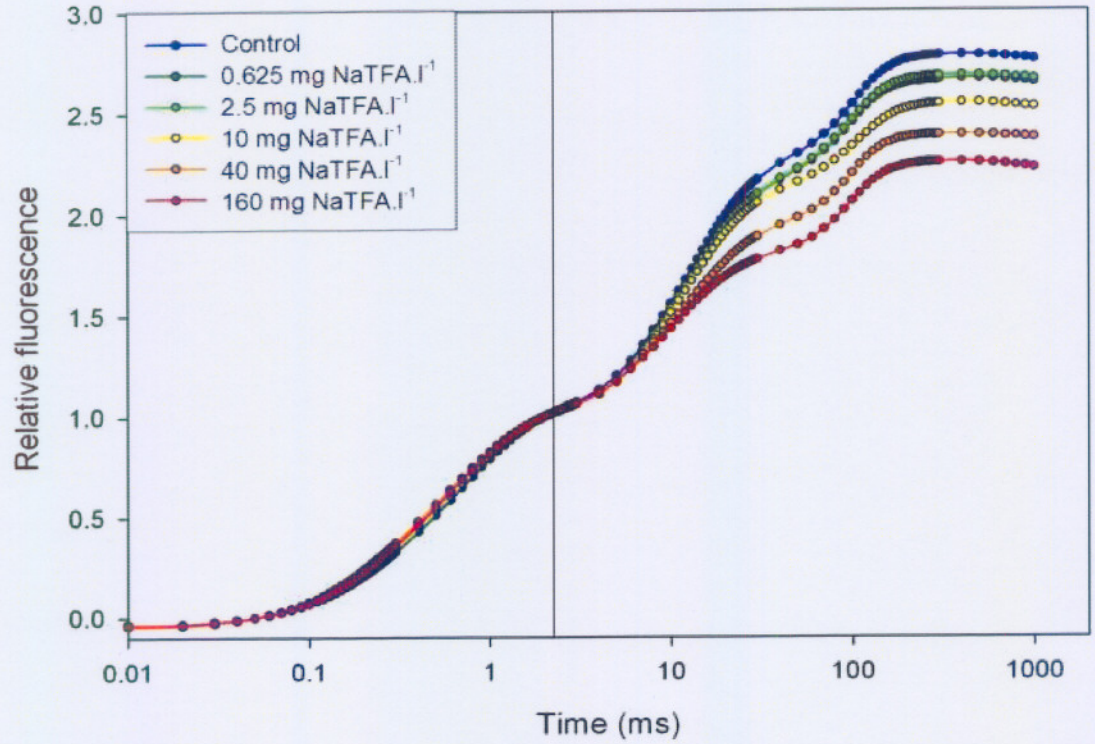

Figure 3.25: Chlorophyll a fluorescence transients normalised between 0.05 ms and 2 ms of *P. vulgaris* plants treated with different NaTFA concentrations in water culture.

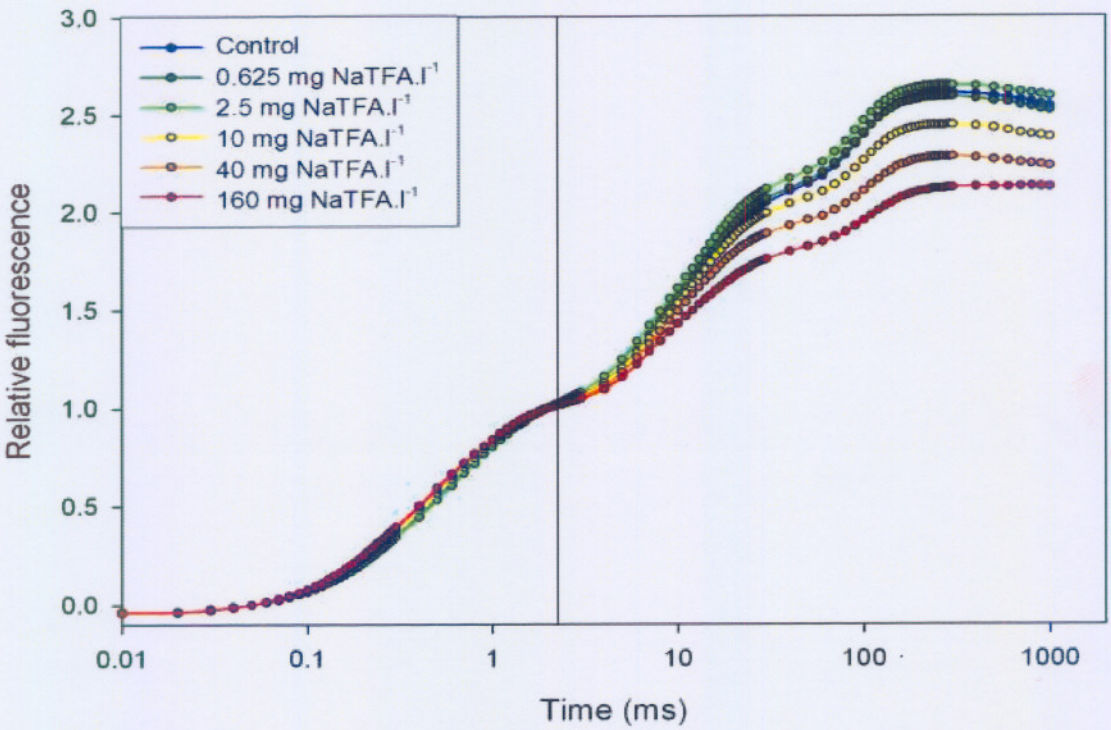

Figure 3.26: Chlorophyll a fluorescence transients normalised between 0.05 ms and 2 ms of *Z. mays* plants treated with different NaTFA concentrations in water culture.

Trifluoroacetate concentration dependant changes were observed in both the specific (per reaction centre) and phenomenological (per cross section) energy fluxes (Figure 3.27 and 3.28) for both *P. vulgaris* and *Z. mays* cultivated in water culture.

For *P. vulgaris* significant decreases in the electron transport per cross section (ET_0/CS_0) of 2% ($p<0.05$), 3% ($p<0.05$) and 12% ($p<0.01$) were apparent from the 10 to the 160 mg NaTFA.l^{-1} treatment (Figure 3.27). Significant increases of 5% ($p<0.05$), 9% ($p<0.01$), 16% ($p<0.01$) and 13% ($p<0.01$) in "antenna size" (ABS/RC), were apparent from the 2.5 to the 160 mg NaTFA.l^{-1} treatment. ABS/RC can be used as a measure of the "antenna size" (Krüger *et al*, 1997; Strasser *et al*, 2004). This increase in "antenna size" (ABS/RC) probably occurred to compensate for the decrease in density of the reaction centres (RC/CS_0) due to inactivation of reaction centres resulting in a very small change in the quantum photochemistry ($\varphi_{P0} = F_v/F_m$, Figure 3.30 & 3.34). Decreases in density of reaction centres (RC/CS_0) of 3%, 6% and 7% ($p<0.01$ for all) were also apparent for the 10 to the 160 mg NaTFA.l^{-1} treatments. The specific trapping flux (TR_0/RC) increased by 4% ($p<0.05$), 3% ($p<0.01$), 14 ($p<0.01$) and 10% ($p<0.01$) respectively, from the 2.5 to the 160 mg NaTFA.l^{-1} treatment. Consequently the quantum efficiency of electron transport (φ_{E0}) decreased by 3% ($p<0.05$), 2% ($p<0.05$), 7% ($p<0.01$), 11% ($p<0.01$) and 16% ($p<0.01$) from the 0.625 to the 160 mg NaTFA.l^{-1} treatments.

Z. mays displayed significant decreases in the electron transport per cross section (ET_0/CS_0) of 8%, 11% and 15% ($p<0.01$ for all) for the 10 to 160 mg NaTFA.l^{-1} treatments (Figure 3.28). A significant increase in antenna size (ABS/RC) of 10%, 15% and 17% ($p<0.01$ for all), due to inactivation of reaction centres, were also apparent from the 10 to the 160 mg NaTFA.l^{-1} treatments. A concomitant decrease in density of reaction centres (RC/CS_0) of 11%, 12% and 8% ($p<0.01$ for all) were also apparent for the 10 to the 160 mg NaTFA.l^{-1} treatments. The specific trapping flux (TR_0/RC) increased by 8%, 12% and 14% ($p<0.01$ for all) from the 10 to the 160 mg NaTFA.l^{-1} treatment respectively. As a result of this the quantum efficiency of electron transport (φ_{E0}) decreased by 6%, 11% and 16% ($p<0.01$ for all) from the 10 to the 160 mg NaTFA.l^{-1} treatments.

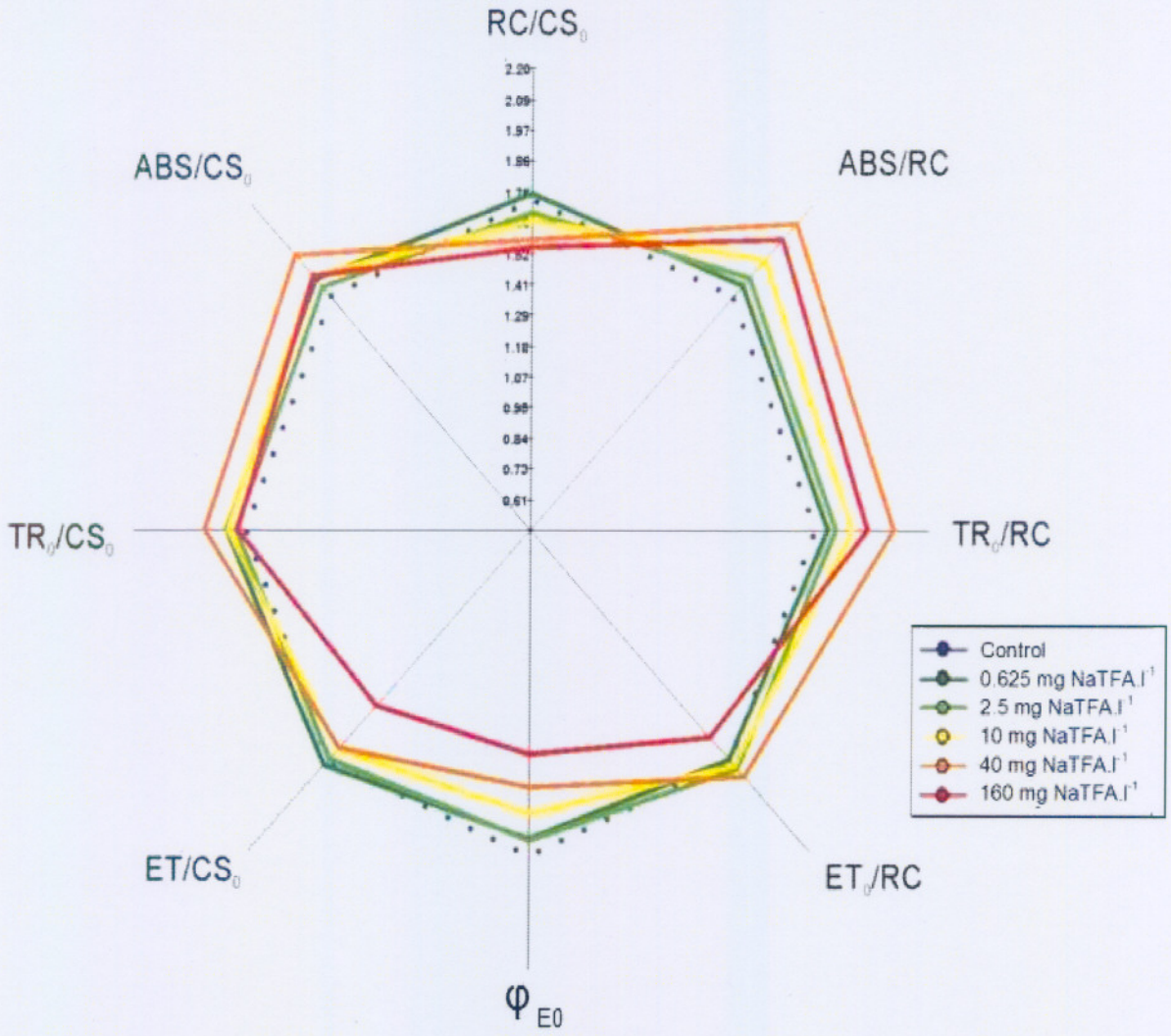

Figure 3.27: Specific and phenomenological energy fluxes through PSII in *P. vulgaris* after 12 days of different NaTFA treatments in water culture.

The same trend in changes with regard to the compensation for inactive reaction centres was also observed in the parameters of "antenna size" (ABS/RC), density of reaction centres (RC/CS_0) and electron transport per cross section (ET_0/CS_0) for *P. vulgaris* and *Z. mays* treated in sand, suggesting the same pattern of inhibition or stimulation (Figures not shown).

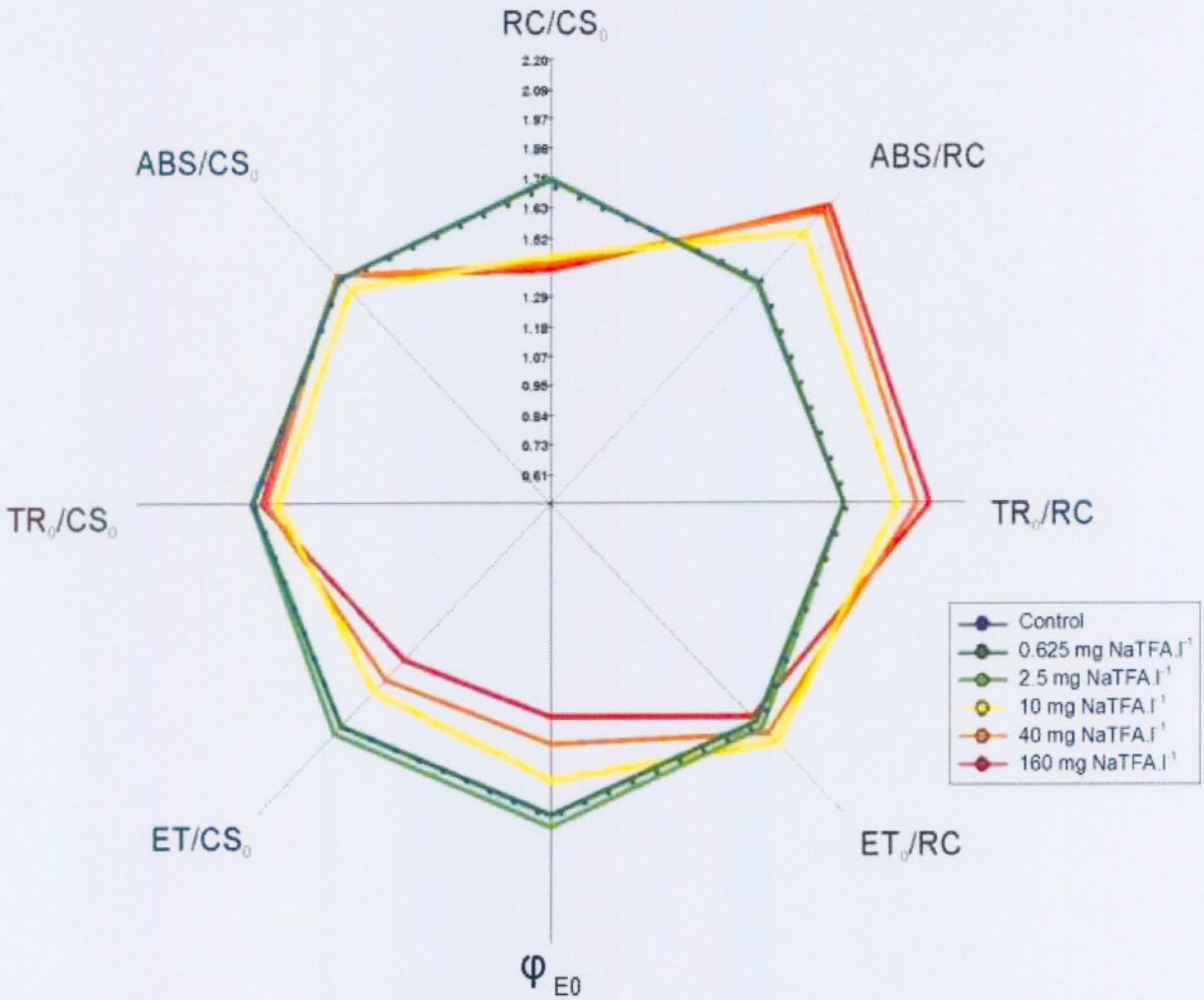

Figure 3.28: Specific and phenomenological energy fluxes of *Z. mays* after 12 days of different NaTFA treatments in water culture.

3.2.2.2 Sand culture

The performance index calculated on absorption basis (PI_{ABS}) proved to be a sensitive indicator of the effect of NaTFA on *P. vulgaris* cultivated in sand (Figure 3.29). The lowest concentration, 0.05 g NaTFA.m^{-2}, displayed no statistically significant change to the control. The PI_{ABS} of the 0.2 g NaTFA.m^{-2} treatment decreased by 19% ($p<0.01$) while the PI_{ABS} of the three higher treatments also displayed a decrease in PI_{ABS} of 7% (not statistically significant), 27% ($p<0.01$) and 40% ($p<0.01$) for the 0.8, 3.2 and 12.8 g NaTFA.m^{-2} treatments. Although the PI_{ABS} of both the 0.2 and 0.8 g NaTFA.m^{-2} treatments were lower than the control these deviated from a typical concentration dependant decrease. No apparent reason for this was evident.

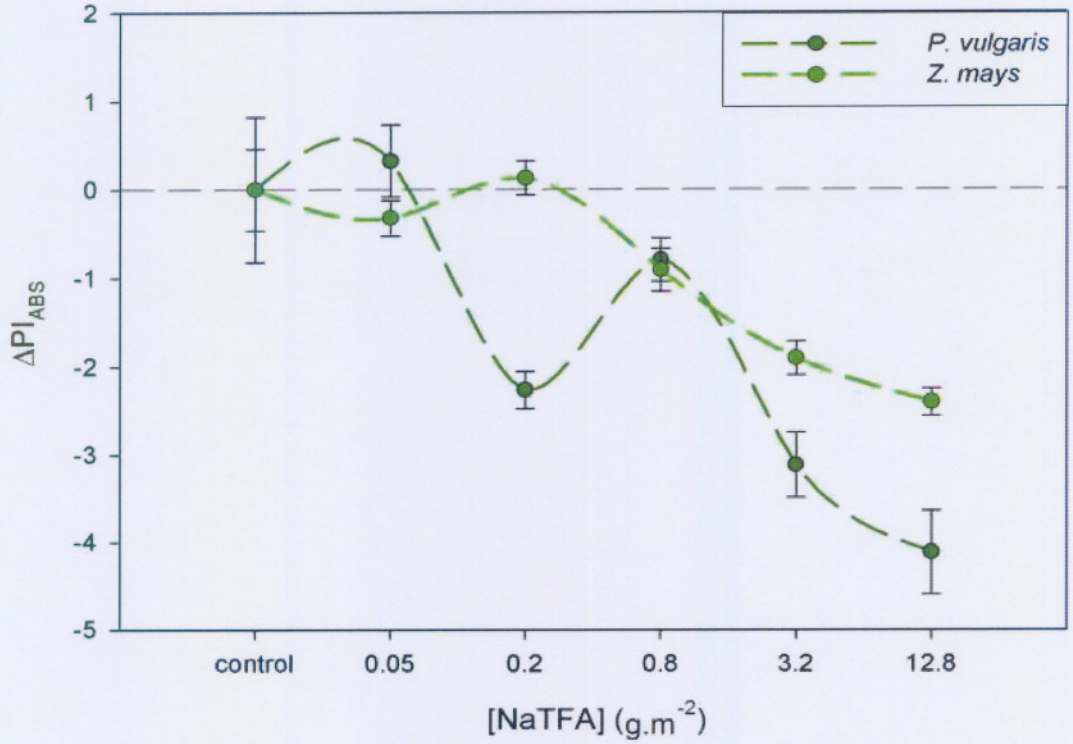

Figure 3.29: Effect of NaTFA treatment on change in performance index (PI_{ABS}) of *P. vulgaris* and *Z. mays* 3 days after treatment in sand culture.

The conversion of excitation energy to electron transport ($\Psi_0/(1-\Psi_0)$) proved to be the most sensitive component of the performance index (PI_{ABS}) for *P. vulgaris*, with an initial increase of 20% ($p<0.01$) at 0.05 g NaTFA.m^{-2} (Figure 3.30). For all the other treatments the conversion of excitation energy to electron transport ($\Psi_0/(1-\Psi_0)$) decreased significantly by 14%, 8%, 20% and 31% ($p<0.01$ for all) at the 0.2, 0.8, 3.2 and 12.8 g NaTFA.m^{-2} treatments. The quantum efficiency of primary photochemistry ($\varphi_{P0}/(1-\varphi_{P0})$) decreased by 8% ($p<0.01$) at the lowest NaTFA treatment of 0.05 g.m^{-2} and at the highest NaTFA treatment of 12.8 g.m^{-2} a significant decrease of 6% ($p<0.01$) was observed. The parameter RC/ABS referring to the chlorophyll content per area, i.e. the efficiency of absorption of light energy, did not change significantly with respect to the control. The quantum efficiency of the formation of reducing equivalents (φ_{R0}) increased from the 0.05 to the 12.8 g NaTFA.m^{-2} with 37%, 26%, 27%, 24% and 16% ($p<0.01$ for all) respectively, corresponding exactly to the measured stimulation in maximal photosynthetic rate (J_{max}) at all NaTFA treatments (Section 3.2.1). Thus it seems as though trifluoroacetate inhibition of electron transport may be mainly contributed to effects after Q_A^- on the photosynthetic electron transport chain and possible inhibition of FNR.

The changes in performance index (PI_{ABS}) of *Z. mays* (Figure 3.29), due to trifluoroacetate treatments, corresponded well with the photosynthetic gas exchange data (Section 3.2.1). The two lowest NaTFA treatments of 0.05 and 0.2 $g.m^{-2}$ displayed no significant changes to the control. Decreases in PI_{ABS} of 10% ($p<0.05$), 21% ($p<0.01$) and 26% ($p<0.01$) were observed at 0.8, 3.2 and 12.8 g $NaTFA.m^{-2}$ treatments.

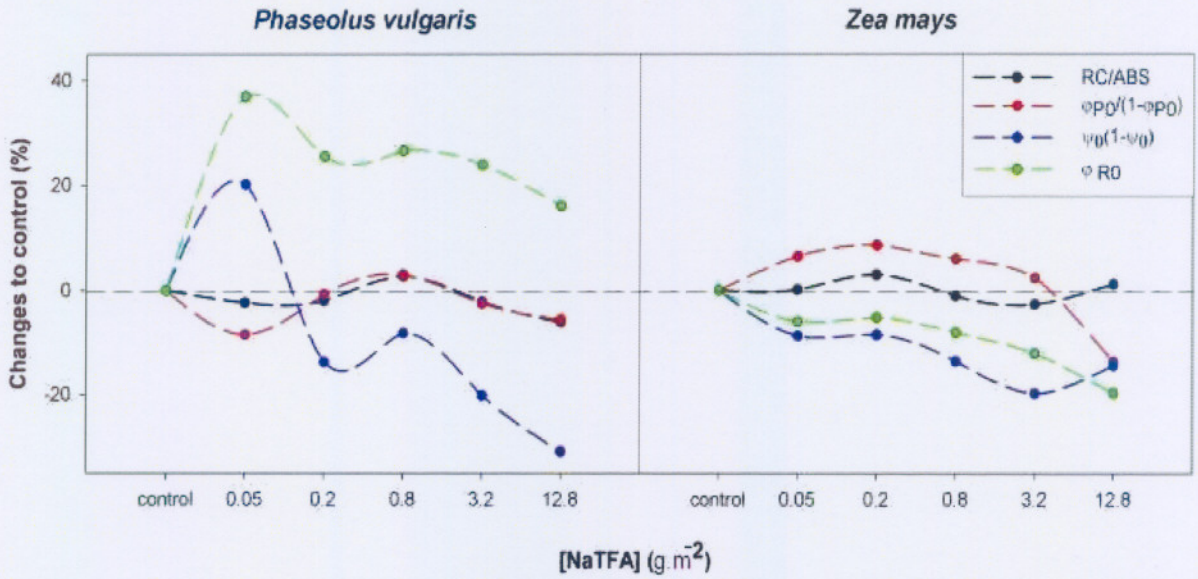

Figure 3.30: The effect of NaTFA treatment on the components of the performance index (PI_{ABS}) and the quantum efficiency of the formation of reducing equivalents of *P. vulgaris* (left) and *Z. mays* (right) cultivated in sand culture. Conversion of excitation energy to electron transport ($\Psi_0/(1-\Psi_0)$) and quantum efficiency of formation of reducing equivalents (φ_{R0}) clearly displays the greatest sensitivity to both stimulation and inhibition.

Just as in the case of *P. vulgaris*, the conversion of excitation energy to electron transport ($\Psi_0/(1-\Psi_0)$) of *Z. mays* proved to be the most sensitive component of the performance index (PI_{ABS}) (Figure 3.30). The treatments displayed a respective significant decrease in $\Psi_0/(1-\Psi_0)$ of 9% ($p<0.05$), 9%, 14%, 20% and 14% ($p<0.01$ for all the rest) from the 0.05 to the 12.8 g $NaTFA.m^{-2}$ treatment. The quantum efficiency of primary photochemistry ($\varphi_{P0}/(1-\varphi_{P0})$) was stimulated by 7%, 9%, 6% and 2% at the 0.05, 0.2, 0.8 and 3.2 g $NaTFA.m^{-2}$ treatments ($p<0.01$ for all). At the highest NaTFA concentration of 12.8 $g.m^{-2}$ a significant decrease in the quantum efficiency of primary photochemistry ($\varphi_{P0}/(1-\varphi_{P0})$) of 14% was observed ($p<0.01$). Except for a stimulation of 3% ($p<0,05$) at the 0.2 g $NaTFA.m^{-2}$ treatment, no other significant variations from the control were observed with respect to the efficiency of light absorption (RC/ABS) of NaTFA treated plants. The quantum efficiency of the formation of reducing equivalents (φ_{R0}) also decreased from the 0.05 to the 12.8 g $NaTFA.m^{-2}$ treatment

with 6% ($p<0.05$), 5% ($p<0.05$), 8% ($p<0.01$), 12% ($p<0.01$) and 19% ($p<0.01$) respectively corresponding to gas exchange data (Section 3.2.1).

3.2.2.3 Water culture

The performance index calculated on an absorption base (PI_{ABS}) also proved to be a very sensitive parameter for quantification of NaTFA-effects for both *P. vulgaris* and *Z. mays* treated in water culture. According to the PI_{ABS} values, both NaTFA treated *P. vulgaris* and *Z. mays* displayed no sign of recovery during the treatment period (Figure 3.31 and 3.33). For *P. vulgaris* leaves of different ages with marked differences in visible symptoms displayed exactly the same tendency with regard to change in performance index (PI_{ABS}), clearly displaying that increased developmental symptoms and effect on photosynthesis were not related (Figure 3.32). For these reasons only chlorophyll a fluorescence data measured on the older leaves after day 12 of treatment were discussed for both *P. vulgaris* and *Z. mays*.

For *P. vulgaris* changes in performance index (PI_{ABS}) corresponded well with the gas exchange data after 12 days of treatment. The performance index (PI_{ABS}) decreased by 7% ($p<0.05$), 27% ($p<0.01$), 39% ($p<0.01$), and 56% ($p<0.01$) for the 2.5 to the 160 mg NaTFA.l^{-1} treatments respectively (Figure 3.30). Efficiency of absorption of light (RC/ABS) decreased by 7%, 15% and 11% ($p<0.01$ for all) from the 10 to the 160 mg NaTFA.l^{-1} treatment respectively (Figure 3.34). The quantum efficiency of primary photochemistry ($\varphi_{P0}/(1- \varphi_{P0})$) displayed a significant decrease of 2% ($p<0.05$), 7% ($p<0.01$), 8% ($p<0.01$) and 13% ($p<0.01$) from the 2.5 to the 160 mg NaTFA.l^{-1} treatment. The quantum efficiency of the conversion of excitation energy to electron transport ($\Psi_0/(1- \Psi_0)$) displayed a decrease of 7% ($p<0.05$), 6% ($p<0.01$), 13% ($p<0.01$), 22% ($p<0.01$) and 30% ($p<0.01$) from the 0.625 to the 160 mg NaTFA.l^{-1} treatment. The quantum efficiency of the formation of reducing equivalents (φ_{R0}) decreased by 13% ($p<0.01$), 7% ($p<0.05$) and 7% ($p<0.05$) from the 10 to the 160 mg NaTFA.l^{-1} treatments respectively.

For *Z. mays*, just as for *P. vulgaris*, changes in performance index corresponded well with the gas exchange data after 12 days of treatment. The performance index (PI_{ABS}) decreased significantly by 26%, 45% and 40% ($p<0.01$ for all) for the 10 to the 160 mg NaTFA.l^{-1} treatments respectively (Figure 3.33).

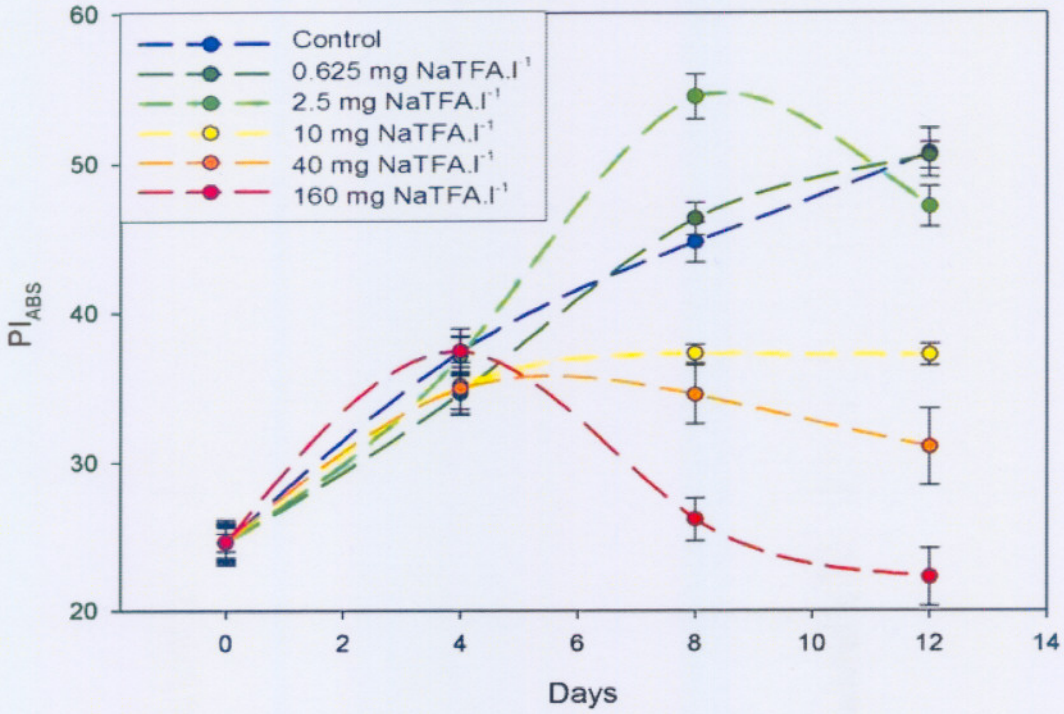

Figure 3.31: The effect of NaTFA treatments on PI_{ABS} of *P. vulgaris* over the treatment period in water culture. Values are normalised at the start of the treatment (day 0).

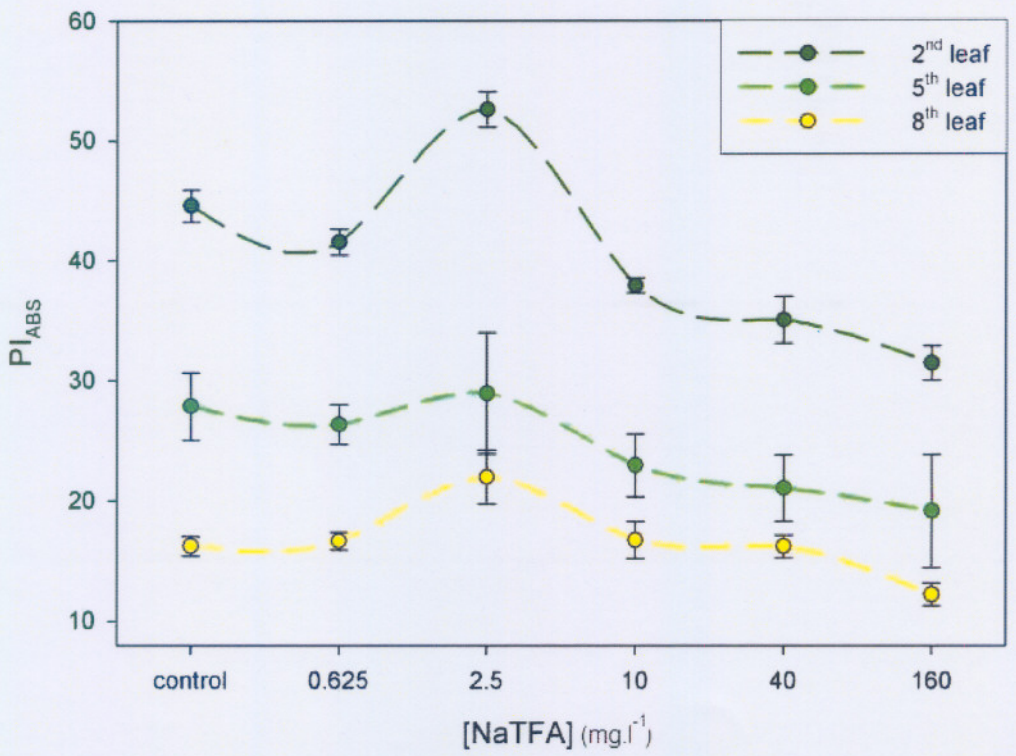

Figure 3.32: Effect of NaTFA treatment on leaves of different developmental stages of *P. vulgaris* after 8 days of treatment in water culture.

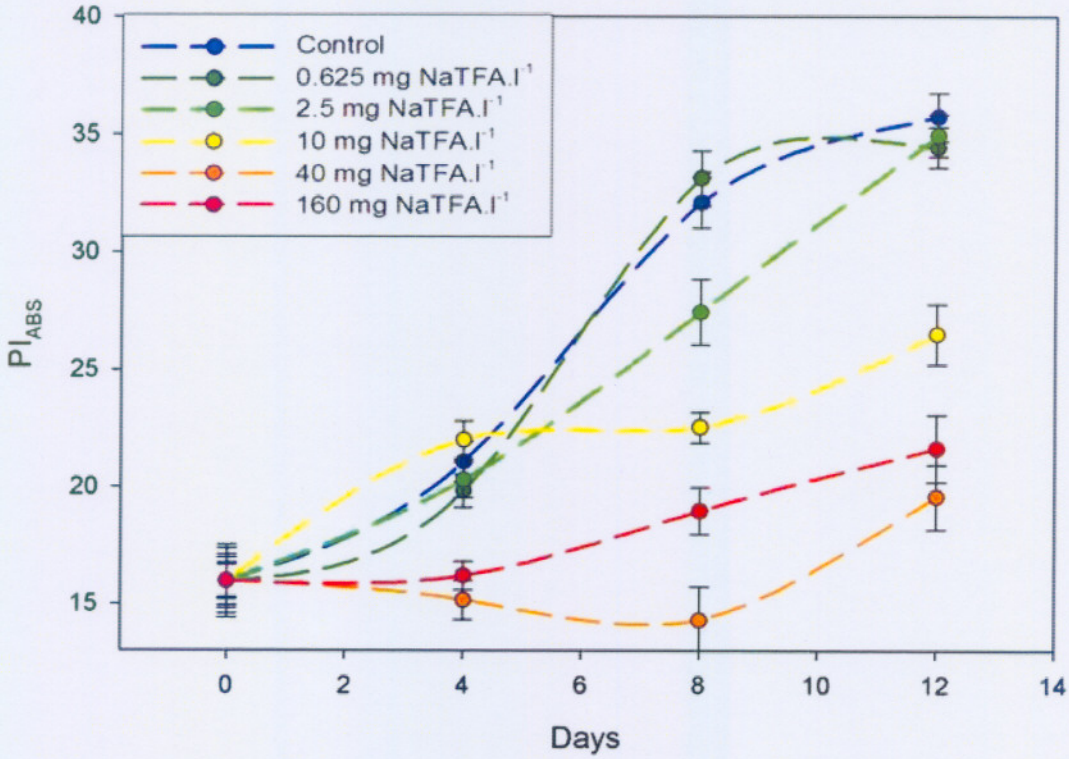

Figure 3.33: The effect of NaTFA treatments on PI_{ABS} of *Z. mays* over the treatment period in water culture. Values are normalised at the start of the treatment (day 0).

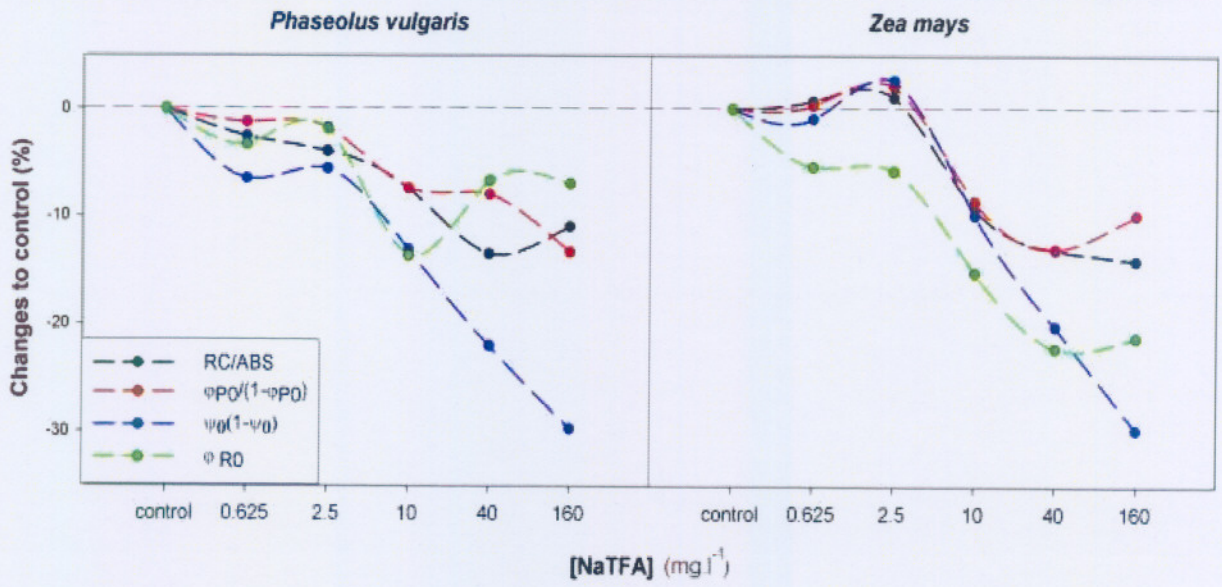

Figure 3.34: The effect of NaTFA treatment on the components of the performance index (PI_{ABS}) and the quantum efficiency of the formation of reducing equivalents of *P. vulgaris* (left) and *Z. mays* (right) cultivated in water culture. The conversion of excitation energy to electron transport ($\Psi_0/(1-\Psi_0)$) and quantum efficiency of the formation of reducing equivalents (φ_{R0}) clearly display the greatest sensitivity to inhibition especially for treated *Z. mays*.

The efficiency of light absorption (RC/ABS) decreased by 9%, 13% and 14% ($p<0.01$ for all) from the 10 to the 160 mg NaTFA.l^{-1} treatment respectively. The quantum efficiency of primary photochemistry ($\varphi_{P0}/(1- \varphi_{P0})$) displayed a significant decrease of 9%, 13% and 10% ($p<0.01$ for all) from the 10 to the 160 mg NaTFA.l^{-1} treatment. The quantum efficiency of the conversion of excitation energy to electron transport ($\Psi_0/(1- \Psi_0)$) displayed a decrease of 10%, 20% and 30% ($p<0.01$) from the 10 to the 160 mg NaTFA.l^{-1} treatment. The quantum efficiency of the formation of reducing equivalents (φ_{R0}) decreased significantly by 5% ($p<0.06$), 6% ($p<0.01$), 15% ($p<0.01$), 22% ($p<0.01$) and 21% ($p<0.01$) from the 0.625 to the 160 mg NaTFA.l^{-1} treatments respectively (Figure 3.34).

The trifluoroacetate treatments clearly displayed concentration dependant changes in the relative fluorescence transients of both *P. vulgaris* and *Z. mays* cultivated and treated in water culture for 12 days (Figure 3.35 and 3.36). So-called K-bands, around 0.3 ms, were not clearly visible for both trifluoroacetate treated *P. vulgaris* and *Z. mays*, since these bands were hidden by the dominating J-peaks. When transients were however normalised between 0.05 ms and 2 ms these K-peaks were noticeable (Figure 3.35a and 3.36a). According to the literature these K-bands can be explained by an imbalance within PSII between the electrons leaving the reaction centres at the acceptor side and the electrons donated by the donor side (Strasser, 1997). This phenomenon has been associated with the dissociation of the oxygen evolving complex (OEC) (Guissé *et al.*, 1995; Srivastava *et al.*, 1997). In *Z. mays,* however, the 2.5 mg NaTFA.l^{-1} treatment of *Z. mays* displayed a stimulation of the OEC function. Dominant J-peaks were also apparent for both trifluoroacetate treated *P. vulgaris* and *Z. mays* around 2 ms. The O to J-phase is related to the photochemical reduction of Q_A in PSII (Strasser *et al.*, 1995). The appearance of a J-peak indicates an inhibition of the dark reactions responsible for the reoxidation of the Q_A^- pool (Tsimilli-Michael *et al.*, 1999), with the exception of the 2.5 mg.l^{-1} treatment of *Z. mays* which displayed a negative J-peak, suggesting stimulation of the dark reactions, i.e. stimulation of the reoxidation of the Q_A^- pool.

So-called I-bands were also apparent (Figure 3.35a and 3.36a) around 30 ms for both *P. vulgaris* and *Z. mays*, but especially apparent in the case of *Z. mays.* According to Schansker *et al.* (2006), fluorescence changes in the I–P phase may provide information on the inactivation state of ferredoxin $NADP^+$ reductase (FNR). The more inactive FNR is, the longer it takes to fully reduce the Q_A pool and reach F_m. According to the curves shown for day 12 the positive ΔI-bands increased almost directly proportional with the concentration of the NaTFA treatments. If the theory of Schansker *et al.* (2006) holds true, it means that increasing NaTFA concentration increases inactivation of FNR, leading to an increased Q_A^- pool. This aspect was also quantified by the newly developed parameter φ_{R0} (Personal communication to GHJ Krüger by RJ Strasser, 2006), which represents the quantum

efficiency of the formation of reducing equivalents (Figure 3.30 and 3.34). When the calculated values for φ_{R0} were compared with the maximal assimilation rate (J_{max}) a remarkable correlation was found, especially for *Z. mays* treated in water culture (Figure 3.37), suggesting that photosynthesis was mainly inhibited due to a decrease in the formation of NADPH.

The same trend regarding the appearance of K-bands, J-peaks and I-bands was also observed in the normalised fluorescence transients of *P. vulgaris* and *Z. mays* cultivated and treated in sand, suggesting a similar pattern of inhibition or stimulation (Figures not shown).

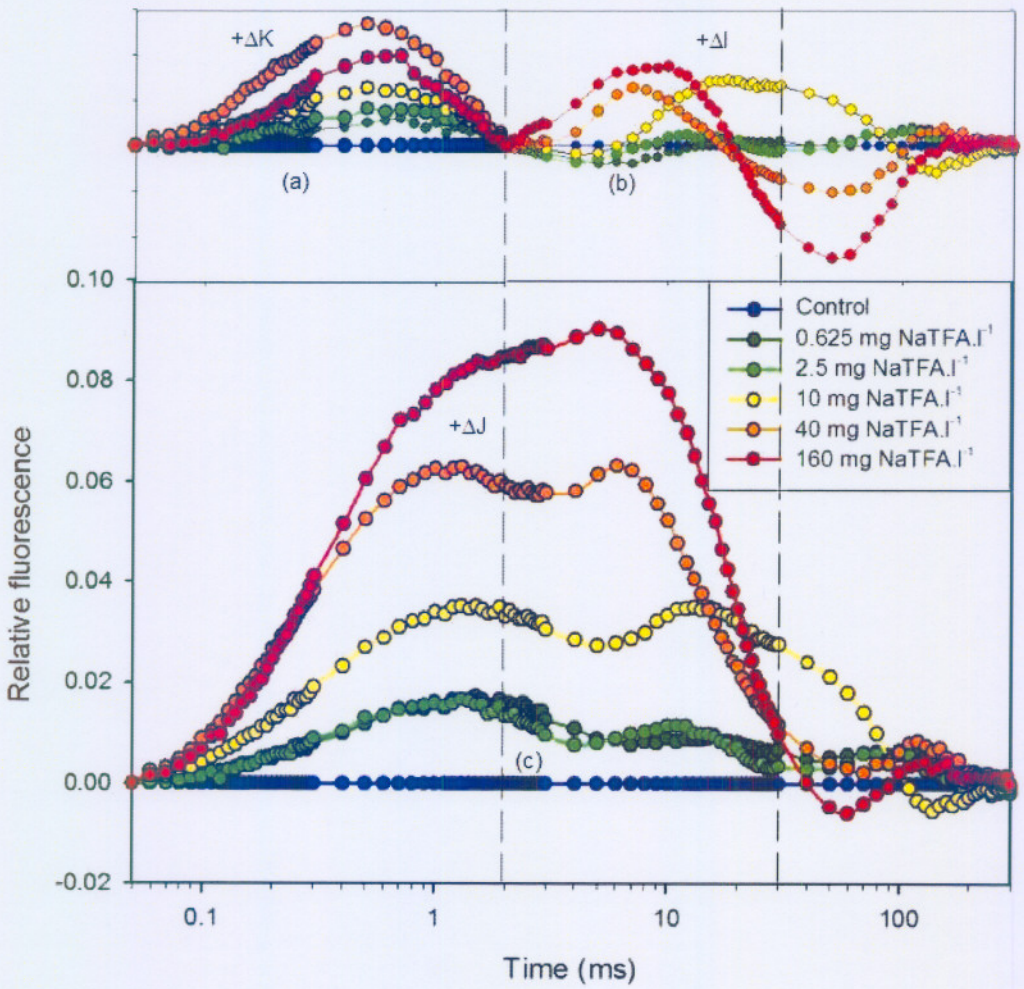

Figure 3.35: Change in the chlorophyll a fluorescence transients of *P. vulgaris* after 12 days of treatment in water culture (expressed as W = f(t)) normalised between F_0 and F_J (W = $(F-F_0)/(F_J-F_0)$, $\Delta W = W_{treatment} - W_{control}$) (a) , F_J and F_m (W = $(F-F_J)/(F_m-F_J)$, $\Delta W = W_{treatment} - W_{control}$) (b) and between F_0 and F_m (W = $(F-F_0)/(F_m-F_0)$, $\Delta W = W_{treatment} - W_{control}$) (c). ΔK-bands and ΔJ-peaks as well as ΔI-bands are clearly visible.

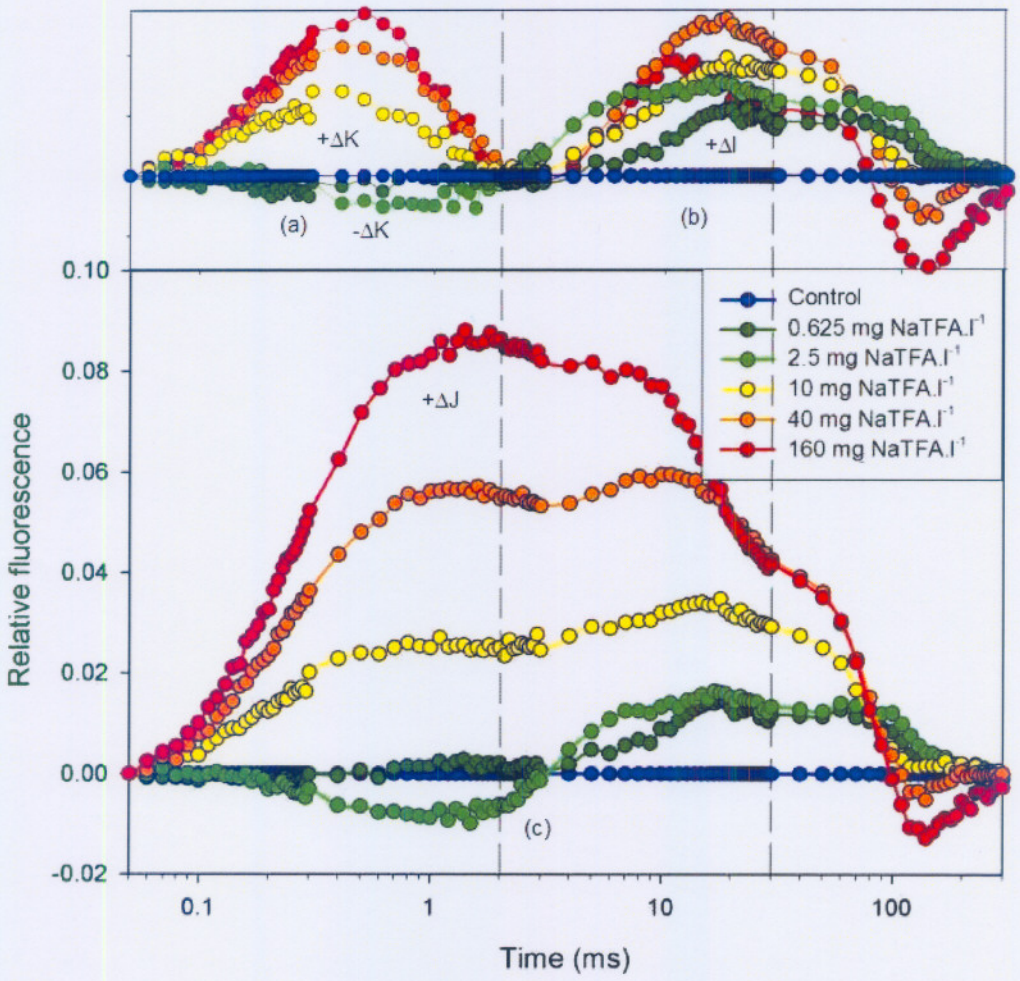

Figure 3.36: Change in the chlorophyll a fluorescence transients of *Z. mays* after 12 days of treatment in water culture (expressed as W = f(t)) normalised between F_0 and F_J (W = $(F-F_0)/(F_J-F_0)$, $\Delta W = W_{treatment} - W_{control}$) (a) , F_J and F_m (W = $(F-F_J)/(F_m-F_J)$, $\Delta W = W_{treatment} - W_{control}$) (b) and between F_0 and F_m (W = $(F-F_0)/(F_m-F_0)$, $\Delta W = W_{treatment} - W_{control}$) (c). ΔK-bands and ΔJ-peaks as well as ΔI-bands are clearly visible.

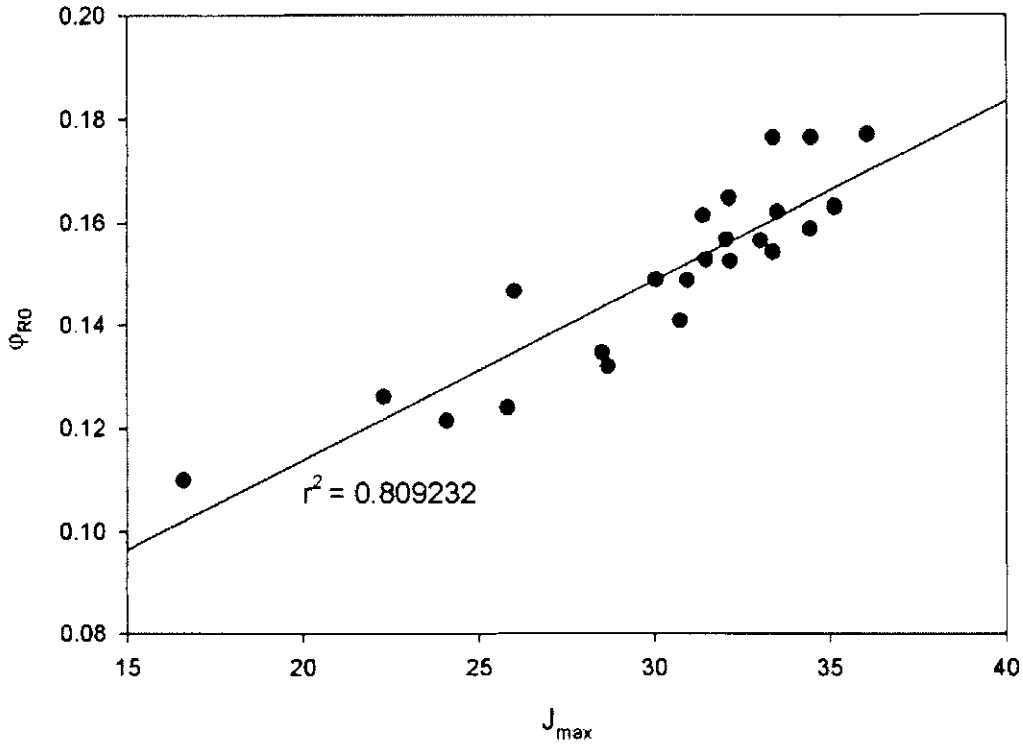

Figure 3.37: Regression showing the relationship between the RuBP regeneration capacity (J_{max}) and the quantum efficiency of the formation of reducing equivalents (φ_{R0}) for *Z. mays* plants after 12 days of different trifluoroacetate treatments in water culture.

3.2.3 Rubisco activity

Trifluoroacetate treatment displayed significant effects on both the initial and total Rubisco activity calculated on a leaf area basis for *P. vulgaris* after 13 days of treatment in water culture (Figure 3.38). A statistically nonsignificant increase of 19% was observed in initial Rubisco activity followed by decreases of 11%, 8% and 3% at the 10 to the 160 mg NaTFA.l^{-1} treatment respectively. Decreases in total Rubisco activity of 8% ($p<0.05$), 14% ($p<0.01$), 29% ($p<0.05$), 27% ($p<0.01$) and 15% for the 0.625 to the 160 mg NaTFA.l^{-1} treatment respectively. The activation state, which is the initial Rubisco activity expressed as the percentage of the total activity, displayed a significant increase of 21% ($p<0.05$) at the 0.625 mg NaTFA.l^{-1} treatment (Data not shown).

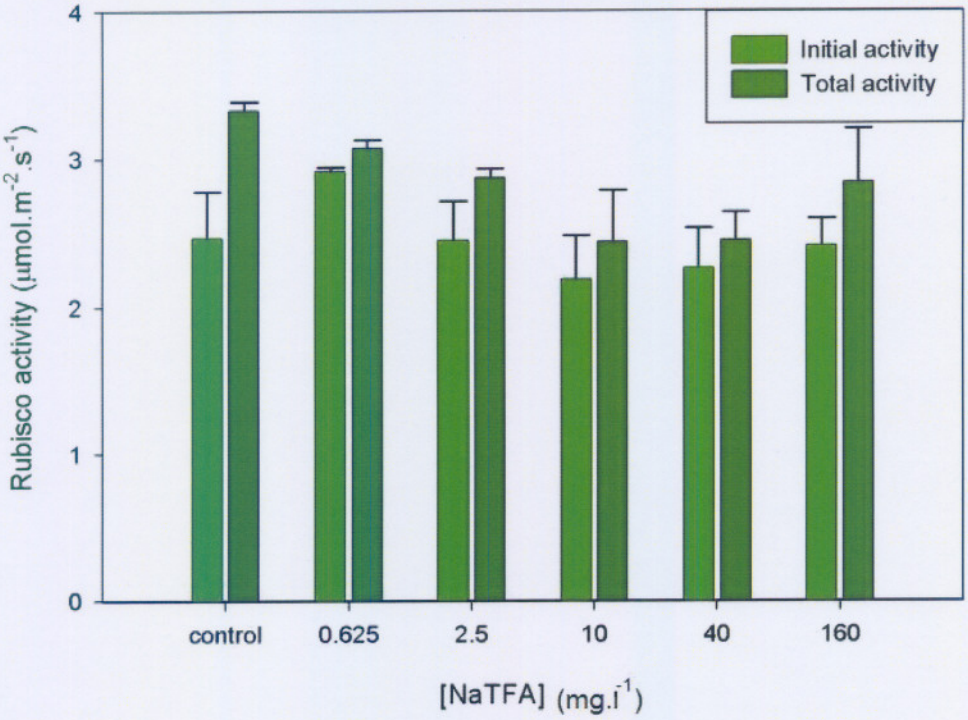

Figure 3.38: Effect of NaTFA treatments on the initial and total Rubisco activity of *P. vulgaris*, cultivated in water culture, expressed as activity on a leaf area basis (13 days of treatment). Each point represents the average of four to five replicates.

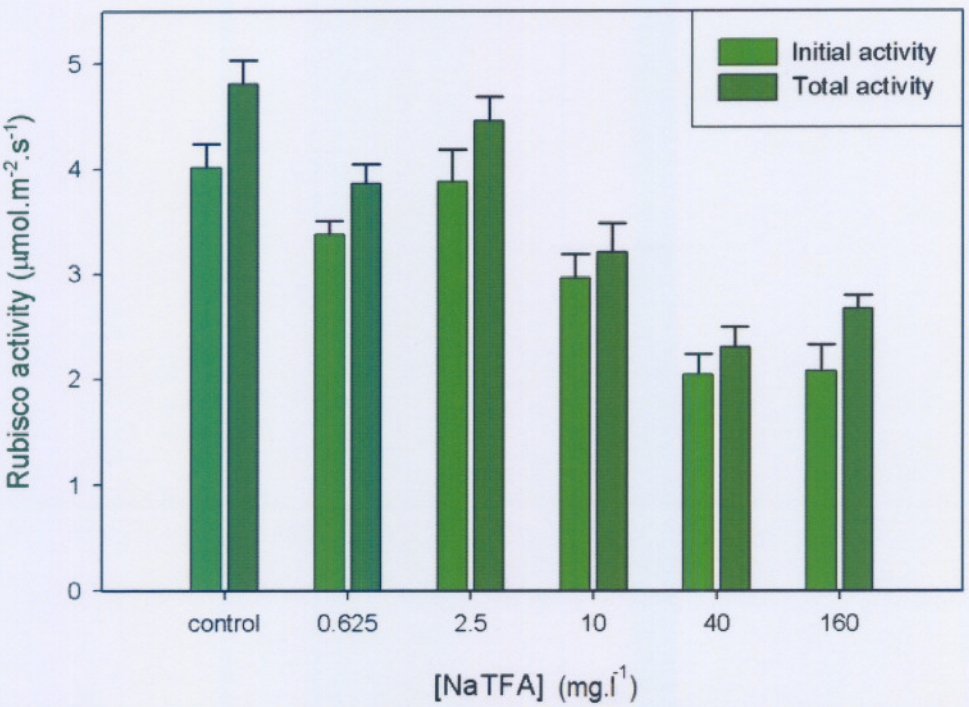

Figure 3.39: Effect of NaTFA treatments on the initial and total Rubisco activity of *Z. mays*, cultivated in water culture, expressed as activity on leaf area basis (13 days of treatment). Each point represents the average of four to five replicates.

Z. mays displayed significant reduction in the initial and total Rubisco activity calculated on a leaf area basis, with increasing trifluoroacetate concentration (Figure 3.39), which corroborates photosynthetic gas exchange data that displayed a decrease in carboxylation efficiency (Section 3.2.1). Decreases in initial activity of 16% ($p<0.05$), 4%, 26% ($p<0.01$), 49% ($p<0.01$) and 48% ($p<0.01$) were observed for the 0.625 to the 160 mg NaTFA.l^{-1} treatment respectively, while decreases in total activity of 20% ($p<0.01$), 8%, 32% ($p<0.01$), 52% ($p<0.01$) and 46% ($p<0.01$) where also observed for these same treatments.

The fact that decreases in both initial activity and total activity were observed for both *P. vulgaris* and *Z. mays* with no great change in the activation state (Data not shown) suggests a decrease in the of Rubisco levels. This decrease in Rubisco may well have been caused by nutrient shortages if one considers the initial loss of root biomass for both *P. vulgaris* and *Z. mays* (Section 3.1.4). Literature however suggests that this decrease can also be caused as a result conformational changes in the protein structure since it is theoretically possible for halogenated acetates to alkylate the sylfhydryl or amino groups in proteins (Hance & Holly, 1963; Foy, 1969). Chang and Cai (2005) also showed that it is possible for trifluoroacetate to methylate aldehydes and possibly some amino acids.

For *Z. mays* the decrease in Rubisco activity corresponded with the decrease in carboxylation efficiency (CE) observed in photosynthetic gas exchange data (Section 3.2.1). *P. vulgaris* however displayed no decrease in carboxylation efficiency (CE), while displaying some decreases in Rubisco activity although not as severe as *Z. mays*.

3.2.4 Photosynthetic electron transport in isolated thylakoids

Both trifluoroacetate and trichloroacetate had marked concentration dependent effects on the electron transport of isolated thylakoid membranes in the system, $H_2O \rightarrow PSII \rightarrow FeCy$ (Figure 3.39). The average oxygen evolution rate for untreated thylakoids was 359 µmol O_2.mg Chl^{-1}.h^{-1}. At the lowest NaTFA treatment of 0.00005 mmol.l^{-1} a significant stimulation of 9% ($p<0.05$) occurred in oxygen evolution rate while a significant decrease ranging from 10% to 52% ($p<0.01$ for all) occurred at concentrations ranging from 0.005 to 100 mmol.l^{-1} respectively. The same trend was observed using NaTCA, but in this case no significant stimulation was observed at low concentrations. Significant decreases ranging from 20% to 61% ($p<0.01$ for all) was observed in the oxygen evolution rate for the 0.005 to the 100 mmol.l^{-1} treatments, respectively.

The inhibition of electron transport by trifluoroacetate in thyakoids correlates with the *in vivo* chlorophyll a fluorescence data. If a bioaccumulation factor of 10 (Thompson *et al.*, 1994b)

were considered, the 0.625 to 160 mg NaTFA.l^{-1} treatments would have an internal NaTFA concentration of 5.24 to 1341 mg trifluoroacetate.l^{-1} respectively (Table 2.2). For these treatments, decreases of 7% to 30% respectively in electron transport past Q_A was observed (measured with chlorophyll a fluorescence, Section 3.2.2). This is comparable to the 0.01 to the 10 mmol NaTFA.l^{-1} (1.37 – 1370 mg trifluoroacetate.l^{-1}) of the *in vitro* treatments and thus falls in the same concentration range which displayed decreases in oxygen evolution of 18% to 27% ($p<0.01$ for all) respectively.

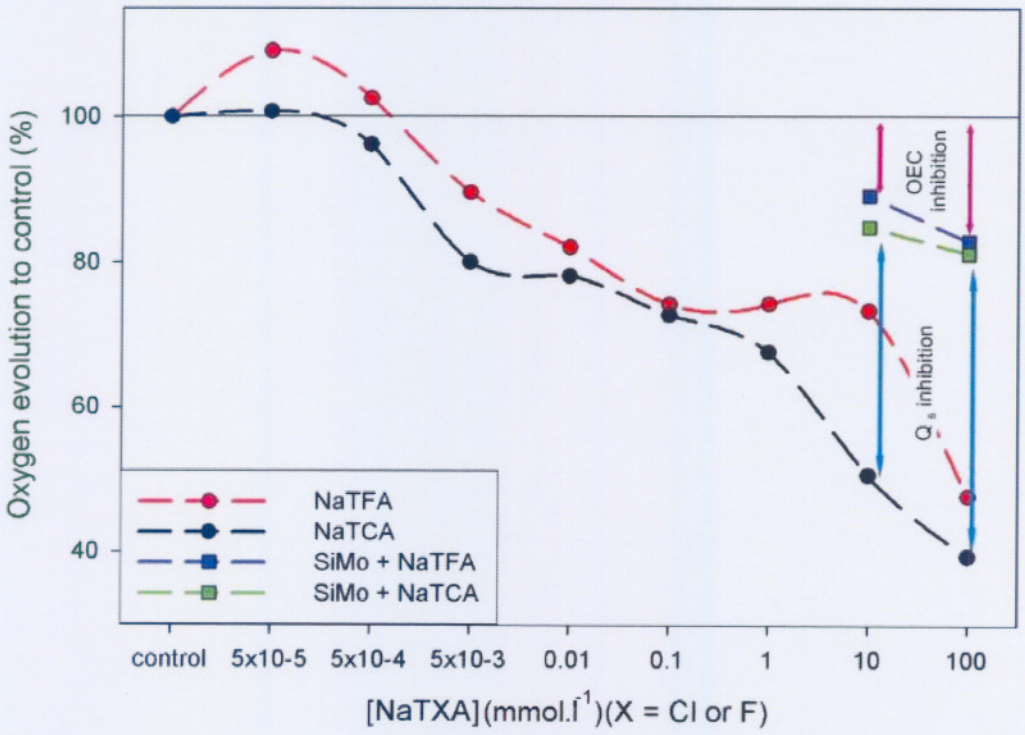

Figure 3.40: Change in oxygen evolution rate of isolated bean thylakoid membranes (within 1 min) treated with different NaTFA and NaTCA concentrations. Inhibition at high concentration is partly alleviated by SiMo indicating both inhibition of Q_B (blue arrows) and the OEC (red arrows) on the photosynthetic electron transport chain by trifluoroacetate.

According to the change in O_2 evolution rate of treated bean thylakoids (Figure 3.39) it is apparent that trichloroacetate has a larger inhibition for all concentrations used compared to trifluoroacetate. This phenomenon is also corroborated by the data of Strauss *et al.* (2004), which displayed greater trichloroacetate inhibition in all gas exchange and chlorophyll a fluorescence parameters measured in plants cultivated and treated in exactly the same sand cultivation experimental setup than the current trifluoroacetate experiment. These differences

in phytotoxicity may be attributed to the differences in chemical structure. Firstly trifluoroacetate is slightly more polar with a resulting lower K_{ow} (-2.1), making trifluoroacetate less capable to intrude into the lipophilic environments of membranes. Secondly trifluoroacetate is very stable with no recorded degradation in plants (Thompson *et al.*, 1994b). It has conversely been shown that the *in vivo* degradation of trichloroacetate to phosgene, chloroform and hydrochloric acid is possible (Weissflog *et al.*, 2007). It is believed that the formation of these toxic degradation products of trichloroacetate, and the concomitant release of protons may be responsible for severe damage to membranes and cell structures (Weissflog *et al.*, 2007).

The oxygen evolution rate recovered by 34% and 42% for the 10 and 100 mmol NaTCA.l^{-1} treatment when SiMo was added to the reaction solution, while 10 and 100 mmol NaTFA.l^{-1} treatments recovered by 18% and 35% respectively. According to literature, SiMo causes conformational changes in the stacking of the thylakoid membranes where PSII is situated, making it able for FeCy to receive an electron directly from Q_A that is situated on PSII (Trebst, 1999). The fact that SiMo alleviates both trifluoroacetate and trichloroacetate inhibition suggests that both these compounds inhibit photosynthetic electron transport between Q_A and the binding of a plastoquinone (PQ) to the Q_A binding site (Q_B). This inhibition between Q_A and Q_B corresponds to the appearance of a J-peak (Figure 3.23 and 3.24) observed for *in vivo* chlorophyll a fluorescence measurements, suggesting a DCMU type inhibition although much less severe. It must however be stressed that the chlorophyll a fluorescence data (Figure 3.35 and 3.36) suggest that the main inhibition is located further on in the electron transport chain due the appearance of an I-peak, indicating negative effects by trifluoroacetate near FNR. A true DCMU type of inhibition is further ruled out by the fact that there was no apparent change in the time to reach F_m (T_{fm}).

The inhibition remaining after the addition of SiMo may be attributed to the possible uncoupling of the OEC, which is also correlated by the so-called K-bands described for the *in vivo* chlorophyll a fluorescence measurements (Section 3.2.2). These observations also corroborates the finding of Govindjee *et al.* (1997) that trichloroacetate inhibits electron transport between Q_A and Q_B, in addition to some minor effects on the electron acceptor side of PSII.

It must however be stressed once again that the inhibition on the OEC and between Q_A and Q_B is not the only point of inhibition on the electron transport chain since normalised chlorophyll a fluorescence transients suggest that inhibition of FNR also occurs (Section 3.2.2). Electron transport measurements further on in the electron transport chain (between PQ and FNR) are however needed to explain these chlorophyll a fluorescence measurements.

Chapter 4

Discussion

4.1 Discussion and integration of data

From the experimental data presented in Chapter 3, it is clear that trifluoroacetate markedly affected photosynthesis as well as growth and development of the experimental C_3 and C_4 plants. Because it appears that the effects on photosynthesis and growth are not directly connected they, will be discussed separately.

A striking observation made in the present study was the phenomenon that, at low concentrations, trifluoroacetate had a stimulatory effect on growth and on some photosynthetic parameters during the course of the experimental growth period. In the literature the terms hormesis or hormoligosis have been used to describe the stimulatory effect of a sub-inhibitory concentration of a toxic substance. This phenomenon is well known for many toxic substances including fluoride. These apparent stimulations should however be interpreted with caution, as this phenomenon is generally just the unnatural re-allocation of resources at the expense of the intended sink (Treshow & Harner, 1968; Bunce, 1985).

4.1.1 Growth and Development

In both *P. vulgaris* and *Z. mays*, trifluoroacetate treatment affected root growth negatively even at the lowest trifluoroacetate levels (0.625 mg $NaTFA.l^{-1}$), while shoot growth was unchanged or even stimulated at these low treatment concentrations and subsequently inhibited at higher treatment concentrations (Section 3.1.2). The inhibition of root growth by trifluoroacetate corresponds to the observed inhibition of root growth caused by Dalapon and trichloroacetate (Ingle & Rogers, 1961).

The changes in shoot to root ratios caused by trifluoroacetate may well be attributed to two factors. Firstly, the stimulatory tendency observed in shoot growth (stimulation in internode length) may well be attributed to an initial increase in auxin levels (Cleland, 1995) caused by low concentrations of trifluoroacetate since this is supported by literature on the changes in auxin levels due to trichloroacetate (Funderburk & Davis, 1960; Mashtakov *et al.*, 1967; Sutinen *et al.*, 1997). This is also further supported by the initial increase in cotyledon mass observed in the bioassay experiment (Section 3.1.5). Secondly, since root growth inhibition was severe, especially in *Z. mays*, it is more likely that the reduction in biomass was due to nutrient shortages caused by reduced root growth. Since Prasad and Blackman (1964)

observed that Dalapon, an analogous compound with similar phytotoxic effects directly inhibited meristematic activity in the root tip, it may be hypothesised that the inhibition of root growth by trifluoroacetate may have a similar origin. The decrease in chlorophyll content in *Z. mays* (Section 3.1.4), the observation of an increase in starch grains (Section 3.1.6) and the reduced Rubisco total activity (Section 3.2.3) in trifluoroacetate treated plants also corresponds to the typical symptoms of nutrient shortages. Nitrogen (N) and phosphate (P) shortages induces changes in carbon partitioning with increases in sucrose and starch in leaves, while similar effects are also displayed in magnesium (Mg) and potassium (K) shortages with additional impairment of phloem transport and consequently a reduction of root growth (Hermans *et al.*, 2006). However it must once again be stressed that no nutrient analyses of plant material has been done as yet.

Higher levels of trifluoroacetate seemed to stimulate axillary bud development and to decrease leaf expansion in *P. vulgaris*, suggesting a possible decrease in auxin levels (Cleland, 1995). Although no literature exists on possible plant hormonal effects induced by trifluoroacetate, studies have been able to show trichloroacetate-induced increases and decreases in auxin levels (Mashtakov *et al.*, 1967; Parshakova & Mashtakov, 1967). Trifluoroacetate's possible effect on auxin levels may have contributed to the observed growth effects. This argument however remains speculative since no analyses of actual hormone levels have been done as yet. One possible explanation for the growth effects observed is the fact that trifluoroacetate can methylate aldehydes as well as similar carbon molecules (Chang & Cai, 2005). It is therefore theoretically possible for trifluoroacetate to methylate auxin molecules and in this manner either increasing or decreasing their auxin activity.

The severely deformed leaves observed in *P. vulgaris* at higher trifluoroacetate can be attributed to two factors. Firstly it could be due to the higher levels of TFA on the tips of leaves slowing down cell growth directly and causing epinasty as described by Davison *et al.* (1997). It is however believed that trifluoroacetate just like trichloroacetate, affects the auxin levels in plants and that the observed symptom of epinasty may well have been caused by changes in hormone levels. Auxin increases the production of aminocyclopropane carboxylic acid (ACC) in the roots, which is then transported via the xylem to the leaves where it is readily converted to ethylene. High ethylene levels are known to induce epinasty (Bradford & Yang, 1980). However, the observation that the symptoms of epinasty disappeared and that leaf expansion in new growth were also severely impaired by the end of the treatment period, suggested that auxin levels became limiting (Taiz, 1984; Cleland, 1995). This decrease in auxin levels was also supported by the apparent stimulation of axillary bud development.

The deformed younger parts of leaves of trifluoroacetate treated *Z. mays* may also be attributed to hormonal effects in the leaf base where leaf expansion and cell division was disturbed by changes in auxin levels (Taiz, 1984).

It is thus likely that only the necrotic spots on the edges of the leaves were directly caused by the higher trifluoroacetate levels and that the epinasty and eventual seizure of leaf expansion may be attributed to changes in auxin levels or activity caused by trifluoroacetate.

4.1.2 Photosynthesis

From the data presented in Chapter 3 (Section 3.2) it is apparent that photosynthesis in both C_3 and C_4 plants were markedly affected by trifluoroacetate treatments. These effects were also clearly dose dependent with initial stimulations apparent in most parameters at low trifluoroacetate concentrations followed by inhibition later on in the experimental period. Although *Z. mays* did not display such striking growth abnormalities compared to those displayed by *P. vulgaris*, *Z. mays* were clearly more sensitive to the effects on photosynthesis by trifluoroacetate. This sensitivity was clearly apparent as *Z. mays* did not only display greater inhibition of photosynthesis but these effects were apparent even after 4 days of treatment compared to *P. vulgaris*, which initially displayed some stimulation followed by inhibition after 8 days of treatment (Section 3.2). This stimulation in photosynthesis of *P. vulgaris* is nowhere more apparent than in the stimulation of the maximal assimilation rate (J_{max}) and quantum efficiency of the production of reducing equivalents (φ_{R0}) in the sand culture experiment (3 day treatment period). Photosynthesis in *P. vulgaris*, a representative of C_3 photosynthesis is thus clearly not as negatively affected by trifluoroacetate. The question can now be asked what the physiological and biochemical basis of inhibition of photosynthesis is and where the key sites of inhibition may be located. The possible mechanism of trifluoroacetate-induced inhibition of photosynthesis in *P. vulgaris* and the possible sites of inhibition will now be discussed with reference to the experimental data and the scheme presented in Figure 4.1:

1) Stomatal limitation contributed markedly to the decrease in photosynthesis in *P. vulagris* (Section 3.2.1). Although a slight stimulation in stomatal conductance was apparent early on (Day 4) after treatment at low NaTFA concentrations (0.625 $mg.l^{-1}$), it soon gave way to increased inhibition with increasing trifluoroacetate dose. Trifluoroacetate thus increased stomatal closure in plants after a period of treatment (Figure 4.1, 1).

2) Enzyme analysis showed that Rubisco activity was reduced with increasing trifluoroacetate concentration (Section 3.2.3). This inhibition may well be attributed to the fact that trifluoroacetate is theoretically able to alkylate or methylate the amino or sulfhydryl groups of proteins, bringing about conformational changes and

subsequently reduced activity (Hance & Holly, 1963; Foy, 1969; Chang & Cai, 2005). Another reason for reduced Rubisco activity may the fact that trifluoroacetate reduces ATP synthesis due to inhibition of photosynthetic electron transport by trifluoroacetate, decreasing the activation state of Rubisco (Section 3.2.3). Trifluoroacetate thus inhibits the assimilation of CO_2 by Rubisco (Figure 4.1, 2).

3) The RuBP regeneration capacity was reduced by increasing trifluoroacetate treatments in *P. vulgaris* (Section 3.2.1). This inhibition may have been caused by the reduction in PCR cycle enzyme reaction rates, since phosphoglycerate kinase and ribulose-5-phosphate kinase requires ATP and glyceraldehyde-3-phosphate dehydrogenase requires NADPH, and reduction in photosynthetic electron transport decreased NADPH and ATP production (Section 3.2.2). Although stimulation in RuBP regeneration capacity (J_{max}) and quantum efficiency for the formation of reducing equivalents (φ_{R0}), by trifluoroacetate was apparent in the sand experiments (3 days of treatment), the water culture (measured after 12 days of treatment) experiments showed that this was only an initial and temporary stimulation. Trifluoroacetate thus probably inhibit the PCR cycle due to reduced production of ATP and NADPH and subsequently RuBP regeneration (Figure 4.1, 3).

4) After the addition of SiMo in the measuring of oxygen evolution rate, i.e. bypassing the Q_B binding site that may have been affected by NaTFA, the restoration of the oxygen evolution rate was not complete. This suggests that the oxygen evolving complex (OEC) was increasingly uncoupled from PS II with increasing trifluoroacetate concentrations and corroborates the finding of Govindjee *et al* (1997) and the appearance of K-bands (Guissè *et al.*, 1995) in the chlorophyll a fluorescence transients (Section 3.2.2). The uncoupling of the OEC once again suggests that trifluoroacetate may induce conformational changes in proteins (Hance & Holly, 1963; Foy, 1969; Chang & Cai, 2005). Trifluoroacetate thus uncouples the OEC from PSII thus inhibiting the photosynthetic electron transport chain (Figure 4.1, 4).

5) The chlorophyll a fluorescence data indicated that the conversion of trapped excitation energy to electron transport beyond Q_A was inhibited (Section 3.2.2) while the oxygen evolution measured in thylakoids (Section 3.2.4) suggested that inhibition on electron transport also occurs between Q_A and Q_B (Govindjee *et al.*, 1997). Although this suggests a DCMU effect, the inhibition was much smaller than a typical DCMU inhibition. The appearance of dominant I-bands in the chlorophyll a fluorescence transients suggested that the main inhibition might be located further on in the photosynthetic electron transport chain (Personal communication to Krüger GHJ; Strasser RJ, 2006). Trifluoroacetate thus inhibits the binding of a

plastoquinone to the Q_B binding site on the D1 protein of PSII due to possible binding of trifluoroacetate close to Q_B (Figure 4.1, 5).

6) The main inhibition on electron transport, as suggested by chlorophyll a fluorescence data (appearance of I-bands), appears to be close to ferredoxin $NADP^+$ reductase (FNR). This inhibition and subsequent reduction in NADPH may well be partly responsible for the reduction in RuBP regeneration. Trifluoroacetate thus inhibits the enzyme FNR and subsequently the formation of NADPH (Figure 4.1, 6).

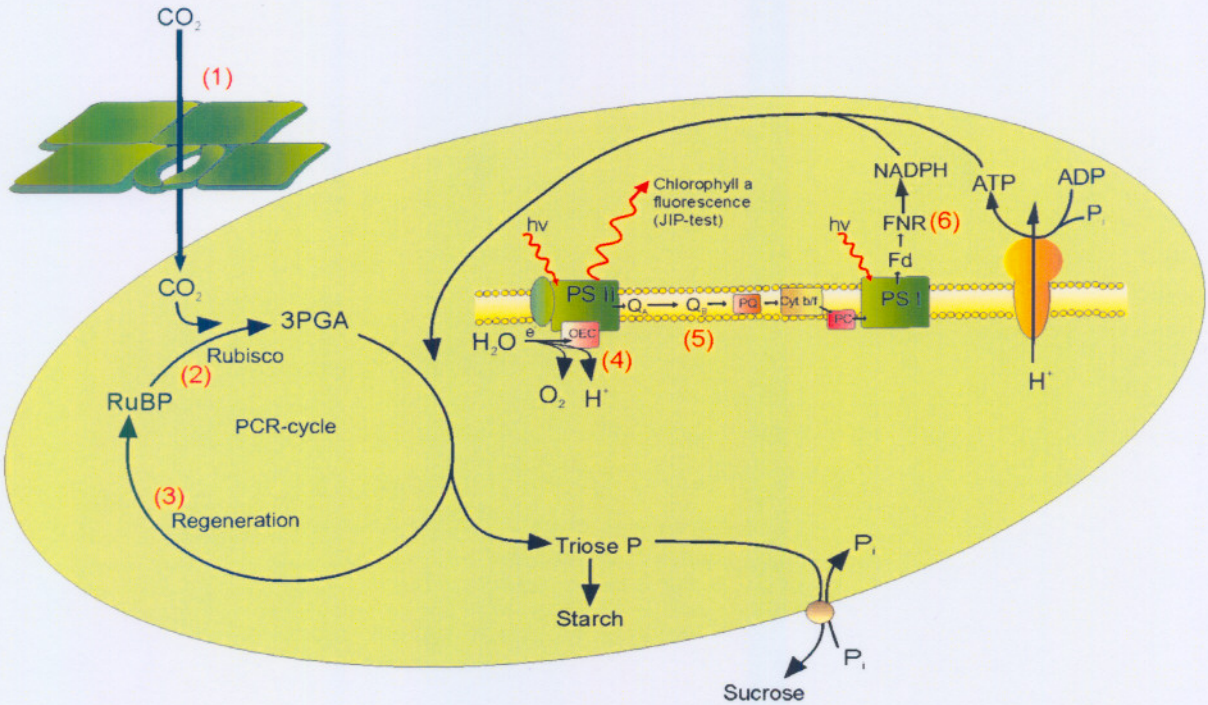

Figure 4.1: The inhibitory effect of trifluoroacetate on C_3 photosynthesis. (1) Stomatal limitation; (2) PEP-case inhibition; (3) Rubisco inhibition; (4) Uncoupling of the OEC; (5) Inhibition of the binding of PQ to Q_B; (6) Inhibition of FNR and subsequent formation of NADPH.

The question can now be asked: why is photosynthesis in *Z. mays* a representative of C_4 photosynthesis more severely affected by trifluoroacetate and where are these points of inhibition located in C_4 photosynthesis:

1) From the data discussed in chapter 3 it is clear that stomatal conductance decreased with increasing trifluoroacetate treatment for *Z. mays* (Section 3.2.1). Although a slight stimulation in stomatal conductance was apparent early on (Day 8) after treatment at low NaTFA concentrations (0.625 $mg.l^{-1}$), it soon gave way to increased inhibition with increasing trifluoroacetate dosage. Trifluoroacetate thus

increases stomatal closure and contributed to inhibition of photosynthesis, but to lesser degree than in *P. vulgaris* (Figure 4.2, 1).

2) The carboxylation by Rubisco and/or PEP-case was severely affected by increasing trifluoroacetate treatment since the carboxylation efficiency displayed considerable declines in *Z. mays* (Section 3.2.1). Once again this may be due to conformational changes and subsequent reduced enzyme activity induced by trifluoroacetate (Hance & Holly, 1963; Foy, 1969; Chang & Cai, 2005). Another possible reason for reduction in carboxylation efficiency is the fact that pyruvate phosphate dikinase, the enzyme that converts pyruvate to PEP, requires ATP while NADP malate dehydrogenase requires NADPH to convert OAA to malate. Since the chlorophyll a fluorescence (decrease in φ_{R0}, Section 3.2.2) and photosynthetic gas exchange data (decrease in J_{max}, Section 3.2.1) discussed in chapter 3 have indicated that photosynthetic electron transport was severely inhibited by trifluoroacetate, it follows that both ATP and NADPH levels were reduced, probably results in the inhibition of the C_4 cycle leading to the accumulation of OAA and pyruvate. It should however be kept in mind that the severe nutrient deficiency experienced by treated *Z. mays* (reduction in chlorophyll content, Section 3.1.4) could also affect enzyme activity since protein synthesis may have been affected. Our conclusion is that trifluoroacetate thus inhibits the C_4 cycle which is responsible for supplying the PCR cycle in the bundle sheath chloroplast with CO_2 and reducing equivalents (Figure 4.2, 2).

3) Enzyme analysis showed that Rubisco activity per leaf area basis was severely decreased by trifluoroacetate treatment in *Z. mays*. This inhibition may well have been caused by the reduced production of ATP and NADPH and decreased Rubisco synthesis as a result of nutrient shortages caused by massive root inhibition (Section 3.2.3). The inhibition of Rubisco activity may have resulted in the decreases in CO_2 assimilation capacity (Section 3.2.1). The literature also suggest that trifluoroacetate may have brought about conformational changes in proteins (Hance & Holly, 1963; Foy, 1969; Chang & Cai, 2005), thus affecting Rubisco activity (Figure 4.2, 3).

4) Data discussed in chapter 3 suggested that RuBP regeneration was negatively affected by trifluoroacetate (Section 3.2.1). This inhibition may have been caused by the reduction in PCR cycle enzyme reaction rates, since phosphoglycerate kinase and ribulose-5-phosphate kinase requires ATP. Furthermore glyceraldehyde-3-phosphate dehydrogenase requires NADPH. The reduction in photosynthetic electron transport and the decreasing NADPH and ATP production (Section 3.2.2)

must have inhibited the activity of the enzyme. This hypothesis is further strengthened by the correlation between RuBP regeneration capacity (J_{max}) and the quantum efficiency of the formation of reducing equivalents (φ_{R0}) (Figure 3.37). It thus seems that trifluoroacetate inhibits the PCR cycle and subsequently RuBP regeneration (Figure 4.2, 4).

5) Export of triosephosphate may have also been negatively affected by trifluoroacetate and nutrient shortages due to the inhibition of root growth. This effect on photosynthate utilisation or translocation was apparent as the increase in starch grains with increased trifluoroacetate treatments, observed in the TEM micrographs (Section 3.1.6). This increase in starch suggests that nutrient shortages may have been caused by root inhibition (Carmi & Heuer, 1972; Hermans *et al.*, 2006). However, sugar and starch analyses still have to be carried out to confirm these observations (Section 3.1.6) (Figure 4.2, 5).

6) The chlorophyll a fluorescence data (Section 3.2.2) suggested that the oxygen evolving complex (OEC) was increasingly uncoupling from PS II with increasing levels of trifluoroacetate treatments. The uncoupling of the OEC once again suggests that trifluoroacetate may induce conformational changes in proteins (Hance & Holly, 1963; Foy, 1969; Chang & Cai, 2005). Trifluoroacetate thus uncouples the OEC from PSII thus inhibiting the photosynthetic electron transport chain (Figure 4.2, 6).

7) The chlorophyll a fluorescence data indicated the inhibition of the efficiency to convert trapped excitation energy to electron transport past Q_A (Section 3.2.2) while the oxygen evolution measured in thylakoids (Section 3.2.4) suggested that inhibition on electron transport by trifluoroacetate occurs between Q_A and Q_B. This observation corresponds to the findings of Govindjee *et al.* (1997) that trichloroacetate inhibits electron transport between Q_A and Q_B. Although this suggests a DCMU effect the inhibition was much smaller than a typical DCMU inhibition. The chlorophyll a fluorescence data suggested that the main inhibition might be located further on in the photosynthetic electron transport chain. Trifluoroacetate thus inhibits the binding of a plastoquinone to the Q_B binding site on the D1 protein of PSII due to possible binding of trifluoroacetate close to Q_B (Figure 4.2, 7).

8) Additionally to the abovementioned inhibition of photosynthetic electron transport an even more severe inhibition of photosynthetic electron transport near FNR was suggested by chlorophyll a fluorescence for *Z. mays*. The main inhibition on electron

transport is located close to FNR according to the chlorophyll a fluorescence data (Appearance of I-bands, Section 3.2.2). This inhibition and subsequent reduction in NADPH may well be partly responsible for the reduction in RuBP regeneration capacity. Trifluoroacetate apparently inhibits the enzyme FNR and subsequently the formation of NADPH (Figure 4.2, 8). The subsequent reduction in NADPH and ATP content may well have contributed to the reduction in RuBP regeneration in the bundle sheath chloroplasts.

Higher sensitivity of mesophyll chloroplasts (compared to normal chloroplasts in *P. vulgaris*) and subsequent greater reduction in the formation of NADPH and ATP may well have contributed substantially to the apparent higher sensitivity of *Z. mays* to trifluoroacetate. The NADPH and ATP formed in the mesophyll chloroplasts have to be transported to the bundle sheath cells. This shuttle system of NADPH and ATP (Lawlor, 1993; Figure 4.2) may well be prone to trifluoroacetate inhibition. The same is also true for the C_4 cycle and transport of assimilated CO_2 from the mesophyll chloroplasts to the bundle sheath chloroplasts in the form of a C_4 acid. The key enzymes in the C4 cycle, namely phosphoglycerate kinase, ribulose-5-phosphate kinase and glyceraldehyde-3-phosphate dehydrogenase may have been affected by reduction in photosynthetic electron transport and resulting decreased NADPH and ATP production. The number of enzymes involved in this complex C_4 photosynthesis mechanism also makes it highly likely that some of these enzymes could have been affected by conformational changes as a result of trifluoroacetate (Hance & Holly, 1963; Foy, 1969; Chang & Cai, 2005). Studies on the chloroplast structures also revealed severe damage to bundle sheath chloroplasts as well as mesophyll chloroplasts membranes by trifluoroacetate or resulting singlet oxygen, which would also severely affect photosynthetic electron transport activity. Any changes in the chemiosmotic potential as a result of membrane damage would have severely affected ATP production (McKersie & Leshem, 1994). The distribution of bundle sheath chloroplasts were also affected since they were located further away from the cell walls adjacent to the mesophyll cells and they were less densely packed. This change in chloroplast distribution may also have hampered the effective translocation of metabolites between the mesophyll and bundle sheath chloroplasts.

Thus the higher sensitivity in C_4 plants to trifluoroacetate may be attributed to the complex nature of C_4 photosynthesis and the resulting increased number of possible points of inhibition by this reactive pollutant trifluoroacetate. The increased sensitivity however may not only be attributed to direct effects on photosynthesis. The fact that root inhibition by trifluoroacetate was more severe in *Z. mays* than in *P. vulgaris*, may in addition be attributed to anatomical differences since *Z. mays* is monocotyledonous and *P. vulgaris* is dicotyledonous. The exact reason for this higher sensitivity of the roots of *Z. mays* remains unknown. Since it was shown that, in both repetitions of the sand experiment and both

repetitions of the water culture experiment, the chlorophyll a fluorescence measurements (φ_{R0}) and the photosynthetic gas exchange (J_{max}) were fully repeatable and exactly comparable (Figure 3.37), the resulting data of the effects of trifluoroacetate on photosynthesis stands on a firm basis.

It should be kept in mind that photosynthesis is probably not the most sensitive process towards trifluoroacetate treatment. According to Sharkey (1985) a build up of starch indicates that the utilisation of photosynthate rather than the production of photosynthate is the most sensitive step towards stress, in this case trifluoroacetate.

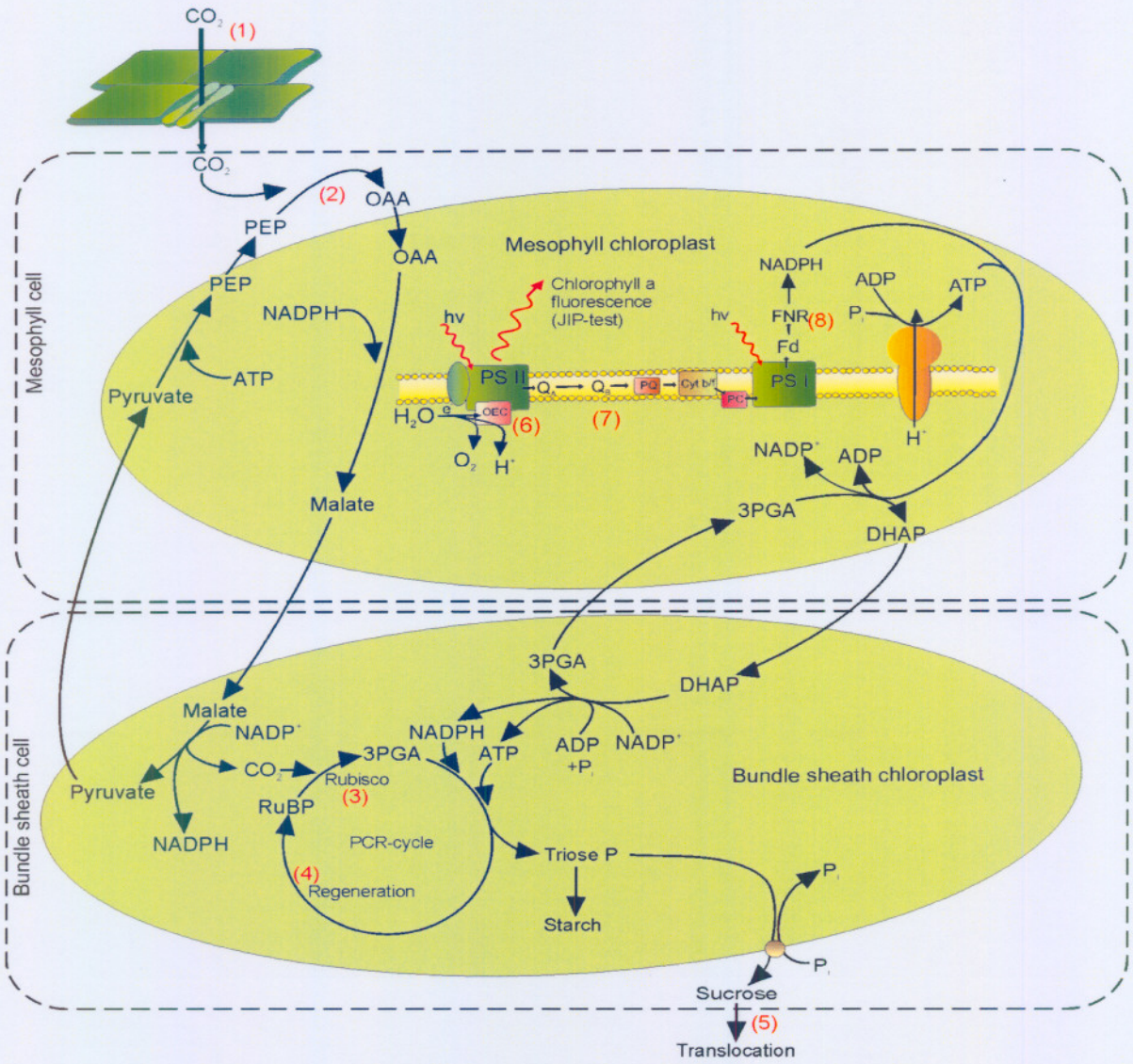

Figure 4.2: The inhibitory effect of trifluoroacetate on C_4 photosynthesis. (1) Stomatal limitation; (2) PEP-case inhibition; (3) Rubisco inhibition; (4) Reduction in RuBP regeneration capacity; (5) Inhibition of triosephoshate export and translocation; (6) Uncoupling of the OEC; (7) Inhibition between Q_A and Q_B; (8) Reduction in the activity of FNR and subsequent formation of NADPH.

4.2 Conclusion

Trifluoroacetate, a persistent substance with a number of anthropogenic sources such as degradation of halogenated hydrocarbons (Tang *et al.*, 1998) and thermolysis of fluoropolymers (Ellis *et al.*, 2000), was shown to result in inhibition of the photosynthetic metabolism as well as other crucial plant processes such as growth.

The hypotheses made before (Section 1.5) the study commenced, were all verified namely that:

- Trifluoroacetate is phytotoxic.
- C_4 plants were indeed more sensitive to trifluoroacetate.
- Trifluoroacetate did inhibit photosynthetic electron transport.
- Although it was not conclusively proven, trifluoroacetate may have affected auxin levels.

Additional information and new hypotheses also arose from the study namely that:

- In all experiments trichloroacetate clearly have shown greater phytotoxicity. These differences in phytotoxicity between trifluoroacetate and trichloroacetate may be attributed to differences in chemical structure. Firstly, trifluoroacetate is slightly more polar with a resulting lower K_{ow} (-2.1), making trifluoroacetate less capable to intrude into the lipophilic environments of membranes. Secondly trifluoroacetate is very stable with no recorded degradation in plants (Thompson *et al.*, 1994b). It has conversely been shown that the *in vivo* degradation of trichloroacetate to phosgene, chloroform and hydrochloric acid is possible (Weissflog *et al.*, 2006a). It is believed that the formation of these toxic substances from trichloroacetate, and the subsequent release of protons may be responsible for severe damage to membranes and cell structures. In the case of trifluoroacetate, decarboxylation is also possible but under extreme conditions which is not environmentally relevant (Hattema *et al.*, 1997). It is this abovementioned stability of trifluoroacetate in nature that possibly makes it as dangerous as trichlororoacetate.
- Trifluoroacetate causes epinasty and other growth irregularities as a result of changes in auxin levels in plants analogous to trichloroacetate (Mashtakov *et al.*, 1967; Parshakova & Mashtakov, 1967). Previously it has been proposed that the higher trifluoroacetate levels on the edges of the leaves directly inhibits cell elongation, causing epinasty and deformities (Davison & Pearson, 1997). In *Z. mays* the effects were apparent near the

leaf base were trifluoroacetate concentrations is supposed to be lower, clearly indicating developmental effects.

- Trifluoroacetate inhibits photosynthetic electron transport, not only by the uncoupling of the OEC and the inhibition of plastoquinone binding to Q_B but also as a result of inhibition of FNR.

- Even though at low concentrations stimulation of some parameters and processes was evident these stimulations may well be disastrous for plants under stress conditions. For example, initial stimulation, although not statistically significant, was measured in stomatal conductance at low trifluoroacetate concentrations. This increase in stomatal conductance resulted in an increased transpiration rate. Stimulation of transpiration with concomitant decrease in root growth, as observed in this study, would lead to severe stress under drought conditions.

- Although build up of starch and sugar could not be conclusively shown, literature suggests that trifluoroacetate, like trichloroacetate, may cause changes in the partitioning of the carbon metabolism (McWhorter, 1961). A current experiment on the effects of trifluoroacetate on trees has raised an interesting question. It was observed that the treated trees were severely attacked by aphids. This may well be caused by increases in starch and sucrose levels in the leaves. Literature reports on the increase in insect herbivory due to changes in sucrose and starch levels in plants affected by pollution (Endress *et al.*, 1985; Hamilton *et al.*, 2005).

Data with regard to visual symptoms on leaves and total biomass corresponds to data from previous ecotoxicological studies on the effect of trifluoroacetate (Davison & Pearson, 1997). The latter studies however failed to identify effects with respect to shoot : root as well as effects on photosynthesis and plant metabolism. This current study has shown that trifluoroacetate affects plants at much lower concentration than previously thought.

Even though some of the severe effects on growth and photosynthesis that were observed at high trifluoroacetate concentrations may be disregarded as these concentration were orders of magnitude higher than those found in nature, it was conclusively shown that the same effects occur to a lesser extent at relevant trifluoroacetate concentrations.

From all the data gathered it seems as though trifluoroacetate is a complex phytotoxin which is able to disturb protein structures and as a result inhibit a number of crucial processes including photosynthesis and hormone metabolism very subtly even at current environmental concentrations.

The controversy surrounding the prediction of future levels and the persistence of trifluoroacetate (Tang *et al.*, 1998, Solomon *et al.*, 2003) highlights the relevance of the research described in this thesis. The results also point to the fact that a lot more work is needed to understand the inhibition mechanisms of trifluoroacetate in plants.

4.3 Future Perspectives

The interpretation of data and formulation of hypotheses from the current study pointed out clear shortcomings in the data. To conclusively proof some of the above mentioned hypotheses the following is proposed:

- Analysis of starch and sucrose levels of samples from both treated plants and current experiments on trees.
- Analysis of auxin levels of treated plants by quantitive techniques.
- Studying the effect of NaTFA on the photosynthetic electron transport between PQ and FNR in isolated thylakoids in an oxygraph system.

References

AFEAS Alternative Fluorocarbons Environmental Acceptability Study (1996). Production sales and atmospheric emissions of fluorocarbons through 1995. Washington, DC.

AFEAS Alternative Fluorocarbons Environmental Acceptability Study (2006). [Web:] www.afeas.org [Date visited: October 22, 2006].

ALHERS J, REGELMANN J, RIEDHAMMER C (2003). Environmental risk assessment of airborne trichloroacetic acid—a contribution to the discussion on the significance of anthropogenic and natural sources. Chemosphere, 52: 531-537.

ARNON DI, WHATLEY FR, ALLEN MB (1958). Photosynthesis by isolated chloroplasts. Science, 127: 1026.

ASHTON FM & CRAFTS AS (1973). Mode of Action of Herbicides. John Wiley & Sons Inc. New York. 19, 54, 111-122.

BENESCH JA & GUSTIN MS (2002). Uptake of trifluoroacetate by *Pinus ponderosa* via atmospheric pathway. Atmospheric Environment. 36: 1233-1235.

BLANCHARD FA (1954). Uptake, distribution, and metabolism of carbon-14-labelled TCA in corn and pea plants. Weeds, 3: 274-278.

BOLHÁR-NORDENKAMPF HR & ÖQUIST G (1993). Chlorophyll fluorescence as a tool in photosynthesis research. In: HALL DO, SCURLOCK JMO, BOLHÁR-NORDENKAMPF HR, LEEGOOD RC, LONG SP (eds). Photosynthesis and Production in a changing Environment: a field and laboratory manual. Chapman & Hall: London. 193-206.

BOUTONNET JC, BINGHAM P, CALAMARI D, DE ROOIJ C, FRANKLIN J, KAWANO T, LIBRE JM, MCCULLOCH A, MALINVERNO G, ODOM JM, RUSCH GM, SMYTHE K, SOBOLEV I, THOMPSON R, TIEDJE JM (1999). Environmental Risk Assessment of Trifluoroacetic Acid, Human and Ecological Risk Assessment, 5: 59-124.

BRADFORD KJ & YANG SF (1980). Xylem transport of 1-aminocylcopropane-1-caboxylic acid, an ethylene precursor in higher plants. Naturwissenschaften, 68: 619-620.

BRADFORD MM (1976). A rapid and sensitive method for the quantification of microgram quantities of protein utilising the principle of protein dye binding. Analytical Biochemistry, 72: 248-254.

BRIAN RC (1976). The history and classification of herbicides. In: AUDUS LJ (ed.). Herbicides: Physiology, Biochemistry, Ecology. Academic Press, London.

BUNCE HWF (1985). Apparent stimulation of tree growth by low ambient levels of fluoride in the atmosphere. Journal of Air Pollution Control Association, 35: 46-48.

CARMI A & HEUER (1981). The role of roots in control of bean shoot growth. Annual Botany. 48: 519-527.

CHANG Y & CAI C (2005). Sodium trifluoroacetate: an efficient precursor for the trifluoromethylation of aldehydes. Tetrahedron letters, 46: 3161-3164.

CHRISTOPH EH (2002). Bilanzierung und Biomonitoring von Trifluoracetat und anderen Halogenacetaten. Dissertation zur Erlangung des Doktorgrades, der Fakultät Biologie, Chemie und Geowissenschaften der Universität Bayreuth.

CLELAND RE (1995). Auxin and cell elongation. In: DAVIES PJ (ed.). Plant Hormones and Their Role in Plant Growth Development. 2nd Ed. Kluwer, Dordrecht, Netherlands. 214-227.

DAVISON AW & PEARSON S (1997). Toxicity of TFA to plants. AFEAS SP91-1823/ BP96-31 University of Newcastle Report.

DEWEY OR, HARTLEY GS, MACKLAUGHLAN JWG (1962). External leaf waxes and their modification by heat-treatment of plants with trichloroacetate. Proceedings of the Royal Society, 155: 432-450.

ELLIS DA & MABURY SA (2000). The aqueous photolysis of TFM and related trifluoromethylphenols. An alternate source of trifluoroacetic acid in the environment. Environmental Science and Technology, 34: 632-637.

ELLIS DA, MABURY SA, MARTIN JW, MUIR DCG (2001). Thermolysis of fluoropolymers as a potential source of halogenated organic acids in the environment. Nature, 412: 321-324.

ELLIS DA, MOODY CA, MABURY SA (2002). Trifluoroacetic Acid and Longer Chain Perfluoro Acids –Sources and Analysis. In: NEILSON AH (ed.). The Handbook of Environmental Chemistry, Vol. 3. Organofluorines, Springer-Verlag, Berlin, Heidelberg. 103-120.

ENDRESS A & POST S (1985). Altered feeding preferences of the Mexican Bean Beetle *Epilachna varivestis* for ozonated soybean foliage. Environmental Pollution, 39: 9-16.

ERICKSON RO & MICHELINI FJ (1957). The plastochron index. American Journal of Botany, 44: 297-305.

FARMAN JC, GARDINER BG, SHANKLIN JD (1985). Large losses of total ozone in Antarctica reveal seasonal ClO_x/NO_x interaction. Nature, 315: 207-210.

FARQUHAR GD & SHARKEY TD (1982). Stomatal conductance & photosynthesis. Annual Review of Plant Physiology, 33: 317-345.

FORCE L, CRITCHLEY C, VAN RENSEN JJS (2003). New fluorescence parameters for monitoring photosynthesis in plants. Photosynthesis Research, 78: 17-33.

FOY CL (1969). Absorption, distribution and metabolism of 2,2-dichloropropionic acid in relation to phytotoxicity. II. Distribution and metabolic fate of dalapon in plants. Plant physiology, 36: 698-709.

FRANICH RA & WELLS LG (1980). Inhibition of *Pinus radiata* Primary Needle Epicuticular Wax Biosynthesis by Trichloroacetate. Journal of Experimental Botany, 31: 829-838.

FRANK H, KLEIN A, RENSCHEN D (1996). Environmental trifluoroacetate. Nature, 382, 34.

FRANKLIN J (1993). The atmospheric degradation and impact of 1,1,1,2-tetrafluoroethane (Hydrofluorocarbon 134a). Chemosphere, 27(8): 1565-1601.

FRANKLIN J (1994). The atmospheric degradation and impact of perchloroethylene. Toxicological Environmental Chemistry, 46:169-182.

FREDERICK JR, ALM DM, WISE RR, HESKETH JD, BELOW FE (1989). Leaf photosynthetic rates, stomatal resistances, and internal CO_2 concentrations of soybean cultivars under drought stress. Photosynthetica, 23(4): 575-584.

FUNDERBURK HH & DAVIS DE (1960). Factors affecting the response of *Zea mays* and *Sorgum halepense* to sodium 2,2-dichloropropionate. Weeds, 8: 6-11.

GIFFORD RM (1974). A comparison of potential photosynthesis, productivity and yield of plant species with differing photosynthetic metabolism. Australian Journal of Botany, 1: 107-117.

GOVINDJEE, XU C, SCHANSKER G, VAN RENSEN JJS (1997). Chloroacetates as inhibitors of photosystem II: Effects on electron acceptor side. Journal of Photochemistry and Photobiology B: Biology, 37: 107-117.

GUISSÉ B, SRIVASTAVA A, STRASSER RJ (1995). The polyphasic rise of the chlorophyll a fluorescence (OKJIP) in heat-stressed leaves. Archives of Science Geneva, 48: 147-160.

HANCE RJ & HOLLY K (1963). Weed Control Handbook: Principles. British Crop Protection Council. Blackwell Scientific Publications. 58-59, 83-84, 201.

HAMILTON JG, DERMODY O, ALDEA M, ZANGERI AR, ROGERS A, BERENBAUM MR, DE LUCIA EH (2005). Anthropogenic changes in tropospheric composition increase susceptibility of soybean to insect herbivory. Environmental Entomology, 34(2): 479-485.

HARNISCH J, FRISCHE M, BORCHERS R, EISENHAUER A, JORDAN A (2000). Naturally fluorinated organics in fluorite and rocks. Geophysical Research Letters, 27: 1883-1886.

HATCH MD & SLACK CR (1966). Photosynthesis by sugarcane leaves. A new carboxylation reaction and the pathway of sugar formation. Biochemical Journal, 101: 103-111.

HATTEMA H, HORE NR, RENNER ND, RUSSEL DK (1997). The Thermal Decomposition of Haloacetic acids: a Laser Pyrolysis and Semiempirical Study. Australian Journal of Chemistry, 50: 363-372.

HERMANS C, HAMMOND JP, WHITE PJ, VERBRUGGEN N (2006). How do plants respond to nutrient shortage by biomass allocation?. Trends in Plant Science, 11: 610-617.

HOAGLAND DR & ARNON DI (1950). The water culture method for growing plants without soil. California Agricultural Experiment Station Circular, 347.

HOEKSTRA EJ & DE LEER EWB (1995). Organohalogens the natural alternatives. Chemistry in Britain, 127-131.

HOPKINS WG (1999). Introduction to Plant Physiology, 2nd Ed. John Wiley & Sons, Inc. New York. 200-206.

HORI H, TAKANO Y, KOIKE K, TAKEUCHI K, EINAGA H (2003). Decomposition of environmentally persistent trifluoroacetic acid to fluoride ions by a homogeneous photocatalyst in Water. Environmental Science and Technology, 37: 418-422.

INGLE M & ROGERS B (1961). Some physiological effects of 2,2-dichloro-propionic acid. Weeds, 9: 264-272.

IPCC Intergovernmental Panel on Climate Change (1996). Climate change 1995: The science of climate change, contribution of Working Group 1 to the Second Assessment Report of the IPCC, HOUGHTON JT, MEIRA FILHO LG, CALLANDER BA, HARRIS N, KATTENBERG A, MASKELL K (eds.). The University Press, Cambridge, UK.

JACOBSON JS & HILL AC (1970). Recognition of air pollution injury to vegetation: a practical atlas. Air Pollution Control Association, Pittsburgh, Pennsylvania.

JORDAN A, FRANK H (1999). Trfluoroacetate in the environment. Evidence for sources other than HCF/HCFCs. Environmental Science and Technology, 33: 522-527.

KAUTSKY H & HIRSCH A (1931). Neue Versuche zur Kohlensäureassimilation. Naturwissenschaften, 19: 96.

KHALIL MAK, MOORE RM, HARPER DB, LOBERT JM, ERICKSON DJ, KOROPALOV V, STURGES WT, KEENE WC (1999). Natural emissions of chlorine-containing gases. Geophysical Research Letters, 104: 8333-8346.

KEPPLER F, EIDEN R, NIEDAN V, PRACHT J, SCHÖLER HF (2000). Halocarbons produced by natural oxidation processes during degradation of organic matter. Nature, 403: 298-301.

KEYS AJ & PARRY MAJ (1990). Ribulose bisphosphate carboxylase/oxygenase and carbonic anhydrase. Methods in Plant Biochemistry, 3: 1-15.

KRAMER PJ (1983). Water relations of plants. New York: Academic Press. 360-364.

KIM BR, SUIDAN MT, WALLINGTON TJ, DU X (2000). Biodegradability of trifluoroacetic acid. Environmental Engineering Science, 17: 337-342.

KRAUSE GH & WEIS E (1991). Chlorophyll fluorescence and photosynthesis: the basics. Annual Review of Plant Physiology, 42: 313-349.

KRÜGER GHJ, TSIMILLI-MICHAEL M, STRASSER RJ (1997). Light stress provokes plastic and elastic modifications in structure and function of photosystem II in camellia leaves. Physiologia Plantarum, 101: 265-277.

LAETSCH WM (1974). The C4 syndrome: a structural analysis. Annual Review of Plant Physiology, 25: 27-52.

LANGE CA, WEISSFLOG L, STRASSER R, KRÜGER GHJ, PFENNINGSDORFF A (2004). Phytotoxic effects of trichloroacetic acid on Scots pine and birch by chl a fluorescence and the JIP-test. South African Journal of Botany, 70: 683-694.

LANGE OL, HARLEY PC, BEYSCHLAG W, TENHUNEN JD (1987). Gas exchange methods for characterizing the impact of stress on leaves. In: TENHUNEN JD (ed.). Plant Response to Stress. Springer-Verlag, Heidelberg, Germany. 3-22.

LAVOREL J & ETIENNE AL (1977). *In vivo* chlorophyll fluorescence. Topics in Photosynthesis, 2: 203-268.

LAWLOR DW (1993). Photosynthesis, Molecular, Physiological and Environmental Processes, 2nd Ed. Longman Scientific & Technical, UK. 177-188.

LAZÁR D & ILÍK P (1997). High-temperature induced chlorophyll fluorescence changes in barley leaves: Comparison of the critical temperatures determined from fluorescence induction and from fluorescence temperature curve. Plant Science, 124: 159-164.

LETHAM DS (1971). Regulation of cell division in plant tissues. A cytokinin bioassay using excised radish cotyledons. Physiologia Plantarum, 25: 391-396.

LONG SP (1985). Leaf gas exchange. In: BARBER J & BAKER NR (eds.) Photosynthetic Mechanisms and the Environment. Elsevier. Amsterdam. 453-500.

LONG SP & HÄLLGREN JE (1993). Measurement of CO_2 assimilation by plants in the field and the laboratory. In: HALL *et al.* (eds.) Photosynthesis and Production in a changing Environment: a field and laboratory manual. Chapman & Hall: London. 129-167.

MANSFIELD TA, DAVIES WJ, WHITMORE ME (1986). Interactions between the responses of plants to pollution and other environmental factors such as drought, light and temperature. In: How are the effects of air pollutants on agricultural crops influenced by the interaction with other limiting factors?. COST Workshop 1986. Denmark. 2-15.

MASHTAKOV SM, DEEVA VP, VOLYNETS AP (1967). Histochemical changes in germinating seeds under the influence of herbicides. In: MASHTAKOV SM (ed.). Physiological Effects of Herbicides on Varieties of Crop Plants. 47-59.

MAUZERALL DL & WANG X (2001). Protecting Agricultural Crops from the Effects of Tropospheric Ozone Exposure: Recoiling Science and Standard Setting in the United States, Europe and Asia. Annual review of Energy and the Environment. 26: 237-268.

MAYER F (1957). Reaction of trichloroacetic acid and other halogen acetates with sulfhydryl groups and amino groups and also vegetable matter. Biochem. Zeitung, 328: 433-442.

MAYORAL ML, ATSMON D, SHIMSHI D, GROMET-ELHANAN Z (1981). Effect of water stress on enzyme activities in wheat and related wild species: Carboxylase activity, electron transport and photophosphorylation in isolated chloroplasts. Australian Journal of Plant Physiology, 8: 385-393.

MCWHORTER CG (1961). Carbohydrate metabolism of Johnsongrass as influenced by seasonal growth and herbicide treatment. Weeds, 9: 229-233.

MCKERSIE BD & LESHEM YY (1994). Stress and Stress Coping in Cultivated Plants. Kluwer. Dordrecht. 28.

MILLS WR & JOY KW (1980). A rapid method for isolation of purified, physiologically active chloroplasts, used to study the intracellular distribution of amino acids in pea leaves. Planta, 148: 75-83.

OEHRLE NW, GREEN LS, KARR DB, EMERICH DW (2004). The HFC/HCFC breakdown product trifluoroacetic acid (TFA) and its effects on the symbiosis between *Bradyrhizobium japonicum* and soybean (*Glycine max*). Soil Biology and Biochemistry 36: 333-342.

OUZOUNIDOU G, MOUSTAKAS M, STRASSER RJ (1997). Sites of action of copper in the photosynthetic apparatus of maize leaves: kinetic analysis of chlorophyll fluorescence, oxygen evolution, absorption changes and thermal dissipation as monitored by photoacoustic signals. Australian Journal of Plant Physiology, 24: 81-90.

PAPAGEORGIOU J (1975). Chlorophyll fluorescence: an intrinsic probe of photosynthesis. In: GOVINDJEE (ed.) Bioenergetics of Photosynthesis, Academic Press, New York. 319-371.

PARSHAKOVA ZP & MASHTAKOV SM (1967). The effect of TCA-sodium on the heteroauxin and tryptophan contents of leguminous plants. Dokl. Akad. Nauk. Belorussk. USSR. 11: 271-273.

PIENAAR JJ & HELAS G (1996). Chemical Transformations of Atmospheric Pollutants. In: HELD G, GORE BJ, SURRIDGE AD, TOSEN GR, TURNER CR, WALMSLEY (eds.). Air Pollution and Its Impacts on the South African Highveld. Environmental Scientific Association, Cleveland & National Association For Clean Air, Parklands. 76-79.

PICKERING ER (1965). Foliar penetration pathways of 2,4 D, monoron and dalapon as revealed by historadioautography. Ph.D. dissertation, University of California. 186.

POSTHUMUS AC (1991). Effects of air pollution on plants and vegetation. In: ROZEMA J & VERKLEIJ JAC (eds.). Ecological Responses to Environmental Stresses. Kluwer Academic Publishers, Netherlands. 191-198.

PRASAD R & BLACKMAN GE (1964). Studies in the physiological action of 2,2-dichloropropionic acid. I Mechanism controlling the inhibition of root elongation. Journal of Experimental Botany, 15: 48-66.

RICHEY DG, DRISCOLL CT, LIKENS GE (1997). Soil retention of trifluoroacetate. Environmental Science and Technology, 31: 1723-1727.

REYNOLDS ES (1963). The use of lead citrate at high pH as an electron-opaque stain in electron microscopy. Journal of Cell Biology, 17: 208-212.

SANTELMANN PW & WILLARD CJ (1955). The absorption and translocation of dalapon. Proceeding of the 9th Northeast Weed control Conference. 21-29.

SCHANSKER G, TÓTH SZ, STRASSER RJ (2006). Dark-recovery of the Chl a fluorescence transient (OJIP) after light adaption: The qT-component of non-photochemical quenching is related to an activated photosystem I acceptor side. Biochimica et Biophysica Acta, 1757: 787-797.

SCHREIBER U & NEUBAUER C (1987). The polyphasic rise of chlorophyll fluorescence upon onset of strong continuous illumination. II. Partial control by photosystem II donor side and possible ways of interpretation. Zeitschrift Naturforschung, 42c:1255-1264.

SCOTT BF, SPENCER C, MARTIN JW, BARRA R, BOOTSMA BA, JONES KC, JOHNSTON AE, MUIR DGG (2005). Comparison of the haloacetic acids in the Environment of the Northern and Southern Hemispheres. Evironmental Science and Technology, 35: 8664-8670.

SHARKEY TD & BADGER MR (1982). Effects of water stress on photosynthetic electron transport, photophosphorylation and metabolite levels of *Xanthium strumarium* mesophyll cells. Planta, 156: 199-206.

SHARKEY TD (1985). Photosynthesis in Intact Leaves of C_3 Plants: Physics, Physiology and Rate Limitations. The Botanic Review, 51: 53-105.

SOLOMON KR, TANG X, WILSON SR, ZANIS P, BAIS AF (2003). Changes in tropospheric composition and air quality due to stratospheric ozone depletion. Journal of Photochemistry and Photobiology, 2: 62-67.

SPURR AR (1969). A low viscosity epoxy resin embedding medium for electron microscopy. Journal of Ultrastructure Research, 26:31-43.

SRIVASTAVA A, GUISSÉ B, GREPPIN H, STRASSER RJ (1997). Regulation of antenna structure and electron transport in photosystem II of *Pisum sativum* under elevated temperature probed by the fast polyphasic chlorophyll a fluorescence transient: OKJIP. Biochimica et Biophysica Acta, 1320: 95-106.

STRASSER RJ & GOVINDJEE A (1992). On the OJIP fluorescence transient in leaves and DI mutants of *Chlamydomonas reinhardtii*. In: MURATA N, (ed.) Research in Photosynthesis. Kluwer Academic Publishers, Dordrecht. 29-32.

STRASSER RJ & STRASSER BJ (1995). Measuring fast fluorescence transients to address environmental questions: The JIP-test. In: MATHIS P (ed.) Photosynthesis: From light to biosphere. Kluwer Academic Publishers, Netherlands. 977-980.

STRASSER BJ (1997). Donor side capacity of photosystem II probed by chlorophyll a fluorescence transients. Photosynthesis Research, 52: 147-155).

STRASSSER RJ, SRIVASTAVA A, GOVINDJEE (1995). Polyphasic chlorophyll a fluorescence transients in plants and cyanobacteria. Journal of Photochemistry and Photobiology, 61: 32-42.

STRASSER RJ & TSIMILLI-MICHAEL M (2001). Stress in plants, from daily rhythm to global changes, detected and quantified by the JIP-test. Chimie Nouvelle (SRC), 75: 3321-3326.

STRASSER RJ, SRIVASTAVA A, TSIMILLI-MICHAEL M (2000). The fluorescence transient as a tool to characterise and screen photosynthetic samples. In: YUNUS M, PATHRE U, MOHANTY P (eds). Probing Photosynthesis: Mechanism, Regulation and Adaptation. Taylor & Francis, London. 443-488.

STRASSER RJ, SRIVASTAVA A, TSIMILLI-MICHAEL M (2004). Analysis of the chlorophyll fluorescence transient. In: PAPAGEORGIOU G, GOVINDJEE (eds.). Chlorophyll Fluorescence a Signiture of Photosynthesis. Kluwer Academic Publishers. Netherlands. 19: 321-362.

STRAUSS AJ, KRÜGER GHJ, VAN HEERDEN PDR, PIENAAR JJ, WEISSFLOG L (2004). Constraints on photosynthesis of C3 and C4 crop plants by trichloroacetic acid, an atmogenically generated pollutant. South African Journal of Botany, 70(5): 1-9.

STRAUSS AJ, KRÜGER GHJ, STRASSER RJ, VAN HEERDEN PDR (2006). Ranking of dark chilling tolerance in soybean genotypes probed by the chlorophyll a fluorescence transient O-J-I-P. Environmental and Experimental Botany, 56: 147 – 157.

STRAUSS AJ, KRÜGER GHJ, STRASSER RJ, VAN HEERDEN PDR (2007). The role of low soil temperature in the inhibition of growth and PSII function during dark chilling in soybean genotypes of contrasting tolerance. Planta, Article submitted.

SUTINEN S, JUUTI S, RYYPPO A (1997). Long-term exposure of Scots pines to monochloroacetic and trichloroacetic acid: Effects on needles and growth. Annual Botany Fennici, 34: 265-273.

TANG X, MADRONICH S, WALLINGTON T, CALAMARI D (1998). Changes in tropospheric composition and air quality. Journal of Photochemistry and Photobiology B, 46, 83-95.

TAIZ L (1984). Plant cell expansion: Regulation of cell wall mechanical properties. Annual Review of Plant Physiology, 35: 585-657.

TAYLOR SE & TERRY N (1984). Limiting factors in photosynthesis. V. Photochemical energy supply co-limits photosynthesis at low values of intercellular CO_2 concentration. Plant Physiology, 75: 82-86.

THOMPSON R & WINDEATT AJ (1994a). Sodium trifluoroacetate: Effects on seed germination (ten species, by aqueous exposure). Brixham Environmental Laboratory Report BL5197/B.

THOMPSON RS, STEWART KM, GILLINGS E (1994b). Trifluoroacetic acid: Accumulation from aqueous solution by the roots of Sunflower (*Helianthus annuus).* Brixham Environmental Laboratory Report BL5042/B.

TREBST A (1999). Linearer und zyklischer Elektronenransport. In: HÄDER D (ed.). Photosynthese. Georg Thieme Verlag. Stuttgart. 115-131.

TRESHOW M & HARNER FM (1968). Growth response of Pinto bean and alfalfa to sublethal fluoride concentrations. Canadian Journal of Botany, 46: 1207-1210.

TRESHOW M & ANDERSON FK (1989). Plant Stress from Air Pollution. John Wiley & Sons Ltd.. The Bath Press, Avon, Great Britain.

TROMP TK, KO MKW, RODRIGUEZ JM, SZE ND (1995). Potential accumulation of a CFC-replacement degradation product in seasonal wetlands. Nature, 376: 327.

TSIMILLI-MICHAEL M, PÊCHEUX M, STRASSER RJ (1999). Light and heat stress adaptation of the symbionts of coral reef and temperate foraminifers probed *in hospite* by the chlorophyll a fluorescence kinetics O-J-I-P. Zeitschrift Naturforsch, 54C: 671-680.

TSIMILLI-MICHAEL M, EGGENBERG P, BIRO B, KÖVES-PECKY K, VÖRÖS I, STRASSER RJ (2000). Synergistic and antagonistic effects of arbuscular mycorrhizal fungi and *Azospirillum* and polyphasic fluorescence transient O-J-I-P. Applied Soil Ecology, 15: 169-182.

UNSWORTH MH (1982). Exposure to gaseous pollutants and uptake by plants. In: UNSWORTH MH & ORMROD DP (eds.) Effects of gaseous air pollution in agriculture and horticulture. Butterworth, London.

U.S Global Change Research Information Office (2006). Atmospheric Production and Fate of Trifluoroacetic Acid. [Web:] www.gcrio.org [Date visited: October 22, 2006].

VAN HEERDEN PDR, STRASSER RJ, KRÜGER GHJ (2004). Reduction of dark chilling stress in N2-fixing soybean by nitrite as indicated by chlorophyll a fluorescence kinetics. Physiologia Plantarum, 121: 239-249.

VON CAEMMERER S & FARQUHAR GD (1981). Some relationships between the biochemistry of photosynthesis and gas exchange of leaves. Planta,153: 376-387.

VISSCHER PT, CULBERTSON CW, OREMLAND RS (1994). Degradation of trifluoroacetate in oxic and anoxic sediments. Nature, 369: 729-731.

WEISSFLOG L, PFENNIGSDORFF A, MARTINEZ-PASTUR G, PULIAFITO E, FIGUEROA D, ELANSKY N, NIKONOV V, PUTZ E, KRÜGER G, KELLNER K (2001). Trichloroacetic acid in the vegetation of polluted and remote areas of both hemispheres- Part I. Its formation, uptake and geographical distribution. Atmospheric Environment, 35: 4511-4521.

WEISSFLOG L , LANGE CA, PFENNINGSDORFF A, KOTTE K, ELANSKY N, LISITZYNA L, PUTZ L, PUTZ E, KRÜGER GHJ (2005). Sediments of salt lakes as a new source of volatile highly chlorinated C1/C2 hydrocarbons. Geophysical Research Letters, 32: doi:10.1029/2004GL020807

WEISSFLOG L, KRÜGER G, ELANSKY N, PUTZ E, LANGE C, LISITZINA L, PFENNIGSDORFF A, KOTTE K (2006). The phytotoxic effect of C_1/C_2-halocarbons and trichloroacetic acid on the steppe plant *Artemisia lerchiana*. Chemosphere, 65: 975-980.

WEISSFLOG L, KRÜGER GHJ, FORCZEK ST, LANGE CA, KOTTE K, PFENNINGSDORFF A, ROHLENOVA J, FUKSOVA K, UHLIROVA H, MATUCHA M, SCHRÖDER P (2007). Oxidative biodegradation of tetrachloroethane in needles of Norway spruce (*Picea abies* L.). South African Journal of Botany, 73: 89-96.

WUJCIK CE, CAHILL TM, SEIBER JN (1999). Determination of trifluoroacetic acid in rain in 1996-1997 precipitation and surface waters in California and Nevada. Environmental Science Technology, 33, 1747-1751.

ZHANG J, ZHANG Y, LI J, HU J, YE P, ZENG Z (2005). Monitoring of trifluoroacetic acid concentration in environmental waters in China. Water research, 39: 1331-1339.

ZEHAVI D & SEIBER JN (1996). An analytical method for trifluoroacetic acid in water and air samples using headspace gas chromatographic determination of the methyl ester. Analytical Chemistry, 68: 3450-3459